AN ABSTRACT OF THE THESIS OF

Robert S. Pennington for the degree of Master of Science in Water Resources Engineering presented on December 04, 2019.

Title: Measurement of Gas Exchange, Stream Metabolism, and Carbon Fluxes of Headwater Streams

Abstract approved:

_____

Roy D. Haggerty

Freshwater systems are an important component of the global carbon cycle as they outgas disproportionately large quantities of carbon compared to the terrestrial landscape. Of particular importance are headwater streams, which represent roughly 90% of the channel network by length and have been conservatively estimated to outgas roughly 36% of the carbon dioxide ($CO_2$) that is evaded from rivers and streams globally. We investigated carbon fluxes of a second order headwater stream that drains a 96 ha forested watershed in western Oregon, USA. Total inorganic carbon imports and exports were estimated to be 1294 kg C $yr^{-1}$ (130 kg C $ha^{-1}yr^{-1}$). Influx from hillslope runoff and groundwater was measured to be 65.6 kg C $ha^{-1}yr^{-1}$, 50% of total imports. The remaining imports were split between stream metabolism at 26% (33.8 kg C $ha^{-1}yr^{-1}$) and near stream riparian sources at 23% (29.9 kg C $ha^{-1}yr^{-1}$). Exports of inorganic carbon as $CO_2$ from the stream to the atmosphere were estimated to be 59% (76.9 kg C $ha^{-1}yr^{-1}$) of total exports. Streamflow exported the remaining 41% (53.1 kg C $ha^{-1}yr^{-1}$) of basin-scaled flux. Results highlight the importance of both external and internal carbon sources to the stream carbon budget.

Aeration rate is an integral parameter for the measurement of $CO_2$ evasion. It is also needed to measure instream metabolic processing. Common field methods to estimate the aeration rate have strengths and weaknesses, and researchers continue to search for better techniques, particularly for steep streams with high rates of gas exchange and low productivity.

We developed the oxygen carbon (OC) method for calculating gas-exchange rates from simultaneous measurement of oxygen ($O_2$) and dissolved inorganic carbon (DIC). Gas-exchange rates are calculated by solving the combined stream transport equation for $O_2$ and DIC. The output is a time series of aeration rates at the same sampling frequency as the input $O_2$ and carbon (C) data. Field tests in a fourth order montane stream in Oregon, USA, were a success. The OC method estimated the aeration rate to 3.25 $h^{-1}$, which agreed well with the value from direct gas injection of 3.22 $h^{-1}$. Sensitivity analysis indicated that application of the OC method is limited to reaches with a suitable change in combined $O_2$ and $CO_2$ concentration $\geq$ ~4 μmol/L and combined $O_2$ and $CO_2$ saturation deficits $\approx$ 4 μmol/L. The OC method was then applied in a second order headwater stream over a wide range of flow conditions, allowing for development of a site-specific regression between discharge and aeration rate.

# Measurement of Gas Exchange, Stream Metabolism, and Carbon Fluxes of Headwater Streams

by
Robert S. Pennington

A THESIS

submitted to

Oregon State University

in partial fulfillment of
the requirements for the
degree of

Master of Science

Presented December 04, 2019
Commencement June 2020

Master of Science thesis of Robert S. Pennington presented on December 04, 2019.

APPROVED:

Major Professor, representing Water Resources Engineering

Director of the Water Resources Graduate Program

Dean of the Graduate School

I understand that my thesis will become part of the permanent collection of Oregon State University libraries. My signature below authorizes release of my thesis to any reader upon request.

Robert S. Pennington, Author

# ACKNOWLEDGEMENTS

I would like to thank my advisor Dr. Roy Haggerty for his support, guidance, and mentorship. I deeply appreciate Roy's trust in my judgement and competence, and his ability to see beyond the trees and convey what is truly important in both science and life. I would also like to thank Dr. Steve Wondzell. His knowledgeable advice has greatly contributed to this research, and his incredible ability to communicate complex ideas and to question what others commonly take for granted has made me a better scientist, might I say a better citizen. Thanks is also due to Dr. Alba Argerich. Her support and collaboration was of tremendous value to this research. I would like to thank staff at the H.J. Andrews Experimental Forest for maintaining the research station and the infrastructure upon which this research was dependent. Special thanks to Satish Serchan, and Jason Brandes for being great companions in the field and office. Thank you to my family for your support and encouragement, but also for the reminder to cherish the moment and to hold close those dearest to you.

# CONTRIBUTION OF AUTHORS

Manuscript 1: Dr. Alba Argerich assisted with field work, analysis, and edits. Dr. Roy Haggerty assisted with study design and edits.

Manuscript 2: Dr. Roy Haggerty helped in the development of this project. Dr. Steve Wondzell assisted with study design, and provided feedback and insight throughout. Satish Serchan provided water chemistry data from the stream and piezometers.

TABLE OF CONTENTS

Page

TABLE OF CONTENTS (CONTINUED)

Page

TABLE OF CONTENTS (CONTINUED)

Page

LIST OF FIGURES

LIST OF TABLES

Table Page

LIST OF APPENDIX FIGURES

# 1 Introduction

The fate and transport of carbon in streams and rivers is important to humans from regional to global scales. On a macroscopic scale, carbon processing in freshwater systems is significant to regional and global scale carbon budgets (Cole et al. 2007; Aufdenkampe et al. 2011a). Aufdenkampe et al. (2011a) reported 2.7 Pg C $yr^{-1}$ is received by freshwater systems, of which only 0.9 Pg C $yr^{-1}$ is transported to the ocean. The balance is outgassed? as $CO_2$ (1.2 Pg C $yr^{-1}$) or stored in sediment (0.6 Pg C $yr^{-1}$); more recent studies estimate $CO_2$ evasion to the atmosphere to be nearly double at 2.1 Pg C $yr^{-1}$ (Raymond et al. 2013). Rates of freshwater carbon transport, processing, and storage are small compared with estimates of terrestrial gross primary production (115 Pg C $yr^{-1}$) or annual carbon emissions from burning of fossil fuels (38 Pg C $yr^{-1}$) (IPCC 2014). However, river carbon fluxes are comparable to estimates of accumulation of carbon on land (2.2 Pg C $yr^{-1}$) and in oceans (2.2 Pg C $yr^{-1}$), making river and stream carbon fluxes important to regional scale carbon budgets. Low-order headwater streams are particularly relevant to what? because they comprise a large fraction (90%) of the channel network (Downing 2012), and their carbon processing and $CO_2$ saturation and evasion rates are large, but poorly constrained (Cole et al. 2007, Battin et al. 2008, Marx et al. 2017). The goal of this research was to expand our knowledge of carbon dynamics in headwater streams in order to better understand the significance of streams in the context of regional and global carbon budgets.

A recent investigation of the complete carbon budget of a headwater stream, Watershed 1 of the H. J. Andrews, Oregon, USA, found that headwater stream carbon fluxes are significant at regional and global scales (Argerich et al. 2016). Total export was measured at 170 kg C $ha^{-1}yr^{-1}$, or 2.1 Pg C $yr^{-1}$. Global averages of net ecosystem production (NEP) are on the order of 143 kg C $ha^{-1}yr^{-1}$ (Koffi et al. 2012). Regional NEP rates can have wide variation in relation to climate and land use. For example, publicly owned lands within the largely forested Pacific Northwest USA had an estimated NEP of -480 kg C $ha^{-1}yr^{-1}$ in the 1980s but a value 1630 kg C $ha^{-1}yr^{-1}$ from 2003 to 2007 (Turner et

al. 2011). Carbon export rates from Watershed 1 are similar in magnitude to terrestrial NEP rates, and support the finding that headwater streams are important landscape features to carbon budgets. This judgement is corroborated by studies that have found increasing dissolved inorganic carbon (DIC) concentrations and $CO_2$ evasion rates with decreasing stream order (Jones and Mulholland 1998, Butman and Raymond 2011, Hotchkiss et al. 2015).

There are a suite of physical and biogeochemical processes significant to carbon dynamics in headwater streams. Most headwater streams are strongly heterotrophic; inputs of terrestrially derived organic carbon are the dominant energy source (Vannote et al. 1980, Minshall et al. 1983). This is because of limited light, relatively large inputs of leaf litter, and inflows of groundwater or hillslope water that may be rich in organic carbon (Vannote et al. 1980, Minshall et al. 1983). The result is often high rates of ecosystem respiration that causes headwater streams to be supersaturated in $CO_2$ relative to the atmosphere (Cole and Caracao 2001, Butman and Raymond 2011). Hillslope and groundwater inflows of high $CO_2$ concentration further elevate $CO_2$ concentrations of the headwater streams (Jones and Mulholland 1998, Hope et al. 2001). The relative proportion of $CO_2$ derived from instream processing versus groundwater or hillslope runoff is a subject of active research (Marx et al. 2017, Wallin et al. 2018).

Regardless of the source, with $CO_2$ concentrations super saturated with respect to the atmosphere, headwater streams perpetually evade $CO_2$ into the atmosphere. The rate at which evasion takes place is driven by the concentration gradient and the aeration rate (Davies et al. 1964). The aeration rate scales with surface turbulence, which is largely a function of hydraulics (Tsivoglou and Neal 1976, Kilpatrick et al. 1989). Headwater streams tend to be steep and turbulent, with high aeration rates and short $CO_2$ residence times (Raymond and Cole 2001, Raymond et al. 2012). The aeration rate is also often a model parameter of great uncertainty (Aristegi et al. 2009, Demars et al. 2015), which results in poorly constrained estimates of $CO_2$ evasion and ecosystem respiration (McCutchan et al. 1998, Butman and Raymond 2011, Riley and Dodds 2013).

Research presented here focuses on the measurement of fluxes of inorganic carbon from the hillslope/groundwater system to the stream, instream processing of organic carbon, and fluxes of $CO_2$ from the stream to the atmosphere. These processes are all highly variable in space and time, and thus the approach included the collection and synthesis of multi-year high resolution carbon, oxygen, temperature, and hydrologic data. Chapter 1 develops a method (oxygen carbon (OC) method) to estimate aeration rates through analysis of $CO_2$ and dissolved oxygen time series data. Chapter 2 applies methods developed in Chapter 1 to determine a carbon budget for a headwater stream on a daily timestep over the course of two hydrologic years. The analysis estimates inputs of inorganic carbon from hillslope/groundwater runoff, stream metabolism, and other near-stream riparian sources. Outflows are partitioned between $CO_2$ evaded to the atmosphere and that exported with streamflow. In sum, this thesis contributes to the growing body of research pertaining to carbon dynamics, carbon fluxes, and stream metabolism of temperate headwater streams.

# 2 Measurement of Gas Exchange Rate by the Oxygen Carbon Method

Robert S. Pennington, Roy Haggerty, Alba Argerich

Freshwater Science

Published by the Society for Freshwater Science and the University of Chicago Press,

1427 E. 60th Street,

Chicago, Illinois 60637

Volume 37, Number 2 | June 2018

## *2.1 Abstract*

The gas-exchange rate between streams and the atmosphere is needed to measure in-stream ecologic processes and C processing in rivers and streams. Current methods include empirical relationships to hydraulics, direct injection of a tracer gas, and modeling based on $O_2$ or C diel curves. All existing methods have strengths and drawbacks and most are limited to point measurements or are unable to measure diel variation in exchange rate. Researchers continue to search for better techniques, particularly for steep streams with high rates of gas exchange and low primary productivity.

We present the oxygen carbon (OC) method for calculating gas-exchange rates via simultaneous measurement of $O_2$ and dissolved inorganic C (DIC). Gas-exchange rates are calculated by solving the combined stream transport equation for $O_2$ and DIC. The output is a time series of aeration rates at the same sampling frequency as the input $O_2$ and C data. Field tests in a 4th-order montane stream in Oregon, USA, indicate that the method is suitable for stream reaches with high downstream gas-concentration gradients and saturation deficits. The mean modeled aeration rate adjusted to 17°C (3.25 $h^{-1}$) agreed well with the value of 3.22 $h^{-1}$ from direct gas injection.

Net ecosystem production calculated with the modeled aeration rate (–1.69 g $O_2$ $m^{-2}$ $d^{-1}$) was consistent with the result obtained with direct gas injection (–1.60 g $O_2$ $m^{-2}$ $d^{-1}$). An assumption of the model is a constant respiration quotient, but results indicated that the respiration quotient may be time variable. Sensitivity analysis indicated that application of the OC method is limited to reaches with a suitable change in combined $O_2$ and $CO_2$ concentration ≥ ~4 μmol/L and combined $O_2$ and $CO_2$ saturation deficits ≈ 4 μmol/L, characteristic of smaller gaining streams. Preliminary application of the OC method indicates it could be useful to practitioners interested in continuous measurement of gas-exchange rates.

## *2.2 Introduction*

Measurement of rates of gas exchange between streams and the atmosphere is fundamental for quantifying stream ecosystem processes including primary productivity

and respiration (Cole et al. 1991, Mulholland et al. 2001) and for calculating catchment to global-scale C budgets (Cole et al. 2007, Raymond et al. 2013). Gas exchange is a model parameter for ecosystem and water-quality models of rivers and lakes concerned with biological $O_2$ demand (Tsivoglou and Neal 1976). However, it is commonly a model parameter with great uncertainty (Aristegi et al. 2009, Demars et al. 2015), which results in poorly constrained estimates of stream metabolism and related rates of net ecosystem production (*NEP*), gross primary production (*GPP*), and community respiration (*CR*) (McCutchan et al. 1998, Riley and Dodds 2013). When evasion of $CO_2$ from rivers to the atmosphere is poorly constrained, large errors in regional and global C budgets are expected (Raymond and Cole 2001).

Many methods are used to estimate gas-exchange rates including direct injection of a semi-inert gas (Rathbun et al. 1978, Kilpatrick et al. 1989, Wanninkhof et al. 1990) and empirical relationships based on hydraulic parameters (Palumbo and Brown 2013). Other methods estimate gas-exchange rates from attributes of a time series of dissolved $O_2$ (*DO*). For example, the nighttime regression method (Hornberger and Kelly 1975) estimates the aeration coefficient of $O_2$ ($K_{DO}$) from the change in DO during nighttime in relation to the change in $O_2$ saturation deficit ($DO_{def}$) when the influence of *GPP* can be neglected. Others use the offset in time between the DO maximum and the solar maximum to estimate $K_{DO}$ (the delta method; (Chapra and Di Toro 1991). Multiparameter inverse models that optimize model parameters, including *CR*, *GPP* and $K_{DO}$, have been applied to fit observed DO time series (Holtgrieve et al. 2010, Riley and Dodds 2013, Birkel et al. 2013).

Of the above methods, all but direct gas injection generally are considered inadequate for studies of stream metabolism in well-aerated streams. Even top-performing empirical relationships to hydraulic parameters applied over a wide range of stream velocities and depths have expected errors of 40 to 50% (Palumbo and Brown 2013). Gas-transfer rates from other indirect methods have similar errors with median discrepancies of 65% between measured and modeled values (Riley and Dodds 2013, Demars et al. 2015). Indirect techniques perform best in productive waters with relatively low aeration rates, and assume substantial lengths of homogenous stream conditions (Chapra and Di Toro

1991, Reichert et al. 2009). For less productive waters, streams with high rates of gas transfer, or heterogeneous reach conditions, indirect methods are generally considered inadequate, and the aeration rate typically is measured through direct gas injection (Bott 2006). However, direct gas injection generally results in a point measurement of the aeration rate representative of conditions at the time of the injection. For prolonged studies under varying hydrologic conditions, multiple gas injections must be made over the range in stream discharge (Roberts et al. 2007). This requirement is logistically challenging and time consuming, so an alternative but robust method to estimate gas-exchange rates is of continued interest.

We present a new approach to measure aeration and stream metabolic rates continuously through the simultaneous measurement of DO and $CO_2$ at an upstream and downstream station. A few investigators have used inorganic C to estimate stream metabolism in rivers (Wright and Mills 1967, Kelly et al. 1974, 1983, Thyssen and Kelly 1985, Crawford et al. 2014), but DO data generally have been used for better accuracy and ease of continuous measurement. Relatively new technology that enables direct measurement of dissolved $CO_2$ at an affordable price is now available and continuous dissolved $CO_2$ can be measured at comparable cost and accuracy to DO (Johnson et al. 2010, Yoon et al. 2016). Simultaneous measurement of DO and $CO_2$ allows direct computation of continuous gas-transfer rates, and stream metabolism by independent data sets. We termed this method the oxygen carbon method (OC method), and it is applicable to streams where assumptions of the 2-station method are valid, and both: 1) measurable offset in combined dissolved gas concentration ($\Delta DO + \Delta\ CO_2$) is present and 2) measurable combined saturation deficit ($CO_2$ saturation deficit + DO saturation deficit) is present. See Table 2.1 for a complete list of variable definitions.

Table 2.1 – Variable definitions.

| Variable | Description | Units |
|---|---|---|
| DO | Dissolved $O_2$ in stream | mol/$L^3$ |
| $DO_l$ | Dissolved $O_2$ of lateral inflow (soil and groundwater) | mol/$L^3$ |
| *DIC* | Total dissolved inorganic C in stream | mol/$L^3$ |
| $DIC_l$ | Total dissolved inorganic C of lateral inflow (soil and groundwater) | mol/$L^3$ |
| $CO_2$ | Dissolved $CO_2$ in stream | mol/$L^3$ |
| $DO_{def}$ | Dissolved $O_2$ deficit | mol/$L^3$ |
| $CO_{2def}$ | Dissolved $CO_2$ deficit | mol/$L^3$ |
| *EC* | Electrical conductivity | µS/cm |
| *t* | Time | T |
| τ | Mean travel time through reach | T |
| *L* | Reach length | L |
| *z* | Mean water depth | L |
| *w* | Mean width | L |
| *p* | Wetted perimeter | L |
| *A* | Stream bed area | $L^2$ |
| $A_x$ | Cross-sectional area | $L^2$ |
| *v* | Stream velocity | L/T |
| *Q* | Stream discharge | $L^3$/T |
| $Q_l$ | Lateral inflow | $L^3$/T |
| *D* | Longitudinal dispersion | $L^2$/T |
| $q_l$ | Lateral inflow per unit stream length | $L^2$/T |
| *SF* | Spatial factor for computation of optimal reach length | – |
| *E* | Measurement error | mol/$L^3$ |
| $K_c$ | Coefficient of gas transfer for gas *c*. Subscript may be DO, $CO_2$, propane, or left as *c* if unspecified. | 1/T |
| $K_{600}$ | Coefficient of gas transfer for $O_2$ at 17°C | 1/T |
| $K_v$ | Gas transfer velocity | L/T |
| *n* | Exponent for calculation of β from *Sc* | – |
| *Sc* | Schmidt number, relation of viscosity to molecular diffusion | – |
| β | Ratio of $K_{CO2}$ to $K_{DO}$ | – |
| *IAP* | Ion activity product | – |
| *SI* | Saturation index | – |
| $K_{sp}$ | Solubility constant | – |
| *NEP* | Net ecosystem production measured as amount of $O_2$ produced | M $L^{-2}$ $T^{-1}$ |
| *CR* | Community respiration measured as amount of $O_2$ produced | M $L^{-2}$ $T^{-1}$ |

| | | |
|---|---|---|
| *G* | Gross primary productivity measured as amount of $O_2$ produced | M $L^{-2}$ $T^{-1}$ |
| *RQ* | Respiratory quotient measured as amount of $CO_2$ released to $O_2$ absorbed | – |
| *PQ* | Photosynthetic quotient measured as amount of $O_2$ released to $CO_2$ absorbed | – |

## *2.3 Methods*

### *2.3.1 Theory*

The DO concentration in a well-mixed river can be modeled with a 1-dimensional solute-transport equation adapted from (Bencala and Walters 1983) to include 1st-order gas transfer with the atmosphere and stream metabolism source and sink terms. The equation accounts for fluxes in and out of an infinitesimally thin, yet entirely well-mixed, cross-section of water considering dispersion (longitudinal mixing), advection (stream flow), lateral inflow (groundwater), aeration, and stream metabolism:

Dispersion Advection Lateral inflow Aeration Stream metabolism

$$\frac{\partial DO}{\partial t} = \frac{1}{A_x}\frac{\partial}{\partial x}\left(A_x D \frac{\partial DO}{\partial x}\right) - \frac{Q}{A_x}\frac{\partial (DO)}{\partial x} + \frac{q_l}{A_x}(DO_l - DO) + \frac{w\,K_v\,DO\_def}{A_x} + \frac{(GPP+CR)\,p}{A_x} \qquad \text{(Eq. 1)}$$

where $A_x$ is the stream channel cross-sectional area, $D$ is dispersion, $Q$ is discharge, $q_l$ is lateral inflow of groundwater and hillslope water per unit stream length, $w$ is stream width, $K_v$ is gas transfer velocity, and $p$ is wetted perimeter ($\approx w$ for shallow channels).

Equation 1 is simplified by assuming that the influence of dispersion is negligible, a nearly ubiquitous assumption in stream metabolism and aeration studies (Knapp et al. 2015). Hensley and Cohen (2016) questioned this assumption through the analysis of a low-gradient spring-fed river, but found that estimates of the influence of dispersion were orders of magnitude less than the influence of aeration or metabolic fluxes at a high-gradient study site. The $wK_v/A_x$ term is substituted by $K_{DO}$, and $p/A_x$ is approximated by the average depth ($z$).

$$\frac{\partial DO}{\partial t} = -v\frac{\partial DO}{\partial x} + \frac{q_l}{A_x}(DO_l - DO) + K_{DO}DO_{def} + \frac{(GPP+CR)}{z} \quad \text{(Eq. 2)}$$

The above partial differential equation is transformed using the method of characteristics into an ordinary differential equation in Lagrangian coordinates (Eq. 3), whereby one can envision moving downstream with a volume or parcel of water (Fischer 1972). In the Lagrangian frame of reference, all aspects of a volume of water, including chemistry, are a function of time, not space.

$$\frac{\Delta DO}{\tau} = \frac{Q_l}{zA}(DO_l - DO) + K_{DO}\,DO_{def} + \frac{(GPP+CR)}{z} \quad \text{(Eq. 3)}$$

An Euler approximation is also made by substituting $\partial t$ with τ, the mean travel time through the reach. ΔDO represents the change in DO from the upstream to downstream end of a study reach. $q_l/A_x$ when scaled up from a thin cross-channel section to an entire reach is equivalent to $Q_l/zA$ where $Q_l$ is total lateral inflow into the reach and $A$ is total stream bed area. Equation 3 is consistent with equations for stream metabolism with groundwater inflow by Hall and Tank (2005).

We developed a transport model of dissolved inorganic C (DIC) similar to the DO model in Eq. 3 and consistent with that formulated by Kelly et al. (1974):

$$\frac{\Delta DIC}{\tau} = \frac{Q_l}{zA}(DIC_l - DIC) + K_{CO_2}CO_{2_{def}} - \frac{\left({}^{GPP}/_{PQ} + RQ\ CR\right)}{z} \quad \text{(Eq. 4)}$$

In this equation, the aeration flux is driven by the $CO_2$ saturation deficit ($CO_{2def}$), but concentration is DIC. DIC includes dissolved $CO_2$ gas, $H_2CO_3$, $HCO_3^-$, and $CO_3^{2-}$. We collectively refer to dissolved $CO_2$ gas and $H_2CO_3$ as $CO_2$. The respiratory quotient (*RQ*) is the molar ratio of $CO_2$ released to $O_2$ used in respiration. The photosynthetic quotient (*PQ*) is the molar ratio of $O_2$ released to $CO_2$ used in photosynthesis. In the production or metabolism of simple carbohydrates *PQ* and *RQ* are both 1. For other organic molecules, *RQ* and *PQ* are generally assumed to range from 0.8 to 1.2 (del Giorgio and Williams 2005), and Bott (2006) recommended a value of 0.85 for *RQ* and 1.2 for *PQ*. The reciprocal of 0.85 is 1.18, a value quite close to 1.2. Therefore, we assume ${}^1/_{PQ} = RQ$.

$$\frac{1}{RQ}\frac{\Delta DIC}{\tau} = \frac{1}{RQ}\frac{Q_l}{zA}(DIC_l - DIC) + \frac{1}{RQ}K_{CO_2}CO_{2def} - \frac{(GPP + CR)}{z} \quad \text{(Eq. 5)}$$

In pursuit of the aeration rate, and after rearranging to solve for the stream metabolism term $\frac{(GPP+CR)}{z}$, Eq. 5 for DIC transport is combined with the transport equation for DO (Eq. 3), and the stream metabolism terms cancel out:

$$\frac{\frac{\Delta DIC}{RQ}+\Delta DO}{\tau} = \frac{Q_l}{zA}\left(\frac{(DIC_l - DIC)}{RQ} + DO_l - DO\right) + K_{DO}\left(\frac{\beta}{RQ}CO_{2_{def}} + DO_{def}\right) \quad \text{(Eq. 6)}$$

The coefficient β relates $K_{DO}$ to $K_{CO2}$. The gas-transfer velocity of 2 gases is commonly related by a friction–velocity model (Bennett 1972, Jähne et al. 1987).

$$\beta = \frac{K_{CO2}}{K_{DO}} = \left(\frac{Sc_{CO2}}{Sc_{DO}}\right)^{-n} \quad \text{(Eq. 7)}$$

Temperature-dependent Schmidt numbers (*Sc*) can be calculated from regression coefficients provided by Raymond et al. (2012).

Equation 6 is rearranged to solve for $K_{DO}$. The resulting equation (Eq. 8) is the generalized form of the OC method and includes a change term, a lateral inputs term, and deficit term.

Change term Lateral inputs term Deficit term

$$K_{DO} = \left(\frac{\frac{\Delta DIC}{RQ}+\Delta DO}{\tau} - \frac{Q_l}{zA}\left(\frac{(DIC_l - DIC)}{RQ} + DO_l - DO\right)\right) \Big/ \left(\frac{\beta}{RQ}CO_{2_{def}} + DO_{def}\right) \quad \text{(Eq. 8)}$$

The temporal resolution of the input variables will define the temporal resolution of the output. A continuous estimate of $K_{DO}$ is made with time series of DO, DIC, and $CO_2$ and estimates of hydraulic and geometric terms (that may generally be related to stream discharge). However, Eq. 8 also could be used with point measurements of DO, DIC and $CO_2$ in time, in which case the output would consist of discrete point estimates of $K_{DO}$.

The ratio of the lateral inputs term to the longitudinal change in concentrations term of Eq. 8 can be used to assess the relative importance of groundwater/hillslope water to

estimates of $K_{DO}$ from OC. If this ratio is <~10%, Eq. 8 may be simplified by assuming that lateral inflows and outflows are negligible:

Change term Deficit term

$$K_{DO} = \left(\frac{\frac{\Delta DIC}{RQ}+\Delta DO}{\tau}\right) \Big/ \left(\frac{\beta}{RQ} CO_{2def} + DO_{def}\right) \quad \text{(Eq. 9)}$$

However, the value of the lateral inputs term may be difficult to define because both the inflow rate and chemistry of groundwater are often poorly constrained.

In low-alkalinity waters (alkalinity < 500 μeq/L), common in geologic settings without limestone and other carbonate type rocks, common in geologic settings without limestone and other carbonate type rocks, ΔDIC can be substituted by $\Delta CO_2$. This substitution is possible because the relation of $CO_2$ to *DIC* is a nearly 1:1 over a large range of $CO_2$ concentrations (see supplemental information). $\frac{\Delta DIC}{\Delta CO_2}$ is ~1 for low-alkalinity water, particularly at higher $CO_2$ concentrations. However, for waters with alkalinity >500 μmol/L, we do not recommend substituting $\Delta CO_2$ for ΔDIC. Under these circumstances *DIC* should be measured or calculated from 2 of the following concentrations: *pH,* $CO_2$, alkalinity, $HCO_3^-$, and $CO_2^{3-}$(Stumm and Morgan 1996). However, practical challenges exist to collection of accurate carbonate chemistry data.

Further caution is recommended for streams draining watersheds with abundant carbonate type rocks, or clastic rocks with carbonate cement that may result in waters being at or near saturation with respect to calcite, aragonite, dolomite, and other carbonates. At such sites, changes in dissolved $CO_2$ and DIC through the reach may occur not only from repartitioning of inorganic carbonate species, stream metabolism, and aeration, but also from precipitation and dissolution (Barnes 1965, Spiro and Pentecost 1991). Tobias and Böhlke (2011) found that 40% of US Geological Survey stream-monitoring stations in the contiguous USA were at or above the equilibrium saturation state for calcite. The OC method, as formulated in our study, should not be applied for water at or above solid-phase saturation. Under continuously or intermittently saturated conditions with respect to solid-phase carbonates, additional kinetic terms for precipitation

and dissolution are necessary (Lorah and Herman 1988, de Montety et al. 2011, Tobias and Böhlke 2011, Khadka et al. 2014).

### *2.3.2 Study site*

The study was conducted at a 60-m-long study reach on McRae Creek in the H. J. Andrews Experimental Forest and Long-Term Ecological Research (LTER) site, Oregon, USA (HJA) during baseflow conditions. The reach had a slope of 3%, boulder and cobble substrate, contributing drainage area of 15.3 $km^2$, and site elevation of 560 m. The study reach was selected with the expectation that complicating factors including lateral inflow was small. No distinct cascades or riffles were present, and the stream could be classified as plane-bed (Montgomery and Buffington 1997). Abundant riparian forest of alder and mixed conifer provided roughly 30% shade to the channel at midday. Water was of low alkalinity and low ionic strength with a background electrical conductivity (EC) of ~30 μS/cm. The bedrock of the catchment is entirely volcanic in origin with no mapped carbonate rocks units (Swanson and James 1975).

### *2.3.3 Measurements*

We conducted stream metabolism measurements 11–14 August 2015 by monitoring DO and $CO_2$ concentrations upstream and downstream following the 2-station open-channel method (Marzolf et al. 1994, 1998, Young and Huryn 1998). We conducted a constant-rate coinjection of NaCl tracer and propane gas on 11 August 2015. We calculated discharge, mean travel time, and mean velocity from the conservative-tracer breakthrough curves (Kilpatrick and Cobb 1985) with EC as a surrogate for concentration (see supplemental information in Appendix A). We measured wetted channel width at 10 locations evenly spaced through the reach, and averaged measurements to give mean channel width. On day 1 of the study, we collected 2 replicate 250-mL water samples at the top and bottom of the reach for alkalinity analysis (see supplemental information in Appendix A).

We measured and logged EC, $CO_2$ concentration, DO, and temperature, at the upstream and downstream end of the reach with WTW (Weilheim, Germany) Cond 3310 meters (EC), modified Vaisala (Vantaa, Finland) Carbocap GMM220 $CO_2$ sensors (Johnson et al. 2010) wired to Campbell Scientific (Logan, Utah) data loggers ($CO_2$) and YSI 600 OMS-V2 sondes (model 6150 ROX DO; Yellow Springs Instruments, Yellow springs, Ohio; DO and temperature). We attached sensors to the bottom of floats to maintain a consistent water depth. We calibrated sensors in the laboratory before and after deployment to check for drift and cross-calibrated them in the field to check for differences between sensors (see Appendix A). No sensor drift was observed through the measurement period.

We calculated $O_2$ saturation for each time step according to equations detailed by Weiss (1970) and used barometric pressure recorded at the HJA PriMet station (4.9 km down-valley at 430 m asl) and transformed to the elevation of the study reach (560 m asl) (US Geological Survey 1981). $CO_2$ data were post-processed and converted to partial pressure $CO_2$ ($pCO_2$) according to barometric pressure, water temperature, and water depth per Johnson et al. (2010).

We calculated DIC and $CO_2$ from the continuous record of $pCO_2$ and mean alkalinity of point samples with CO2SYS (version 1.1; coded in Matlab; Lewis and Wallace 1998) and temperature-dependent equilibrium constants published by Millero (1979). To estimate dissolved $CO_2$ at saturation, necessary to compute $CO_{2def}$, we assumed a constant value of 400 μatm for atmospheric $CO_2$ concentration, equal to the global annual mean $CO_2$ concentration for 2015 (NOAA 2016).

### *2.3.4 Assumptions and model validation*

We calculated $K_{DO}$ by the OC method with Eq. 9, which assumes negligible lateral inputs of groundwater. Potential bias related to this assumption was explored.

To validate the estimated, we measured the gas-transfer coefficient independently of the OC method by co-injecting propane gas into the stream with an air-stone and a salt

tracer to correct for dilution. We collected 6 gas samples at each of 3 stations along the reach during steady-state and analyzed them within 24 h on an Agilent (Santa Clara, California) 7890A gas chromatograph system. We calculated the value of the gas-transfer coefficient for propane ($K_{propane}$) from the decline in dilution-adjusted propane concentration following Tsivoglou and Neal (1976) and Kilpatrick et al. (1989):

$$K_{propane} = \frac{1}{\tau} ln \left[\frac{Propane_{upstream} EC_{downstream}}{Propane_{downstream} EC_{upstream}}\right] \quad \text{(Eq. 10)}$$

We used Eq. 7 and the *Sc* calculated from regression coefficients provided by Raymond et al. (2012) to convert $K_{propane}$ to $K_{DO}$. $K_{DO}$ was converted to $K_{600}$, the aeration coefficient of $O_2$ at 17°C when water has a *Sc* value of 600, by Eq. 7 and temperature-dependent *Sc* from regression coefficients provided by Raymond et al. (2012).

To ensure that stream water was under saturated with respect to carbonate minerals, we calculated calcite ($CaCO_3$) and dolomite ($CaMg(CO_3)_2$) saturation indices using solubility constants (*Ksp*) published by Plummer and Busenberg (1982) and Sherman and Barak (2000), respectively. The saturation index (SI) of a given mineral is equal to the logarithm of the ratio of the ion activity product (IAP) to the mineral's *Ksp*. A positive SI indicates the mineral is oversaturated and precipitation is thermodynamically favored, whereas a negative SI indicates that the mineral is undersaturated and the dissolution of the mineral is thermodynamically favored. IAP at low concentrations is approximated by the product of concentrations (e.g., for calcite, IAP = $[Ca^{2+}][CO_3^{2-}]$). We obtained $[Ca^{2+}]$ and $[Mg^{2+}]$ during August 2015 from the HJA long-term chemistry data set at Lookout Creek (Johnson and Fredriksen 2016).

To check whether our assumption of a constant *RQ* = 0.85 was reasonable, we rearranged Eq. 9 to solve for *RQ* and used $K_{DO}$ obtained from direct gas injection:

$$RQ = \left(\tau \beta K_{DO} CO_{2def} - \Delta DIC\right) / \left(\Delta DO - \tau K_{DO} DO_{def}\right) \quad \text{(Eq. 11)}$$

To check whether our assumption of constant 400 µL/L atmospheric $CO_2$ was reasonable, we rearranged Eq. 9 to solve for $CO_{2def}$, then converted $CO_{2def}$ to partial pressure atmospheric $CO_2$.

### *2.3.5 Error analysis*

We used a Monte-Carlo approach to estimate the confidence intervals of modeled $K_{DO}$ based on the OC method. For each input parameter and constant of the Monte-Carlo model, we estimated a 95% confidence interval (CI). DO and $CO_2$, temperature, and travel time were all given an error of 1%. Atmospheric $CO_2$, alkalinity, and β values were given an error of 5%, and *RQ* was given an error of 10%. We assumed variables were normally distributed and independent. We assumed errors were systematic, rather than random. For time series with thousands of data points, random errors (noise) tend to be insignificant to summary results. In contrast, systematic errors can alter summary results substantially (Birnbaum et al. 1967, Kadmon et al. 2003). A systematic error of +1% for temperature means that all values of temperature in the time series are 1% higher than the measured value for that model run. We coded model equations in Matlab and evaluated 10,000 model runs. The model calculated and saved $K_{DO}$ for each time-step of each run. After all model runs were complete, 2.5, 50, and 97.5 percentiles from the results were computed for each time-step to estimate the $K_{DO}$ 95% CI.

### *2.3.6 Analysis of sensitivity to site conditions*

To create a rough guideline for application of the OC method, we performed a sensitivity analysis of the OC method to the longitudinal change in the combined DO and DIC concentrations through the study reach and to the reach-averaged combined DO and $CO_2$ deficits. We used simple rules of error propagation for addition and division on Eq. 9 and assumed error was primarily attributed to measurement errors of DO and $CO_2$. For a more complete error analysis, we advise using a Monte-Carlo method based on site-specific data and error distributions of all input parameters (discussed above). We assumed that CIs were ~±0.1 µatm for DO and ±20 µatm $CO_2$. When converted into consistent molar units, error ($E$) for both the combined longitudinal change in concentrations (ΔDIC + ΔDO) and combined deficit ($CO_{2def} + DO_{def}$) terms were ~4 µmol/L. We approximated the % error of $K_{DO}$ by the OC method as:

$$\%\ \text{error}\ K_{DO}\ \text{by OC} \approx 100\left(\frac{E}{\Delta DIC+\Delta DO} \pm \frac{E}{CO_{2def}+DO_{def}}\right) \quad \text{(Eq. 12)}$$

For the purpose of considering where best to apply the OC method, we calculated % error by Eq. 12 over a range of possible reach conditions.

### *2.3.7 Stream metabolism*

We calculated NEP with the 2-station open-channel method, accounting for the influence of lateral inflow (Odum 1956, Marzolf et al. 1994, 1998, McCutchan et al. 2002, Hall and Tank 2005), assuming that $CR_{nighttime} = NEP_{nighttime}$ and that $CR_{nighttime} = CR_{daytime}$. We applied various combinations of aeration-rate and stream-chemistry data, including $K_{DO}$ from propane injection with either DO or carbonate data sets or $K_{DO}$ from OC with either DO or carbonate data sets.

Aeration/advection Lateral inputs

$$NEP_{from\ DO} = z\left(\frac{\Delta DO}{\tau} - K_{DO}\ DO_{def}\right) - \frac{Q_l}{A}(DO_l - DO) \quad \text{(Eq. 13)}$$

or

$$NEP_{from\ carbon} = \frac{\left[-z\left(\frac{\Delta DIC}{\tau} - K_{CO2}\ CO_{2\,\mathrm{def}}\right) + \frac{Q_l}{A}(DIC_l - DIC)\right]}{RQ} \quad \text{(Eq. 14)}$$

We calculated instantaneous *NEP* for each 5-min time step. For summary results, we averaged instantaneous *NEP*, *CR*, and *GPP* for each day, then over the 4-d period.

We generally assumed that lateral inflows were 0, but we used the ratio of the lateral inputs term to aeration/advection to explore the potential influence of lateral inflows on *NEP* estimates.

## *2.4 Results*

### *2.4.1 Hydraulic conditions*

Our study was conducted during steady summer baseflow conditions over a 72 h period (11–14 August 2015). Dilution gauging on August 11 measured *Q* as 17.0 L/s at the

downstream end of the 60 m long reach and 17.7 L/s at a point 140 m farther downstream. Day (1976) found that median errors for dilution gauging ranged from 4.7 to 7.3%. Thus, measured increase in streamflow of 4% over the 140-m distance was within the error of *Q* measurements. Median travel time between the upstream and downstream DO and $CO_2$ sensors was 13.7 min, median channel width was 4.5 m, and mean depth was 5.2 cm. No precipitation events occurred over the study period, nor had any rain fallen for weeks prior to the experiment, resulting in steady flow conditions through the study period. US Geological Survey gauging station 14161500, 5 km downstream of the study site on Lookout Creek, recorded no change in streamflow through the study period. Thus, hydraulic conditions for 11–14 August were well-represented by the 11 August propane/solute injection.

We calculated a dimensionless spatial factor ($SF = LK_{DO}/v$), where *L* was reach length, to assess the potential influence of *L* and spatial heterogeneity on our results (Reichert et al. 2009). Optimum reach lengths have *SF* values between 0.4 and 1. Applying the aeration rate from direct gas injection (2.88 L/h; see below) we estimated $SF = 0.66$, indicating effective station spacing.

### *2.4.2 Time-series data*

Time-series data for temperature, solar radiation, DO, $CO_2$, and DIC showed expected diel fluctuations (Figure 2.1A–C), but % saturation of $CO_2$ was high compared to DO (Figure 2.1B). DO curves roughly resembled incoming solar radiation with a defined peak near solar noon close to 100% saturation and a broad, flat trough through the night at ~95% saturation (Figure 2.1A, B). $CO_2$ and DIC concentration curves followed an inverse DO pattern, and unlike DO, concentrations were far from saturation with the atmosphere (Figure 2.1C). $CO_2$ concentrations ranged between 250 and 450% saturation, and at midday, when DO was near equilibrium with the atmosphere, $CO_2$ was at a minimum but still well above saturation.

DO concentration was consistently higher upstream than downstream with a mean offset of 1.7 μmol $O_2$/L (0.05 mg $O_2$/L), but this apparent offset was within sensor error. $CO_2$ and DIC concentrations were consistently higher up- than downstream with a mean

offsets of 14.4 µmol C/L (0.17 mg C/L) and 14.6 µmol C/L (0.17 mg C/L), respectively, which were an order of magnitude larger than the observed change in DO. Changes in $CO_2$ and DIC were nearly identical, an expected result given the low alkalinity and relatively high $CO_2$ concentration of the stream (Figures A.1 and A.2).

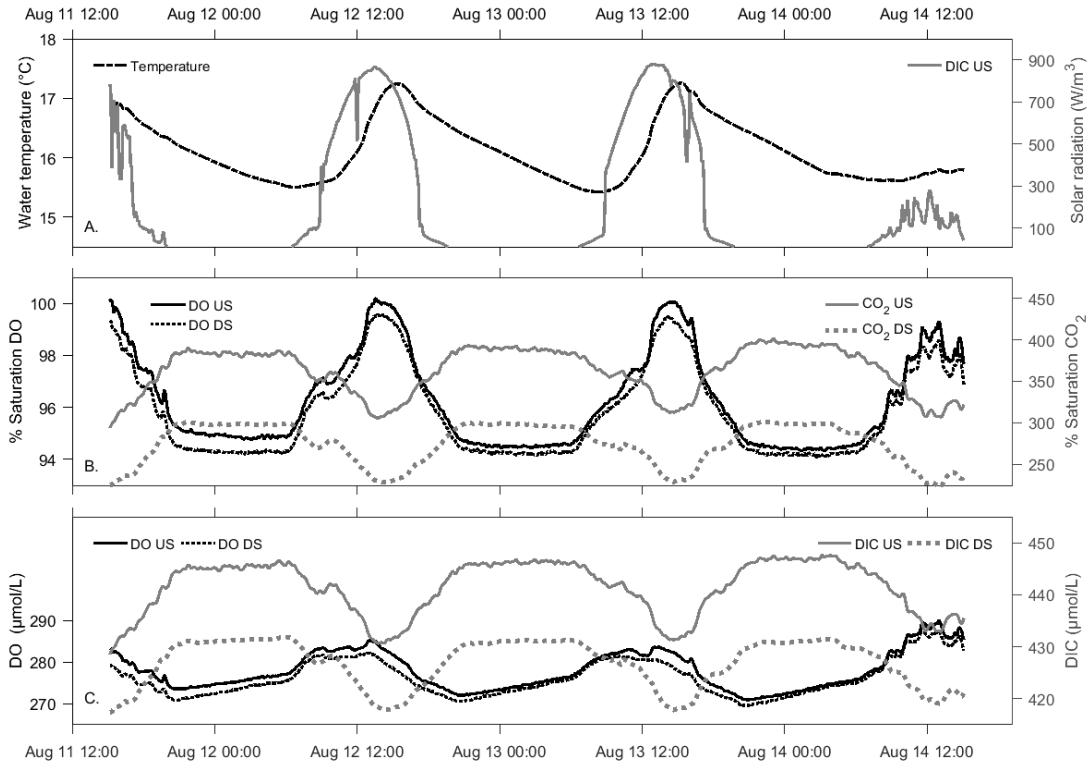


Figure 2.1 – Upstream (US) and downstream (DS) changes in water temperature, solar radiation, and streamflow (A); dissolved $O_2$ (DO) and $CO_2$ saturation (B); and DO and dissolved inorganic C (DIC) concentration (C). Water temperature has a diel fluctuation that lags behind incoming solar radiation. $CO_2$, DO, and DIC curves follow expected diel patterns attributable to photosynthesis and respiration. Note the large change in DIC from upstream to downstream compared with change in DO. This difference in behavior is necessary to constrain errors of the oxygen carbon (OC) method.

### *2.4.3 Aeration rates and model validation*

Based on our estimates of uncertainty, we found no meaningful differences between aeration estimates from the OC method and direct tracer-addition studies (Figure

2). $K_{600}$ from propane injection was 3.2/h ± 1.2%, whereas mean estimated $K_{600}$ from OC was 3.3/h ± 0.7% (Figure 3A). The mean estimates were nearly identical and well within confidence bounds. Instantaneous estimates of $K_{600}$ by OC showed a clear diel fluctuation of ~30% (0.7/h). The values had a repeating diel structure with a steady value through the night, a minimum near solar noon, and a maximum in late afternoon.

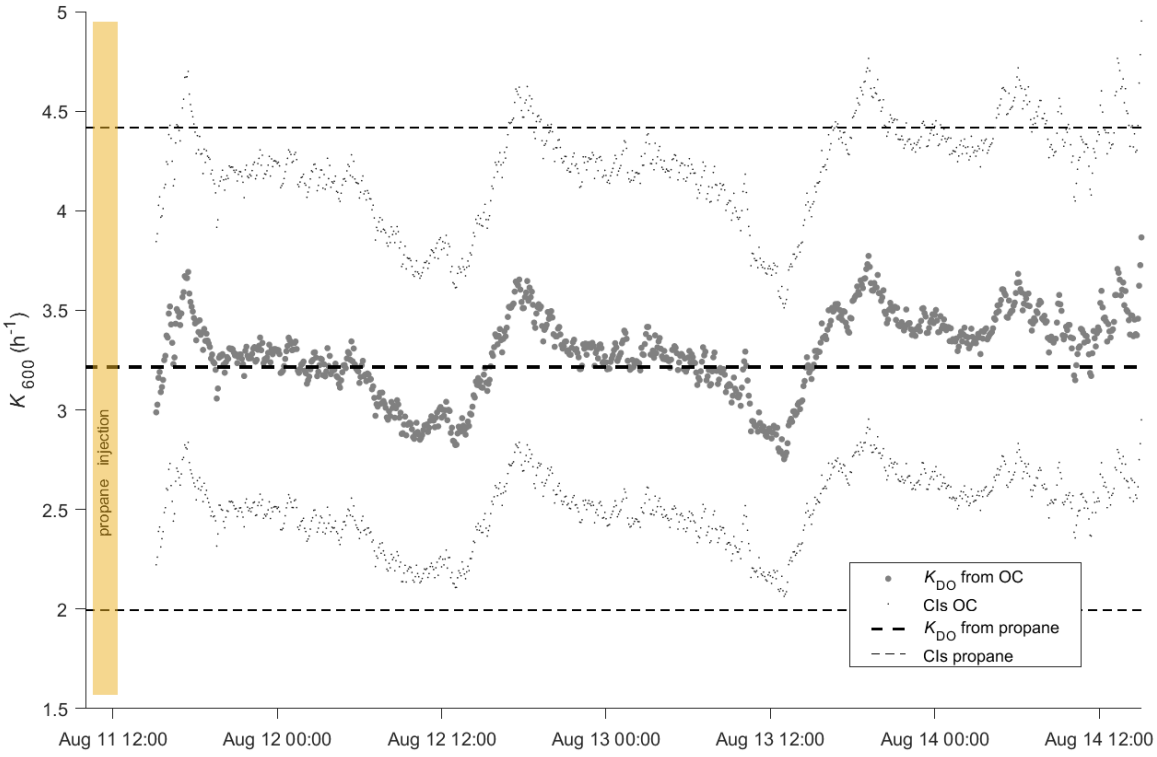


Figure 2.2 – Mean (95% CI) K600 (aeration coefficient of $O_2$ [KDO] corrected to 17°C) from the oxygen carbon (OC) method and from propane injection. K600 from propane is extrapolated from a 1.5-h steady-state gas injection that was performed prior to the beginning of the time series conducted on 11 August. Estimates of K600 by the two methods are in general agreement. However, the diel structure of the OC method indicates that transient factors, such as wind, are important to the diel signal or assumed constants (respiratory quotient, photosynthesis quotient, and atmospheric $CO_2$) change through the day and affect modeled aeration rates.

Alkalinities measured from samples collected 11 August at the up- and downstream ends of the study reach were equal (382 µeq/L). EC was relatively steady through the study period (±2 µS/cm), and we assume that alkalinity was constant through the study period

because of the strong correlation between alkalinity and EC for streams at the HJA ($R^2$ = 0.95 for Lookout Creek; Johnson and Fredriksen 2016). Nevertheless, we built a 5% error for alkalinity into the error analysis.

Calcite and dolomite concentrations were well below equilibrium saturation state ($SI$ = –1.57 and –2.6, respectively). The bedrock of the HJA is entirely volcanic, with low rates of chemical weathering relative to water-residence time (Fredriksen et al. 1983). The apparent result that solute concentrations are below equilibrium saturation states supports the assumption that precipitation and dissolution fluxes are negligible in regard to reach-scale processes.

We calculated $RQ$ for every time step based on $K_{DO}$ from the propane injection and ambient $CO_2$ (400 μatm; Figure 3B). The mean calculated $RQ$ was 0.83 and the median was 0.81, suggesting that the assumed value of 0.85 was generally appropriate. However, calculated $RQ$ presented diel fluctuations. $RQ$ was ~0.85 through the night, rose rapidly to a maximum of 1.5 near midday, when $K_{600}$ based on the OC method was at a minimum, and dropped to a minimum of ~0.6 around 1800 h, when $K_{600}$ by the OC method was at a maximum.

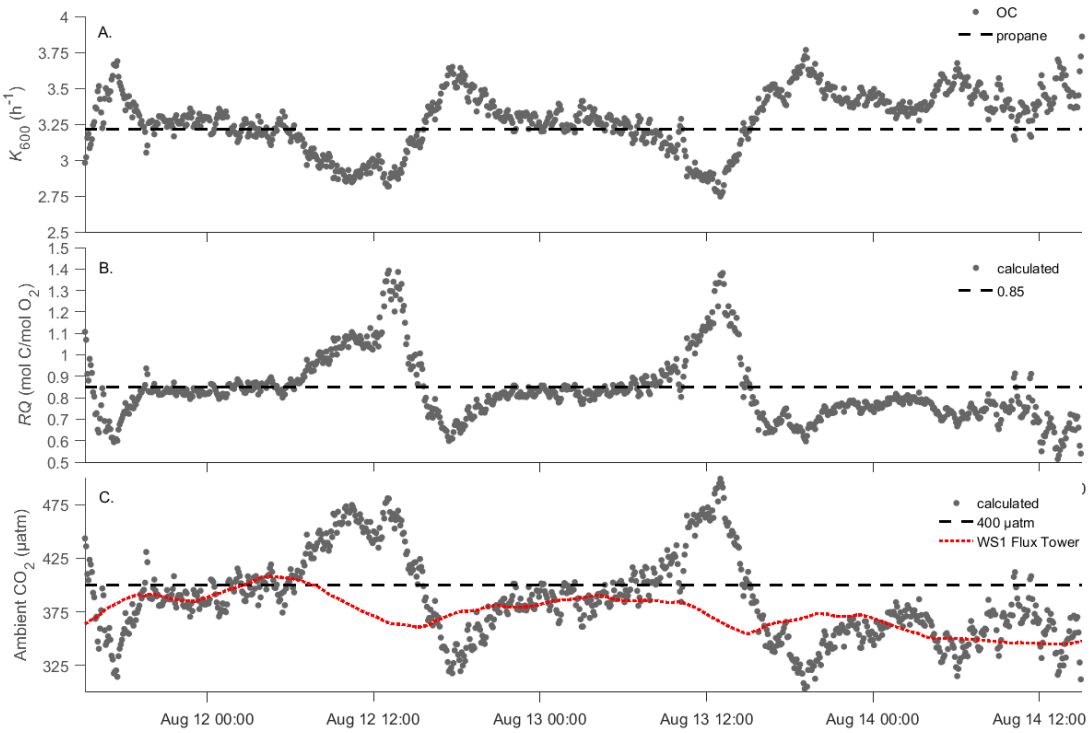


Figure 2.3 – Calculated timeseries of $K_{600}$, *RQ*, and atmospheric $CO_2$. Plot A. – $K_{600}$ (aeration coefficient of $O_2$ [$K_{DO}$] corrected to 17°C) from the oxygen carbon (OC) method, calculated assuming a respiratory quotient (*RQ*) = 0.85 and atmospheric $CO_2$ = 400 µL/L, demonstrating diel structure with minimum near midday and maximum in later afternoon. Plot B. – *RQ* calculated assuming constant $K_{DO}$ from propane injection and atmospheric $CO_2$ = 400 µatm. Calculated *RQ* had a diel structure with large maximum through the day and minimum in late afternoon. Given that hydraulic conditions were steady and calculated $CO_2$ was inconsistent with measured values, we suspect diel structure of $K_{600}$ was related to variation in metabolic rates and parameters, including *RQ*. Plot C – Atmospheric $CO_2$ calculated assuming a constant $K_{DO}$ from propane injection and *RQ* = 0.85. Also shown is atmospheric $CO_2$ concentration measured at the flux tower at Watershed 1, H. J. Andrews Experimental Forest. The calculated and measured values were in general agreement at night, but deviated substantially during the day.

Calculated atmospheric $CO_2$ followed a similar pattern (Figure 3C). The calculated $CO_2$ remained close to 385 µatm through the first 2 nights, with peaks of up to 500 µatm near midday, when $K_{600}$ by the OC method was at a minimum. After the midday peak, calculated ambient $CO_2$ dropped to a minimum of ~325 µatm at ~1800 h. The mean calculated ambient $CO_2$ was 386 µatm and median was 382 µatm, suggesting the assumed

value of 400 μatm was ~15 μatm too high. Measured $CO_2$ concentrations at Watershed 1, HJA, a tributary stream 5 km downstream, showed similar concentrations.

### *2.4.4 Method sensitivity to site conditions*

We tested model sensitivity to longitudinal change in combined $CO_2$ and DO, and combined $CO_2$ and DO saturations deficits to help define suitable conditions for application of the OC method (see Eq.12). When either the combined change or the combined deficit was ≤~4 μmol/L, the 95% CI in modeled $K_{DO}$ increased rapidly to values >100% (Figure 1.4). The study reach selected for this proof-of-concept study had a large longitudinal change in DIC (mean = 14.6 μmol C/L or 350 μatm) compared with change in DO (mean = 1.7 μmol $O_2$/L). The mean combined change in DO + DIC was 16.0 μmol/L. The mean combined deficit was 25 μmol/L. Thus, the study reach was well suited for the OC method with a 95% CI = ~41% according to Eq. 12. This value was higher than estimated through our Monte-Carlo analysis (22%).

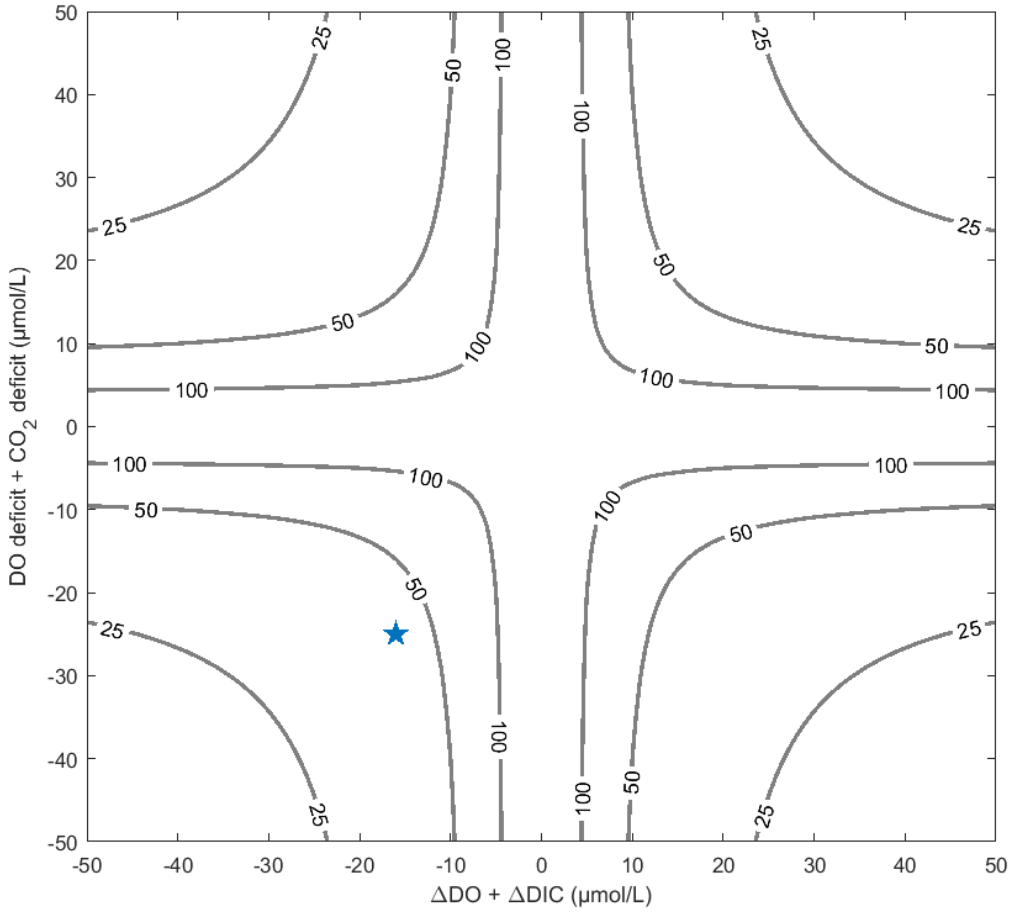


Figure 2.4 – Approximate % error for KDO (aeration coefficient of $O_2$) by the oxygen carbon (OC) method contoured over a range of possible combined gas gradients (x-axis) and combined gas deficits (y-axis). Errors are >100% if either the combined change or the combined deficit term is <~4 µmol/L. The star indicates average conditions for our study.

### *2.4.5 Stream metabolism*

Stream metabolic metrics estimated for various combinations of aeration rates with DO and $CO_2$ data sets were relatively consistent (Table 2). All estimates of *NEP* were negative, indicating the reach was net heterotrophic. Ranges were –1.56 to –1.69 g $O_2$ $m^{-2}$ $d^{-1}$ for *NEP*, –2.00 to –2.15 g $O_2$ $m^{-2}$ $d^{-1}$ for *CR*, and 0.44 to 0.46 g $O_2$ $m^{-2}$ $d^{-1}$ for *GPP*. Note that stream metabolic rates based on $K_{DO}$ from the OC method gave identical results

regardless of whether DO or $CO_2$ data sets were used. This result is inherent to the OC method, which solves for aeration rate by canceling out the stream metabolism terms.

Table 2.2 – Mean stream metabolism estimates for the period 11–14 August obtained by 4 different combinations of data. Positive values indicate production of $O_2$, and consumption of C. KDO from the propane injection and instantaneous values calculated from the OC method were applied independently to DO and $CO_2$ time series. Estimates from $CO_2$ time series assume RQ = 1/PQ = 0.85. Stream metabolism rates of NEP, CR, and GPP are in general agreement by all pairs of data and applied gas exchange rate. See Table 1 for abbreviations.

| Aeration rate origin | Time series used as input | *NEP* (g $O_2$ $m^{-2}$ $d^{-1}$) | *CR* (g $O_2$ $m^{-2}$ $d^{-1}$) | *GPP* (g $O_2$ $m^{-2}$ $d^{-1}$) |
|---|---|---|---|---|
| OC method | DO[a] | –1.69 | –2.15 | 0.46 |
| OC method | $CO_2$[a] | –1.69 | –2.15 | 0.46 |
| Propane injection | DO | –1.64 | –2.09 | 0.45 |
| Propane injection | $CO_2$ | –1.56 | –2.00 | 0.44 |
| Mean | | –1.63 | –2.08 | 0.45 |

[a] Stream metabolism rates obtained using $K_{DO}$ from OC were identical whether DO or $CO_2$ data sets were used. This result is inherent to the OC method, which solves for aeration rate by canceling out the stream metabolism terms.

### *2.4.6 Influence of lateral inflow*

Lateral inflow of hillslope/groundwater to the study reach was estimated to be <2% of stream flow. *Q* measured at the downstream end of the study reach and a point 140 m farther downstream indicated a lateral inflow rate of 0.005 L $s^{-1}$ $m^{-1}$, a 4% increase in stream flow over this distance. The increase in stream flow was within the error of gauging measurements, but for consideration of the influence of lateral inflow, we assumed it was real. Over the 60-m study reach, lateral inflow was estimated to be 0.3 L/s (1.8% of stream

flow). If stream flow was proportional to contributing area, it would have would have increased by 0.09 L/s (0.5%).

Based on expected lateral inflow rates and chemistry, potential bias to stream metabolic rates attributed to lateral inflows was moderate when based on DO data and large when based on C data. In contrast, lateral inflows had little influence on $K_{DO}$ estimated by the OC method. DO and $CO_2$ concentrations of groundwater/hillslope waters were not measured at the study site. However, DO < 5 mg/L has rarely been observed in hillslope/groundwater-dominated piezometers at nearby Watershed 1, and observed DO is usually closer to saturation (S. Serchan Oregon State, CEOAS, unpublished data). We applied values of 5 mg DO/L and 0.3 L/s lateral inflow and found a mean *NEP* correction factor of –28%, a value we consider moderate. Maximum values of DIC observed in the same piezometers were ~9.4 mg C/L, equivalent to equilibrium with 10,000 μatm $CO_2$ at 16°C and alkalinity of 382 μeq/L (Corson-Rikert et al. 2016). Applying a value of 9.4 mg DIC/L and 0.3 L/s lateral inflow, we found a mean *NEP* correction factor of –99%, a value we consider large. A similar check can be made for $K_{DO}$ by the OC method from the ratio of the lateral-inflow term to the longitudinal change in concentrations term in Eq. 8. After applying expected groundwater chemistries, we found a correction of only +1%. Thus, for our study site, the potential influence of lateral inflows to estimated rates of stream metabolism were moderate to large, but potential influence on the estimated aeration rate was small. However, correction factors may be sizeable at sites with relatively little lateral groundwater input, depending on water chemistry, and should be checked based on site-specific conditions.

### *2.5 Discussion*

We estimated the gas-transfer velocity and stream metabolic metrics of a 4$^{th}$-order montane stream by applying the 2-station open-channel method for estimating stream metabolism combined with measurement of both DO and $CO_2$. Estimated values of $K_{DO}$ based on the OC method were consistent with and had similar CI to values obtained through the standard technique of direct-gas injection.

An advantage provided by the OC method is the ability to monitor rates of gas transfer continuously over days to weeks to months in small streams without the need for multiple gas-tracer injections spread over the range in discharge. The nighttime regression method, the delta method, and multiparameter inverse-modeling methods also provide continuous estimates of gas-exchange rates, but work best in productive waterbodies that have relatively low gas-transfer rates (Chapra and Di Toro 1991, Holtgrieve et al. 2010, 2016, Demars et al. 2015). Holtgrieve et al. (2016) clarified that inverse modeling is not limited to productive/low gas-transfer-rate waterbodies because the method relies on a dynamic DO signal, which may be driven by temperature fluctuation in place of photosynthesis, but sites with little fluctuation in the DO signal are difficult to model with confidence. Another important characteristic is that these methods provide a temporally averaged estimate of gas-transfer rate, commonly at a daily interval. The OC method differs from methods that use attributes or inverse modeling of a DO time series because it is best suited to low-order streams and provides instantaneous estimates of gas transfer rather than daily means. The OC method has no inherent limitation related to productivity or aeration rate. Thus, if site conditions permit, the OC method is suitable for extended monitoring at high temporal resolution, which enables observation of the influence of transient factors on stream metabolism including discharge, wind, and rain, among others.

### *2.5.1 Method application and limitations*

The greatest limiting factor of the OC method is the need for a large longitudinal change in combined gas concentrations and combined gas deficits through the study reach. Combined concentration changes and combined deficits (defined in relation to Eq. 12) should both be >~4 μmol/L or CIs become large (Figure 4). How frequently suitable longitudinal changes in concentration and deficit conditions occur and whether they persist throughout the year are not clear, but we expect them to be common to the Oregon Cascades and to gaining headwater streams and spring-fed systems in general. Stream $CO_2$ concentrations recorded in a 2$^{nd}$-order stream 5.0 km downstream (Watershed 1, HJA) exhibited large longitudinal gas concentration gradients with differences in $pCO_2$ as high

as 1000 μatm over tens of meters (Dosch 2014) and DO concentrations near saturation with little longitudinal change. Crawford et al. (2013) observed differences in $pCO_2$ up to 1000 μatm (~40 μmol/L or 0.5 mg C/L) over reach lengths of hundreds of meters throughout the year in an investigation of a boreal stream. We suspect that the elevated $CO_2$ concentrations that we observed in our study reach were caused by high-DIC lateral inflows *above* the upstream end of the study reach. Lateral inflows of hillslope/groundwater emerging at the transition from hillslope to riparian zone have been observed at the HJA. These inflows were supersaturated in $CO_2$ (with values 10–25× that of saturated conditions (400 μatm) and had DO concentrations near saturation (Corson-Rikert et al. 2016). These seemingly contradictory concentrations are thought to be a result of soil and vadose-zone processes, where soil water equilibrates with the high-$CO_2$ and high-$O_2$ soil atmosphere typical of well-drained upland soils (Oh and Richter 2004, Luo 2006). Thus, lateral inflow of hillslope/groundwater provides a potential mechanism to create large combined gas concentration changes and deficits appropriate for the OC method.

The requisite combined gas-concentration change (ΔDIC and ΔDO) may preclude the application of the OC method based on the 1-station open-channel method. In our experience, concentration changes between time steps (e.g., 10 min) at a single sensor location are typically small (<1 μmol/L). Thus, accurate estimates of aeration rates (given current sensor technology) with the OC method based on a single station would be unlikely. Furthermore, the additional requirement for a suitably large combined gas-deficit term also may be limiting. We have not tested application of the OC method using a single-station. In locations with suitably large and well-defined lateral inputs of groundwater, the OC method based using a single-station might prove useful. In this circumstance, the numerator and denominator terms of Eq. 8 may both be suitably large to constrain errors. However, a site-specific error analysis would be necessary to define uncertainty.

Accurate in situ measurements of DO and $CO_2$ are important to the OC method. Recent technological advancements allow maintenance-free deployment of sensors for

weeks or even longer periods. Optical DO sensors have become increasingly robust, and minimal drift has been observed over periods of 2 to 3 wk (Johnston and Williams 2006). In-stream $CO_2$ sensors are a relatively young technology and less proven, but none of the multiple investigators who deployed submersible infrared gas analyzer (IRGA) $CO_2$ sensors in headwater streams for extended periods documented significant sensor drift (Johnson et al. 2010, Crawford et al. 2013, Leith et al. 2015). In more productive waters, biofouling may be problematic and frequent maintenance may be required. Yoon et al. (2016) recommended service every 3 to 5 d for sensors deployed in an urbanized river system in South Korea. When protected by Cu mesh the IRGA-type sensor-maintenance interval was extended to 1 to 2 wk. Thus, even in productive waters continuous monitoring of DO and $CO_2$ is possible. One additional limitation to $CO_2$ measurement for long-term deployment is that current technology needed for $CO_2$ measurement is energy intensive compared with DO sensors. We found that a 35 amp-h deep-cycle battery allowed ~2 wk of data collection at a 5-min sampling interval when using a Vaisala Carbocap GMM220 $CO_2$ sensor wired to a Campbell Scientific CR200 data logger. By comparison, the relatively lightweight YSI 600 OMS-V2 sonde powered by AA alkaline batteries allowed 1 mo of sampling on 5-min intervals. For remote sites and extended monitoring, transporting and maintaining charged batteries for $CO_2$ data collection may be a challenge.

### *2.5.2 Field recommendations*

The OC method is viable for reaches with a relatively large combined gas concentration change and combined gas deficit when fluxes related to dissolution or precipitation of carbonates can be quantified or disregarded. Watershed geology may be helpful in considering potential for dissolution and precipitation fluxes. Characterization of SIs for calcite, dolomite, and other possible carbonate minerals is recommended. To this end, measurement of carbonate chemistry and knowledge of the expected range of $[Ca^{2+}]$, $[Mg^{2+}]$, and other relevant solutes is necessary (Stumm and Morgan 1996). If near or above saturation with respect to a given carbonate mineral, then reformulation of the OC method derived in this paper to include precipitation or dilution fluxes would be necessary (de

Montety et al. 2011). To verify that suitably large combined gas-concentration changes and combined gas deficits exist, we recommend a reconnaissance longitudinal survey of DO and $CO_2$ through the study reach before deciding to apply the OC method. Ideally, the longitudinal survey should be conducted in a Lagrangian frame by moving with the stream at the average water velocity, following and sampling a parcel of water. In practice, this type of survey may be difficult, so care should be taken to consider whether observed changes in combined concentration are representative of a discrete parcel of water (as they should be for application of the OC method), or a temporal signal. It is also important that sensors are given time to equilibrate, submersible $CO_2$ sensors require ~10 min (dependent on water flow) to achieve ~100% equilibration (Yoon et al. 2016).

Once a reach with a suitable longitudinal change in gas concentrations and deficits is found and selected, standard methods to measure reach hydraulics, including wetted width, travel time, stream gauging, and groundwater inflow, are necessary (Bott 2006). In our study, inclusion of relatively small lateral inflows of high-DIC groundwater, on the order of 1.7% of stream flow with 10,000 μatm $CO_2$ and 5 mg DO/L increased estimated aeration rates by only 1%. However, if lateral inputs had been 5% of stream flow, with a DO concentration at saturation with the atmosphere and 10,000 μatm $CO_2$, the estimated aeration rate would have been 79% higher. Thus accurate estimates of groundwater inflow and chemistry are important. Demars et al. (2011) noted that groundwater commonly does not enter a stream evenly distributed in space, but travels along preferential flow paths and enters the stream in spatially concentrated seeps. Spatial anomalies in EC during a plateau solute injection could indicate areas of lateral inflow. Longitudinal surveys of DO and $CO_2$ may also be useful for detecting inflows of groundwater, but we know of no investigators that have used this technique to evaluate lateral inflows. Conceptually, an abrupt increase in $CO_2$ could indicate high-$CO_2$ groundwater inflow.

DO and $CO_2$ sensors should be placed at the up- and downstream ends of the study reach. Ideally, a 3$^{rd}$ $CO_2$ sensor should be deployed in the air above the stream to measure atmospheric $CO_2$ concentrations. In our experience, well-calibrated and cross-checked sensors are very important. Calibration procedures for Vaisala-type $CO_2$ sensors were

detailed by Johnson et al. (2010). We advise further cross checks in the field before and after sampling. All $CO_2$ sensors should be hung together above the stream in the shade for 2 h, then placed together in the stream at the station with highest $CO_2$ concentration for another 2 h. These readings can be used to cross-check sensors over the expected range of $CO_2$ values. This process should be reversed at the end of the study, or intermittently, for long-term deployment.

In general, DIC also must be measured or calculated at the up- and downstream ends of the study reach. We made point measurements of alkalinity and assumed it was constant over the 4-d study period. For low-alkalinity waters <~500 μeq/L, particularly if $CO_2$ concentrations are ≥~800 μatm, $\Delta DIC \approx \Delta CO_2$ and calculation or measurement of DIC is unnecessary (see Appendix A). However, if this substitution is unwarranted, DIC can be calculated from $CO_2$ and pH, $CO_2$ and alkalinity, or another combination of 2 carbonate-related variables (Stumm and Morgan 1996).

### *2.5.3 Reach-scale metabolic quotients*

The OC method has a number of assumptions related to environmental and biologic processes that influence ratios of C to $O_2$ consumption and production. We assumed metabolic quotients $RQ = 1/PQ = 0.85$. This value was prescribed by Bott (2006) and supported by *RQ* values referenced by del Giorgio and Williams (2005) and *PQ* values referenced by Ryther (1956). *RQ* ranges from 0.5 for methane to 1.33 for glycolic acid for aerobic respiration, whereas simple sugars and carbohydrates have *RQ* values of 1.0. Values of *RQ* associated with anaerobic respiration including denitrification or fermentation are much higher, so reaches with substantial anaerobic respiration may have a larger *RQ*. To our knowledge, no values of metabolic quotients at the reach scale have been published, and recent studies pairing DO and $CO_2$ data have been based on assumed metabolic quotients of 1.0 (Roberts et al. 2007, Crawford et al. 2014, Hotchkiss et al. 2015). We found consistent rates of *NEP*, *CR*, and *GPP* from independent DO and $CO_2$ datasets that support the applied *RQ* value of 0.85. Estimates of *NEP* based on C were

3.7% less than those based on DO. If *RQ* = 1.0 were applied, the discrepancy would increase to 18.5%.

We assumed constant *RQ* with respect to time. However, evidence suggests that *RQ* might change during the day. Modeled $K_{600}$ had an unexpected diel signal given that stream flow was recorded as stable and the reach was sheltered from the wind. Assuming $K_{600}$ was truly constant, the apparent signal could be attributed to time-variable *RQ* or atmospheric $CO_2$. Calculated atmospheric $CO_2$ concentrations (assuming the aeration rate and other parameters were constant) were inconsistent with diel patterns observed at nearby Watershed 1 (Figure 3C). Thus, we suspect that RQ is time variable. Calculated *RQ* (assuming the aeration rate and other parameters are constant) had a repeating diel structure with peak at midday and minimum in late afternoon (Figure 3B). A number of recent investigators using $\delta^{18}O_2$ found large increases in respiration rates during the day (Tobias et al. 2007, Hotchkiss and Hall 2014). Increases in respiration are hypothesized to result from a combination of multiple processes including: 1) increased respiration of bioavailable C produced and released in association with photosynthesis (Kaplan and Bott 1982, del Giorgio and Williams 2005), 2) photorespiration (Raven and Beardall 2005), 3) photoreactions of organic C and respiration of newly produced of bioavailable by-products (Moran and Zepp 1997), and 4) increased respiration with temperature (Perkins et al. 2012). The variety of respiration pathways, photoreactions, and the potentially changing character of bioavailable C suggests that *RQ* would change through the day. Similar changes in respiration pathways and C character probably also occur seasonally. A lack of studies pertaining to *RQ* in riverine environments makes formation of a hypothesis regarding temporal dynamics of *RQ* difficult. Further study is certainly needed to better define metabolic quotients in stream systems at the reach scale.

### *2.6 Chapter Summary*

Predicted gas-exchange rates by the OC method over a 3-d period during steady baseflow conditions were consistent with the measured aeration rate found through direct

gas injection. The method is based on the dual measurement of DO and $CO_2$ according to general procedures of the commonly applied 2-station open-channel method for measurement of stream metabolism. Submersible $CO_2$ sensors are now common and inexpensive, making automated and continuous collection of DO and carbonate chemistry data easily attainable. Thus, the OC method can be easily applied to measure gas-exchange rates continuously in real time over extended periods if suitable reach conditions are present. The method hinges on the existence of a suitable downstream change in combined DO and $CO_2$, a common condition in low-order streams of the Oregon Cascades. Our study provides added impetus for dual measurement of DO and $CO_2$ of streams for estimation of gas exchange and characterization of C sources, processing, and transport. Our study is based on a single short-duration study of a single reach. We hope the greater community will implement and verify whether the OC method is broadly applicable, accurate, and convenient.

## *2.7 Acknowledgements*

This research was made possible through support from the National Science Foundation (1417603). Meteorological data and site access were provided by the HJ Andrews Experimental Forest research program, funded by the National Science Foundation (NSF) LTER (DEB 1440409), US Forest Service Pacific Northwest (USFS PNW), and Oregon State University (OSU). Additional funding was provided from USFS PNW and OSU through the joint venture agreement 10-JV-11261991-055. Water-chemistry samples were run by OSU and the USFS Cooperative Chemical Analytical Laboratory (CCAL).

## *2.8 Literature Cited*

Aristegi, L., O. Izagirre, and A. Elosegi. 2009. Comparison of several methods to calculate reaeration in streams, and their effects on estimation of metabolism. Hydrobiologia 635:113–124.

Barnes, I. 1965. Geochemistry of Birch Creek, Inyo County, California a travertine depositing creek in an arid climate. Geochimica et Cosmochimica Acta 29:85–112.

Bencala, K. E., and R. A. Walters. 1983. Simulation of solute transport in a mountain pool-and-riffle stream: a transient storage model. Water Resources Research 19:718–724.

Bennett, J. P. 1972. Reaeration in open-channel flow. Geological Survey Professional Paper 737. US Geological Survey, Washington, DC.

Birkel, C., C. Soulsby, I. Malcolm, and D. Tetzlaff. 2013. Modeling the dynamics of metabolism in montane streams using continuous dissolved oxygen measurements. Water Resources Research 49:5260–5275.

Birnbaum, Z. W., E. Lukacs, P. Révész, and P. Révész. 1967. The laws of large numbers. Academic Press/Elsevier Science, Burlington.

Bott, T. L. 2006. Primary productivity and community respiration. Pages 663–690 *in* F. R. Hauer and G. A. Lamberti (editors). Methods in stream ecology. 2nd edition. Academic Press, San Diego, California.

Chapra, S., and D. Di Toro. 1991. Delta method for estimating primary production, respiration, and reaeration in streams. Journal of Environmental Engineering 117:640–655.

Cole, J. J., Y. T. Prairie, N. F. Caraco, W. H. McDowell, L. J. Tranvik, R. G. Striegl, C. M. Duarte, P. Kortelainen, J. A. Downing, J. J. Middelburg, and J. Melack. 2007. Plumbing the global carbon cycle: integrating inland waters into the terrestrial carbon budget. Ecosystems 10:172–185.

Cole, J., G. Lovett, S. Findlay, and Cary Conference. 1991. Comparative analyses of ecosystems : patterns, mechanisms, and theories. Springer-Verlag, New York.

Corson-Rikert, H. A., S. M. Wondzell, R. Haggerty, and M. V. Santelmann. 2016. Carbon dynamics in the hyporheic zone of a headwater mountain stream in the Cascade Mountains, Oregon. Water Resources Research 52:7556–7576.

Crawford, J. T., N. R. Lottig, E. H. Stanley, J. F. Walker, P. C. Hanson, J. C. Finlay, and R. G. Striegl. 2014. $CO_2$ and $CH_4$ emissions from streams in a lake-rich landscape:

patterns, controls, and regional significance. Global Biogeochemical Cycles 28:197–210.

Crawford, J. T., R. G. Striegl, K. P. Wickland, M. M. Dornblaser, and E. H. Stanley. 2013. Emissions of carbon dioxide and methane from a headwater stream network of interior Alaska. Journal of Geophysical Research: Biogeosciences 118:482–494.

Day, T. J. 1976. On the precision of salt dilution gauging. Journal of Hydrology 31:293–306.

del Giorgio, P. A., and P. J. L. Williams. 2005. Respiration in aquatic ecosystems. Oxford University Press, New York.

Demars, B. O. l., J. Russell Manson, J. S. Ólafsson, G. M. Gíslason, R. Gudmundsdóttir, G. Woodward, J. Reiss, D. E. Pichler, J. J. Rasmussen, and N. Friberg. 2011. Temperature and the metabolic balance of streams. Freshwater Biology 56:1106–1121.

Demars, B. O. L., J. Thompson, and J. R. Manson. 2015. Stream metabolism and the open diel oxygen method: Principles, practice, and perspectives. Limnology and Oceanography: Methods 13:356–374.

de Montety, V., J. B. Martin, M. J. Cohen, C. Foster, and M. J. Kurz. 2011. Influence of diel biogeochemical cycles on carbonate equilibrium in a karst river. Chemical Geology 283:31–43.

Dosch, N. T. 2014. Spatiotemporal dynamics and drivers of stream $pCO_2$ in a headwater mountain catchment in the Cascade Mountains, Oregon. Masters Thesis, Oregon State University, Corvallis, Oregon.

Fischer, H. B. 1972. A Lagrangian method of predicting pollutant dispersion in Bolinas Lagoon, Marin County, California. Geological Survey Professional Paper 582-B. US Geological Survey, Reston, Virginia.

Fredriksen, R. L., F. M. McCorison, and F. J. Swanson. 1982. Material transfer in a western Oregon forested watershed. In: Edmonds, Robert L., ed. Analysis of coniferous forest ecosystems in the western United States. US/IBP Synthesis Series 14. Stroudsburg, PA: Hutchinson Ross Publishing Company: 233-266.(Available from: https://andrewsforest.oregonstate.edu/publications/877)

Hall, R. O., and J. L. Tank. 2005. Correcting whole-stream estimates of metabolism for groundwater input. Limnology and Oceanography: Methods 3:222–229.

Hensley, R. T., and M. J. Cohen. 2016. On the emergence of diel solute signals in flowing waters. Water Resources Research 52:759–772.

Holtgrieve, G. W., D. E. Schindler, T. A. Branch, and Z. T. A'mar. 2010. Simultaneous quantification of aquatic ecosystem metabolism and reaeration using a Bayesian statistical model of oxygen dynamics. Limnology and Oceanography 55:1047–1063.

Holtgrieve, G. W., D. E. Schindler, and K. Jankowski. 2016. Comment on Demars et al. 2015, "Stream metabolism and the open diel oxygen method: Principles, practice, and perspectives." Limnology and Oceanography: Methods 14:110–113.

Hornberger, G., and M. Kelly. 1975. Atmospheric reaeration in a river using productivity analysis. Journal of the Environmental Engineering Division-ASCE 101:729–739.

Hotchkiss, E. R., and R. O. Hall. 2014. High rates of daytime respiration in three streams: use of $\delta^{18}O$ and $O_2$ to model diel ecosystem metabolism. Limnology and Oceanography 59:798–810.

Hotchkiss, E. R., R. O. Hall, R. A. Sponseller, D. Butman, J. Klaminder, H. Laudon, M. Rosvall, and J. Karlsson. 2015. Sources of and processes controlling $CO_2$ emissions change with the size of streams and rivers. Nature Geoscience 8:696–699.

Jähne, B., K. O. Münnich, R. Bösinger, A. Dutzi, W. Huber, and P. Libner. 1987. On the parameters influencing air–water gas exchange. Journal of Geophysical Research: Oceans 92:1937–1949.

Johnson, M. S., M. F. Billett, K. J. Dinsmore, M. Wallin, K. E. Dyson, and R. S. Jassal. 2010. Direct and continuous measurement of dissolved carbon dioxide in freshwater aquatic systems—method and applications. Ecohydrology 3:68–78.

Johnson, S., and R. Fredriksen. 2016. Stream chemistry concentrations and fluxes using proportional sampling in the Andrews Experimental Forest, 1968 to present. Long-Term Ecological Research, Forest Science Data Bank, Corvallis, Oregon. (Available from: http://andrewsforest.oregonstate.edu/data/abstract.cfm?dbcode=CF002).

Johnston, M. W., and J. S. Williams. 2006. Field comparison of optical and Clark cell dissolved oxygen sensors in the Tualatin River, Oregon, 2005. US Geological Survey, Reston, Virginia. (Available from: https://pubs.usgs.gov/of/2006/1047/ )

Kadmon, R., O. Farber, and A. Danin. 2003. A systematic analysis of factors affecting the performance of climatic envelope models. Ecological Applications 13:853–867.

Kaplan, L. A., and T. L. Bott. 1982. Diel fluctuations of DOC generated by algae in a piedmont stream. Limnology and Oceanography 27:1091–1100.

Kelly, M. G., M. R. Church, and G. M. Hornberger. 1974. A solution of the inorganic

carbon mass balance equation and its relation to algal growth rates. Water Resources Research 10:493–497.

Kelly, M. G., N. Thyssen, and B. Moeslund. 1983. Light and the annual variation of oxygen- and carbon-based measurements of productivity in a macrophyte-dominated river1. Limnology and Oceanography 28:503–515.

Khadka, M. B., J. B. Martin, and J. Jin. 2014. Transport of dissolved carbon and $CO_2$ degassing from a river system in a mixed silicate and carbonate catchment. Journal of Hydrology 513:391–402.

Kilpatrick, F. A., and E. D. Cobb. 1985. Measurement of discharge using tracers. Page 52 *in* Techniques of water-resources investigations of the US Geological Survey. Book 3. US Geological Survey, Reston, Virginia.

Kilpatrick, F. A., R. E. Rathbun, N. Yotsukura, G. W. Parker, and L. L. DeLong. 1989. Determination of stream reaeration coefficients by use of tracers. Pages 37–43 *in* Techniques of water-resources investigations of the US Geological Survey. Book 3. US Geological Survey, Denver, Colorado.

Knapp, J. L. A., K. Osenbrück, and O. A. Cirpka. 2015. Impact of non-idealities in gas-tracer tests on the estimation of reaeration, respiration, and photosynthesis rates in streams. Water Research 83:205–216.

Leith, F. I., K. J. Dinsmore, M. B. Wallin, M. F. Billett, K. V. Heal, H. Laudon, M. G. Öquist, and K. Bishop. 2015. Carbon dioxide transport across the hillslope–riparian–stream continuum in a boreal headwater catchment. Biogeosciences 12:1881–1892.

Lewis, E., and W. R. Wallace. 1998. Program developed for $CO_2$ system calculations. ORNL/CDIAC-105. Carbon Dioxide Information Analysis Center, Oak Ridge National Laboratory, Oak Ridge, Tennessee.

Lorah, M. M., and J. S. Herman. 1988. The chemical evolution of a travertine-depositing stream: geochemical processes and mass transfer reactions. Water Resources Research 24:1541–1552.

Marzolf, E. R., P. J. Mulholland, and A. D. Steinman. 1994. Improvements to the diurnal upstream–downstream dissolved oxygen change technique for determining whole-stream metabolism in small streams. Canadian Journal of Fisheries and Aquatic Sciences 51:1591–1599.

Marzolf, E. R., P. J. Mulholland, and A. D. Steinman. 1998. Reply: Improvements to the diurnal upstream-downstream dissolved oxygen change technique for determining whole-stream metabolism in small streams. Canadian Journal of Fisheries and

Aquatic Sciences 55:1786–1787.

McCutchan, J. H., W. M. Lewis, Jr, and J. F. Saunders. 1998. Uncertainty in the estimation of stream metabolism from open-channel oxygen concentrations. Journal of the North American Benthological Society 17:155–164.

McCutchan, J. J. H., J. I. F. Saunders, W. J. M. Lewis, Jr, and M. G. Hayden. 2002. Effects of groundwater flux on open-channel estimates of stream metabolism. Limnology and Oceanography 47:321–324.

Millero, F. J. 1979. The thermodynamics of the carbonate system in seawater. Geochimica et Cosmochimica Acta 43:1651–1661.

Montgomery, D. R., and J. M. Buffington. 1997. Channel-reach morphology in mountain drainage basins. Geological Society of America Bulletin 109:596–611.

Moran, M. A., and R. G. Zepp. 1997. Role of photoreactions in the formation of biologically labile compounds from dissolved organic matter. Limnology and Oceanography 42:1307–1316.

Mulholland, P. J., C. S. Fellows, J. L. Tank, N. B. Grimm, J. R. Webster, S. K. Hamilton, E. Martí, L. Ashkenas, W. B. Bowden, W. K. Dodds, W. H. Mcdowell, M. J. Paul, and B. J. Peterson. 2001. Inter-biome comparison of factors controlling stream metabolism. Freshwater Biology 46:1503–1517.

NOAA (National Oceanic and Atmospheric Administration). 2016. Annual mean carbon dioxide data. National Oceanic and Atmospheric Administration, Washington, DC. (Available from: https://www.esrl.noaa.gov/gmd/ccgg/trends/global.html)

Odum, H. T. 1956. Primary production in flowing waters. Limnology and Oceanography 1:102–117.

Oh, N. H., and D. D. Richter. 2004. Soil acidification induced by elevated atmospheric $CO_2$. Global Change Biology 10:1936–1946.

Palumbo, J., and L. Brown. 2013. Assessing the performance of reaeration prediction equations. Journal of Environmental Engineering 140(3).

Perkins, D. M., G. Yvon-Durocher, B. O. L. Demars, J. Reiss, D. E. Pichler, N. Friberg, M. Trimmer, and G. Woodward. 2012. Consistent temperature dependence of respiration across ecosystems contrasting in thermal history. Global Change Biology 18:1300–1311.

Plummer, L. N., and E. Busenberg. 1982. The solubilities of calcite, aragonite and vaterite in $CO_2$-$H_2O$ solutions between 0 and 90°C, and an evaluation of the aqueous model for the system $CaCO_3$-$CO_2$-$H_2O$. Geochimica et Cosmochimica Acta 46:1011–

1040.

Rathbun, R. E., D. Y. Tai, D. J. Shultz, and D. W. Stephens. 1978. Laboratory studies of gas tracers for reaeration. Journal of the Environmental Engineering Division 104:215–229.

Raven, J. A., and J. Beardall. 2005. Respiration in aquatic photolithotrophs. Pages 36–46 *in* P. A. del Giorgio and P. J. L. Williams (editors). Respiration in aquatic ecosystems. Oxford University Press, New York.

Raymond, P. A., and J. J. Cole. 2001. Gas exchange in rivers and estuaries: choosing a gas transfer velocity. Estuaries 24:312–317.

Raymond, P. A., J. Hartmann, R. Lauerwald, S. Sobek, C. McDonald, M. Hoover, D. Butman, R. Striegl, E. Mayorga, C. Humborg, P. Kortelainen, H. Dürr, M. Meybeck, P. Ciais, and P. Guth. 2013. Global carbon dioxide emissions from inland waters. Nature 503:355–359.

Raymond, P. A., C. J. Zappa, D. Butman, T. L. Bott, J. Potter, P. Mulholland, A. E. Laursen, W. H. McDowell, and D. Newbold. 2012. Scaling the gas transfer velocity and hydraulic geometry in streams and small rivers. Limnology and Oceanography: Fluids and Environments 2:41–53.

Reichert, P., U. Uehlinger, and V. Acuña. 2009. Estimating stream metabolism from oxygen concentrations: effect of spatial heterogeneity. Journal of Geophysical Research: Biogeosciences 114:G03016.

Riley, A. J., and W. K. Dodds. 2013. Whole-stream metabolism: strategies for measuring and modeling diel trends of dissolved oxygen. Freshwater Science 32:56–69.

Roberts, B. J., P. J. Mulholland, and W. R. Hill. 2007. Multiple scales of temporal variability in ecosystem metabolism rates: results from 2 years of continuous monitoring in a forested headwater stream. Ecosystems 10:588–606.

Ryther, J. H. 1956. The measurement of primary production. Limnology and Oceanography 1:72–84.

Sherman, L. A., and P. Barak. 2000. Solubility and dissolution kinetics of dolomite in Ca–Mg–HCO/CO solutions at 25°C and 0.1 MPa carbon dioxide. Soil Science Society of America Journal 64:1959–1968.

Spiro, B., and A. Pentecost. 1991. One day in the life of a stream—a diurnal inorganic carbon mass balance for a travertine-depositing stream (Waterfall Beck, Yorkshire). Geomicrobiology Journal 9:1–11.

Stumm, J., and J. Morgan. 1996. Aquatic chemistry: chemical equilibria and rates in

natural waters. Pages 370–388 *in* Morgan (editor). Environmental science and technology. 3rd edition. Wiley, New York.

Swanson, F. J., and M. E. James. 1975. Geology and geomorphology of the HJ Andrews Experimental Forest, western Cascades, Oregon. Research Paper PNW-188. Pacific Northwest Forest and Range Experiment Station, US Department of Agriculture, Forest Service, Portland, Oregon.

Thyssen, N., and M. G. Kelly. 1985. Water-air exchange of carbon dioxide and oxygen in a river: measurement and comparison of rates. Archiv für Hydrobiologie 105:219–228.

Tobias, C., and J. K. Böhlke. 2011. Biological and geochemical controls on diel dissolved inorganic carbon cycling in a low-order agricultural stream: implications for reach scales and beyond. Chemical Geology 283:18–30.

Tobias, C. R., J. K. Böhlke, and J. W. Harvey. 2007. The oxygen-18 isotope approach for measuring aquatic metabolism in high productivity waters. Limnology and Oceanography 52:1439–1453.

Tsivoglou, E. C., and L. A. Neal. 1976. Tracer measurement of reaeration: III. Predicting the reaeration capacity of inland streams. Journal of the Water Pollution Control Federation 48:2669–2689.

US Geological Survey. 1981. Water quality—new tables of dissolved oxygen saturation values. Water Quality Branch Technical Memorandum. No. 81.11. US Geological Survey, Reston, Virginia . (Available from: https://water.usgs.gov/admin/memo/QW/qw81.11.html.)

Wanninkhof, R., P. J. Mulholland, and J. W. Elwood. 1990. Gas exchange rates for a first-order stream determined with deliberate and natural tracers. Water Resources Research 26:1621–1630.

Weiss, R. F. 1970. The solubility of nitrogen, oxygen and argon in water and seawater. Deep Sea Research and Oceanographic Abstracts 17:721–735.

Wright, J. C., and I. K. Mills. 1967. Productivity studies on the Madison River, Yellowstone National Park. Limnology and Oceanography 12:568–577.

Yoon, T. K., H. Jin, N.-H. Oh, and J.-H. Park. 2016. Technical note: applying equilibration systems to continuous measurements of $pCO_2$ in inland waters. Biogeosciences Discussions 2016:1–34.

Young, R. G., and A. D. Huryn. 1998. Comment: Improvements to the diurnal upstream-downstream dissolved oxygen change technique for determining whole-stream

metabolism in small streams. Canadian Journal of Fisheries and Aquatic Sciences 55:1784–1785.

# 3 Carbon Fluxes of a Headwater Stream

## *3.1 Abstract*

Per unit area, aquatic systems play a disproportionately large role in the global carbon cycle. Of particular importance are headwater streams, which represent roughly 90% of the channel network by length. Headwater streams have been conservatively estimated to outgas roughly 36% of the $CO_2$ that is evaded from rivers and streams globally; however, there is great uncertainty to this estimate and researchers hypothesize that the actual value may be much higher. We investigated carbon fluxes in a second order headwater stream that drains a 96 ha forested watershed in western Oregon, USA. Total imports and exports were estimated to be 1294 kg C $yr^{-1}$ (130 kg C $ha^{-1}yr^{-1}$). Through measurement of dissolved inorganic carbon (DIC) and $pCO_2$ in a network of near stream piezometers, influx from hillslope runoff and groundwater was estimated to be 65.6 kg C $ha^{-1}yr^{-1}$ or 50% of total imports. The remaining imports were split between stream metabolism at 26% (33.8 kg C $ha^{-1}yr^{-1}$) and near stream riparian sources at 23% (29.9 kg C $ha^{-1}yr^{-1}$). Exports of inorganic carbon as $CO_2$ from the stream to the atmosphere were estimated to be at 59% (76.9 kg C $ha^{-1}yr^{-1}$) of exports. Carbon exports with streamflow were 41% (53.1 kg C $ha^{-1}yr^{-1}$) of basin-scaled flux. Estimated fluxes are generally consistent with past studies, and highlight the importance of both external and internal carbon sources to the stream carbon budget.

## *3.2 Introduction*

Streams and rivers are important to the global carbon (C) cycle as they receive, process, and evade quantities of C comparable to terrestrial net ecosystem production (NEP) (Cole et al. 2007, Turner et al. 2013, Ward et al. 2017). Low-order headwater streams are particularly relevant because they comprise a large fraction of the channel

network (Downing 2012), and their organic carbon processing, $CO_2$ concentrations, and evasion rates are large, but poorly constrained (Cole et al. 2007).

There are a suite of physical and biogeochemical processes significant to carbon dynamics in headwater streams. Most headwater streams are strongly heterotrophic; inputs of terrestrially derived organic carbon are the dominant energy source (Vannote et al. 1980, Minshall et al. 1983). This is because of limited light, relatively large inputs of leaf litter, and inflows of groundwater or hillslope water that may be rich in organic carbon (Vannote et al. 1980, Minshall et al. 1983). The result is often high rates of ecosystem respiration that causes headwater streams to be supersaturated in $CO_2$ relative the atmosphere (Cole and Caracao 2001, Butman and Raymond 2011). Hillslope and groundwater inflows of high DIC concentration further elevate $CO_2$ concentrations of headwater streams (Jones and Mulholland 1998, Hope et al. 2001). The relative proportion of $CO_2$ derived from instream processing versus groundwater or hillslope runoff is a subject of active research (Hotchkiss et al. 2015, Marx et al. 2017).

Recent studies have estimated that, for small streams in the USA, internal processing accounts for roughly 25% of the $CO_2$ that is evaded to the atmosphere (Hotchkiss et al. 2015). A complete carbon budget of a headwater stream in Oregon on the same study site as this investigation estimated instream processing to account for 27% of evasion (Argerich et al. 2016). However, the $CO_2$ evasion rate, and other components of the carbon budget, were poorly constrained. This is true of most studies of headwater streams because $CO_2$ outgassing is generally calculated using measured $CO_2$ concentrations in the stream and aeration rates estimated from hydraulics. Spatial variability in $CO_2$ concentration is often high with variation of over 100% within 50 m (Crawford et al. 2014, Dosch 2014). Rapid changes in concentration from high $CO_2$ groundwater inflow source locations occurs over short distances. For example, Öquist et al. (2009) found that within 200 m of a spring, approximately 65% of the C in groundwater was evaded to the atmosphere. Thus, estimates of $CO_2$ evasion often have large errors, and studies that explicitly measure lateral inflows of terrestrial C have been recommended (Hotchkiss et al. 2015).

Models of stream carbon budgets generally include two source terms of inorganic carbon: inflows of inorganic carbon with hillslope runoff and groundwater, and internal production of $CO_2$ from metabolism of organic carbon. However, there is evidence that wetlands are a third source of inorganic carbon in which aerial vegetation with submerged roots transport $CO_2$ into the water (Abril et al. 2014). Unlike stream metabolism, $CO_2$ is injected without a stoichiometrically balanced loss in DO. For large tropical wetlands, this process has been found to be significant; C import rates for the Amazon basin was estimated to be 0.21 Pg C $yr^{-1}$. However, few publications pertaining to this process with respect to stream carbon budgets are available. We hypothesize here that the near stream riparian zones of headwater streams are a third source of C to the stream that is not accounted for through stream metabolism or lateral inflows.

In this study we develop a carbon budget for a headwater stream on a daily timestep over the course of two hydrologic years. Imports of DIC are partitioned between lateral inflows, stream metabolism, and riparian source areas. Exports are partitioned between $CO_2$ outgassed to the atmosphere and DIC transported with discharge.

## *3.3 Site Description*

### *3.3.1 Watershed 1 Description*

This study was conducted in Watershed 1 (WS1) of the H. J. Andrews Experimental Forest Long-Term Ecological Research site (LTER) (Figure 3.1). WS1 is a steep, forested catchment with an area of 95.5 ha, and ranges in elevation from 450 to 1027 m. The geology of the WS1 comprises silicic volcanic type rocks, largely tuffs and breccias, with no mapped carbonate rocks (Swanson and Dooge 1975, Priest et al. 1988). WS1 has steep valley walls (>50% slope), and a narrow confined riparian zone with an average channel gradient of roughly 12% in the lower reaches. The stream is within a channeled colluvial valley of step-pool morphology with some short bedrock dominated reaches (Montgomery and Buffington 1997). The colluvial deposits are made up of a poorly sorted mixture of logs, boulders, cobbles, gravels, sands, and finer sediments that rarely exceed 2 m in depth (Wondzell 2006).

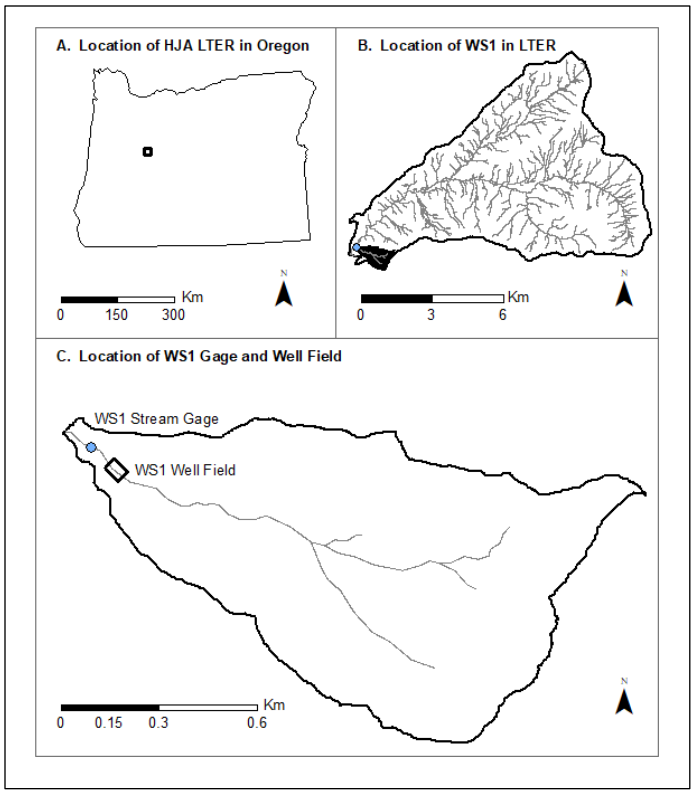


Figure 3.1 Term Ecologic Research Station (LTER) within Oregon. B) Watershed 1 (WS1) within the LTER. C) Stream gage and well field within Watershed 1 (WS1).

The climate of the study site is temperate with cool, wet winters, and warm, dry summers. WS1 has an average annual precipitation of approximately 2300 mm which falls primarily as rain from November to April. Precipitation may fall as snow, but snow generally melts away during warm periods or warmer storms within days or weeks of snowfall. Streamflow in WS1 is greatest through the winter wet season and declines dramatically in dry summer months. In the late summer the wetted channel may become intermittent with isolated pools separated by patches of dry alluvium. In bedrock dominated reaches, flow is perennial with minimum flows as low as 0.1 L/s. The LTER maintains a long-term gaging station near the bottom of WS1 that records streamflow, water and air temperature, and electrical conductivity (EC) every 5 minutes. Precipitation, discharge, and spatial data are available from H. J. Andrews Experimental Forest Data Catalog. The LTER also collects bulk water samples which are analyzed for DOC, POC, alkalinity, cations, and anions (Johnson and Fredriksen 2016). Bulk sample data were used in development of the comprehensive carbon budget for WS1 by Argerich et al. (2016). WS1 was clear-cut logged between 1962 to 1966; logging debris (slash) was burned in 1966. Many burned logs and debris were left in the riparian zone. Some charcoal covered logs and stumps are visible today.

WS1 is now densely forested with second growth Douglas fir with some western hemlock. Red alder dominates the riparian zone with some maple and cottonwood present. In recent years numerous red alders have fallen during storms, particularly when precipitation came as heavy wet snow.

### *3.3.2 Watershed 1 Well Field*

Data from an intensively monitored sub-reach near the bottom end of the WS1 (well field) was used to develop a carbon budget for the greater watershed (Figure 3.2). The well field is the study site of numerous past publications pertaining to carbon dynamics (Dosch 2014, Argerich et al. 2016, Corson-Rikert et al. 2016, Brandes 2017) and many studies related to hyporheic flows (Kasahara and Wondzell 2003, Wondzell 2006, Ward et al. 2012).

The WS1 well field consists of roughly 40 piezometers oriented in seven transects that cross a relatively flat valley bottom area of approximately 45 m in length and 20 m in width. The valley floor material is composed of colluvium, consisting of a heterogenous mixture of sediments of all size classes, soil, and numerous logs and boulders. The valley floor deposits are dissected by the stream such that the active channel is roughly 1 to 2 meters below the vegetated valley floor. The stream has eroded to bedrock at downstream piezometer transects C and D. Deposits are roughly 1 meter deep within the active channel in upstream transects. Even during very high flows, the stream does not overtop its banks and is contained to an active channel that is bounded on either side by valley floor areas vegetated with predominantly red alder and ferns. Past studies have documented significant hyporheic flow travels from the stream through the valley floor deposits and back to the stream (Kasahara and Wondzell 2003, Wondzell 2006, Ward et al. 2014).

Piezometers were originally installed in the summer of 1997, and were replaced in September 2013. Piezometers constructed of 1.25 inch diameter PVC pipe were replaced with pre-fabricated stainless steel piezometers with a diameter of 2 inches. Stainless steel piezometers were installed in the identical surface location, or as near as possible, to the original PVC piezometers. An additional upstream transect (transect I) was also added. The stainless steel piezometers have a cone at the bottom to facilitate impact driven

installation, and a 10 cm screened interval above the cone. The piezometers were driven to refusal using a pneumatic fence post driver (Rhino PD 55), and sledge hammer. Final depths below ground surface ranged from 0.5 to 2 meters; bottom elevations of the screened intervals were generally consistent with the retired PVC piezometers. The bottom point of the piezometer is expected to coincide with the contact of the colluvium and underlying volcanic bedrock. Very little hyporheic flow is expected to pass through the bedrock, while relatively large hyporheic exchange flows pass through the overlying colluvial and alluvial substrate.

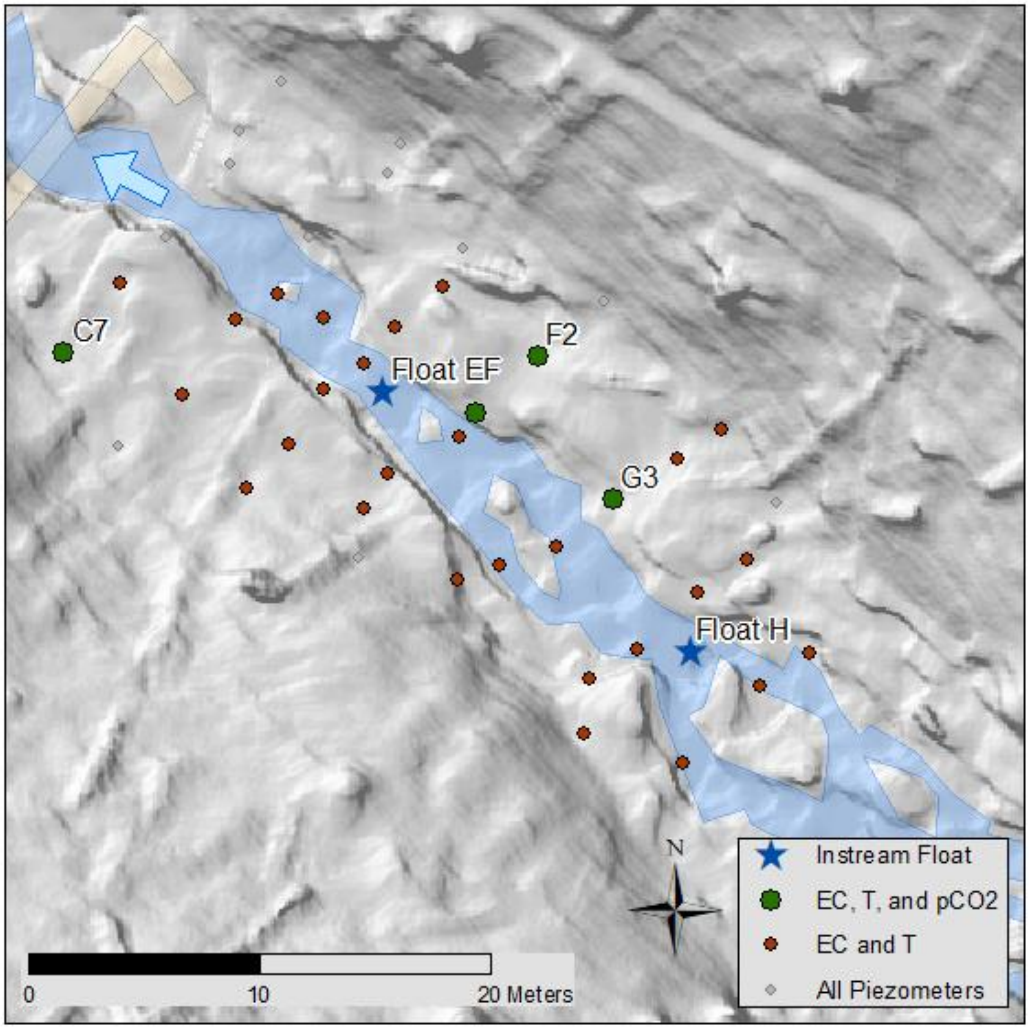


Figure 3.2 – WS1 well field and location of stainless-steel piezometers and instream monitoring locations (instream float).

Sites with continuous deployment of Electrical Conductivity (EC) and Temperature (T) and $pCO_2$ shown.

### *3.4 Conceptual Model and Methods*

The carbon budget was developed using the conceptual model of inputs and exports

inputs exports

$$DIC_{lateral} + DIC_{metabolism} + DIC_{riparian} = DIC_{discharge} + CO2_{evasion}$$

(Eq. 1)

where $DIC_{lateral}$ is the import of DIC to the stream from groundwater, hillslope or soil water. This study does not attempt to partition DIC inflows from different lateral source areas. $DIC_{metabolism}$ is the carbon production through stream metabolism, quantified as net ecosystem production (NEP). $DIC_{riparian}$ is the carbon imported to the stream along hyporheic flow paths that cannot be attributed to metabolism. Within WS1, and common to many stream systems, hyporheic flow paths extend laterally from the wetted channel through forested floodplain or terrace deposits. Along hyporheic flow paths, C from the overlying soil, root respiration, or other sources are hypothesized to infiltrate hyporheic water, result in high DIC hyporheic water, and be imported back to the stream with hyporheic return flow. $DIC_{riparian}$ is hypothesized to represent a significant source of DIC to the stream that is separate from $DIC_{metabolism}$. $DIC_{discharge}$ is the export of DIC from the watershed with stream discharge. $CO_{2\text{evasion}}$ is the $CO_2$ evaded from the stream to the atmosphere. See Table 3.1 for a complete list of variable definitions. The sections below detail methods specific to estimates of each DIC import and export to and from the stream.

Table 3.1 – Variable definitions.

| Variable | Description | Units |
|---|---|---|
| *DO* | Dissolved $O_2$ in stream water | $mol/L^3$ |
| $DO_l$ | Dissolved $O_2$ of lateral inflow (soil and groundwater) | $mol/L^3$ |
| $DO_{def}$ | Dissolved $O_2$ deficit | $mol/L^3$ |
| $CO_{2def}$ | Dissolved $CO_2$ deficit | $mol/L^3$ |
| *DIC* | Total dissolved inorganic C in the stream water | $mol/L^3$ |

| | | |
|---|---|---|
| $DIC_l$ | DIC of lateral inflow (soil and groundwater) | mol/$L^3$ |
| $DIC_{sat}$ | DIC at equilibrium with atmosphere $CO_2$ and given temperature and alkalinity | mol/$L^3$ |
| $DIC_{lateral}$ | Import flux of DIC from groundwater or hillslope runoff | M $L^{-2}$ $T^{-1}$ |
| $DIC_{riparian}$ | Import flux of DIC from near stream riparian | M $L^{-2}$ $T^{-1}$ |
| $DIC_{metabolism}$ | Import flux of DIC from instream processing - NEP | M $L^{-2}$ $T^{-1}$ |
| $DIC_{evasion}$ | Export flux of C as $CO_2$ from the stream to atmosphere | M $L^{-2}$ $T^{-1}$ |
| $DIC_{discharge}$ | Export flux of C with stream discharge | M $L^{-2}$ $T^{-1}$ |
| $EC$ | Electrical conductivity | µS/cm |
| $\tau$ | Mean travel time through reach | T |
| $L$ | Reach length | L |
| $A$ | Wetted stream bed area of the study reach | |
| $A_s$ | Wetted stream bed area above the WS1 gage | $L^2$ |
| $A_w$ | Area of the watershed or catchment above the WS1 gage | $L^2$ |
| $v$ | Stream velocity | L/T |
| $Q$ | Stream discharge | $L^3$/T |
| $Q_l$ | Lateral inflows to the reach | $L^3$/T |
| $K_c$ | Coefficient of gas transfer for gas *c*. Subscript may be DO, $CO_2$, propane, or left as *c* if unspecified. | 1/T |
| $K_{600}$ | Coefficient of gas transfer for $O_2$ at 17.5°C | 1/T |
| $RQ$ | Respiratory quotient measured as amount of $CO_2$ released to $O_2$ absorbed | – |
| $NEP_c$ | Production of $O_2$ through stream metabolism per unit stream area. Subscript indicates source data used to calculated NEP and may be DO or DIC timeseries | M $L^{-2}$ $T^{-1}$ |

### *3.4.1 DIC Imports from Lateral Inflows*

Lateral DIC import (scaled to the watershed area) was estimated from measurement of time-variable DIC concentrations of water within piezometers that were found to be dominated by lateral inputs from groundwater or hillslope water, multiplied by the stream discharge rate ($Q$) measured at the WS1 stream gage.

$$Q_l = DIC_l \, Q \, / A_w \qquad \text{(Eq. 2)}$$

Time variable concentrations of DIC in lateral inflows ($DIC_{lateral}$) was estimated from a combination of data sources including, continuous measurements of $pCO_2$, EC, and temperature, and discrete measurements DIC in lateral inflow dominated piezometers. Lateral inflow dominated piezometers were identified from analysis of EC break through curves of salt tracer injections and natural temperature signals (see Appendix B for greater discussion). Piezometers C7, D7, E7, and F7 were identified as lateral inflow dominated through most of the year. Other piezometer sites were found to fluctuate between being hyporheic water or lateral inflow dominated. While other sites, mostly those near or within the active channel, were found to always be hyporheic water dominated.

A strong correlation between EC and alkalinity was found in flow proportional water samples collected at the WS1 gage, allowing measured EC to be converted to alkalinity (Johnson and Fredriksen 2016, see Figure C.1). DIC was then calculated from the continuous record of $pCO_2$ and alkalinity at piezometer C7 which was instrumented with both a $pCO_2$ and EC sensor. DIC and carbonate speciation was calculated using CO2SYS (version 1.1; coded in Matlab; Lewis and Wallace 1998) using temperature-dependent equilibrium constants published by Millero (1979).

A regression relationship was developed between DIC in C7 and other groundwater dominated sites, and used to convert DIC timeseries at C7 to $DIC_{lateral}$. For short periods of time when data was not available for C7, correlations with stream discharge were used.

Lateral inflow rate was assumed to be equivalent to stream discharge. This is considered valid because nearly all streamflow in the headwater stream is derived from lateral inflows of soil or groundwater, excepting the small fraction of precipitation that falls directly into the active channel. During all field visits, including periods of heavy precipitation, overland flow was never observed.

### *3.4.2 DIC Imports from Stream Metabolism*

Input of DIC from instream processing of organic carbon was estimated from correlations of NEP to stream temperature. DO timeseries in the stream was available for roughly eight months of the two year study. Using these data, NEP was estimated using

the 1-station or 2-station open-channel method, accounting for lateral inflow to reach ($Q_l$) (Odum 1956, Marzolf et al. 1994, 1998, McCutchan et al. 2002, Hall and Tank 2005).

Advection Aeration Lateral inputs

$$NEP_{DO} = z\left(\frac{\Delta DO}{\tau} - K_{DO}\, DO_{def}\right) - \frac{Q_l}{A}(DO_l - DO) \quad \text{(Eq. 3)}$$

In the above equation for stream metabolism, all variables, other than *RQ*, are considered time-variable. Average depth ($z$), stream bed area ($A$), mean travel time ($\tau$), and $Q_l$, were modeled as functions of $Q$ measured at the WS1 gage. Regression relationships between $Q$ and $A$ from Argerich et al. (2016) were applied. Salt tracer injections conducted over a range of flows from this study and Ward et al. (2010) were used to develop a regression relationship between $Q$ and stream velocity, which was then used to calculate $\tau$.

Measured discharge was scaled linearly with contributing drainage area to estimate $Q_l$

$$Q_l = Q\ \frac{Area\ DS - Area\ US}{A_w} \quad \text{(Eq. 4)}$$

where *Area DS* is the contributing drainage area above the downstream sensor, *Area US* is the contributing drainage area above the upstream sensor, and $A_w$ is the contributing drainage area above the WS1 gage. This method is consistent with that used by Schmadel, Ward, and Wondzell (2017) for estimating spatially variable groundwater inflow.

The final time variable parameter in Eq. 3 for stream metabolism is the aeration rate ($K_{DO}$), which was estimated as a function of discharge and temperature. The oxygen carbon method was used estimate $K_{DO}$ over a wide range of flow conditions using the equation below from Pennington et al. (2018):

$$K_{DO} = \left(\frac{\frac{\Delta DIC}{RQ} + \Delta DO}{\tau} - \frac{Q_l}{zA}\left(\frac{(DIC_l - DIC)}{RQ} + DO_l - DO\right)\right) \Big/ \left(\frac{\beta}{RQ} CO_{2_{def}} + DO_{def}\right) \quad \text{(Eq. 5)}$$

The oxygen carbon method is described in detail in the previous chapter of this thesis. Measured values of $K_{DO}$ were converted to $K_{600}$, the aeration coefficient of oxygen

at 17.5°C when oxygen in water has a Schmidt value of 600, temperature-dependent Schmidt values from regression coefficients provided by Raymond et al. (2012). Once normalized to $K_{600}$, the aeration rate was regressed with $Q$ to develop a discharge-dependent aeration rate.

In order to develop a continuous estimate of NEP through the study period, $NEP_{DO}$ measurements were binned into daily values and regressed with mean daily temperature using the commonly used Arrhenius equation for respiration (Arrhenius 1915). $NEP_{DO}$ was then converted into $DIC_{metabolism}$

$$DIC_{metabolism} = -RQ \; A_s/A_w \; NEP_{DO} \quad \text{(Eq. 6)}$$

where $RQ$ is the molar ratio of $CO_2$ released to $O_2$ consumed in respiration, used to convert $NEP$ into units of C. In the metabolism of simple carbohydrates $RQ$ is 1. For other organic molecules, $RQ$ is generally assumed to range from 0.8 to 1.0 (del Giorgio and Williams 2005). Bott (2006) recommended a value of 0.85 for $RQ$ for studies of stream metabolism. This value is supported by recent studies of aeration rates and stream metabolism in nearby McRae Creek (Pennington et al. 2018). Note, $NEP_{DO}$ is in units of $O_2$ produced per unit stream area, while $DIC_{metabolism}$ is in units of C imported per unit watershed area, hence the multiplication by the wetted stream area upstream of the WS1 gage ($A_s$) and division by $A_w$.

### *3.4.3 DIC Imports from Riparian Sources*

Similar to using DO timeseries, NEP was estimated using $CO_2$ and DIC timeseries data

$$NEP_{DIC} = \frac{z}{RQ}\left(\frac{\Delta DIC}{\tau} - K_{CO2}\, CO_{2_{def}}\right) - \frac{Q_l}{A \cdot RQ}(DIC_l - DIC) \quad \text{(Eq. 7)}$$

Through Eq. 3.7, $NEP_{DIC}$ assumes DIC imported from riparian sources, then measured in the stream, was produced through stream metabolism. This contrasts with $NEP_{DO}$ which does not consider additional DIC imported to the stream from riparian sources that was not associated with respiration (oxygen consumption) in the stream or

along a hyporheic flow path. Thus, $NEP_{DIC}$ is expected to approximate $DIC_{metabolism}$ + $DIC_{riparian}$, while $NEP_{DO}$ represents only $DIC_{metabolism}$. Differencing the two NEP estimates is expected to approximate the additional DIC imported to the stream from the riparian zone (Eq. 3.6).

$$DIC_{riparian} = RQ \; A_s/A_w \; (NEP_{DIC} - NEP_{DO}) \quad \text{(Eq. 6)}$$

### *3.4.4 DIC Exports from Stream Discharge*

DIC exported with streamflow was estimated as DIC outflow with the assumption that stream water was at saturation, in equilibrium with the atmosphere. This assumption is considered valid if aeration rates are high compared with advective rates. Under these circumstances (if not for continued imports) stream water would approach equilibrium with the atmosphere in a relatively short distance. For WS1, the distance necessary to attain equilibrium, if not for additional imports of DIC, would be less than 50 meters. Thus, DIC export was estimated by multiplying Q and concentrations of DIC at saturation with the atmosphere in stream water ($DIC_{sat}$), as shown below.

$$DIC_{discharge} = DIC_{sat} \; Q \quad \text{(Eq. 7)}$$

$DIC_{sat}$ was derived from, temperature, alkalinity, and atmospheric $pCO_2$, consistent with methods used for lateral inflows. Barometric pressure, recorded at the H. J. Andrews PRIMET meteorological station, was scaled to the elevation of the WS1 gage. Atmospheric $pCO_2$ at the site was then calculated, assuming a constant value of 434 μatm $CO_2$ partial pressure at sea level, equal to the average observed at 2.5 cm above the stream (Argerich et al. 2016).

## *3.5 Field Methods*

### *3.5.1 Time Series Data*

Continuous $pCO_2$ and DO were measured in the stream and in select piezometers (Figure 3.2) using Vaisala (Vantaa, Finland) Carbocap GMM220 $CO_2$ sensors (Johnson et al. 2010, Dosch 2014) wired to Campbell Scientific (Logan, Utah) data loggers ($CO_2$) and YSI 600 OMS-V2 sondes (model 6150 ROX DO; Yellow Springs Instruments, Yellow springs, Ohio; DO and temperature). Data was collected continuously at 10-minute intervals. For instream measurements, $CO_2$ sensors were attached to the bottom of floats to maintain a consistent water depth. YSI sondes were attached to the streambed. The $CO_2$ sensors were calibrated before deployment by insertion into an airtight chamber with gas of a known $CO_2$ concentration (1010 ppm). $CO_2$ measurements were validated by comparing data with measurements from discrete water samples (discussed below). Little offset from discrete water samples were observed, and correction to $pCO_2$ data was not performed after original deployment. YSI sondes were downloaded and calibrated monthly in water saturated air.

Continuous EC and temperature were observed in the stream and 30 piezometers within the well field (Figure 3.2) using EC/temperature sensors (Campbell 547A) wired to Campbell Scientific dataloggers. Linear drift correction was performed on all temperature and EC time series data at all sites when the value measured was offset by greater 0.5 °C or 5 µS/cm compared with the value from discrete sampling. The GCE Data Toolbox for Matlab Version 3.9.9b was used to organize and post process time series data.

### *3.5.2 Discrete Water Chemistry Samples*

Water samples were collected from the stream and piezometers monthly from July 2014 through June 2015 and analyzed for a suite of cations, anions, alkalinity, DO, and DIC (Serchan, unpublished data). Several other sampling events took place between June 2015 and March 2017. Discrete sampling data were used for QA/QC of time series data, and to develop regression relationships of water chemistry (DO or DIC) to continuous time series such as WS1 discharge or DIC at piezometer C7.

## *3.6 Results*

### *3.6.1 Time Series Data*

The field component of the study was conducted over a roughly two year period from October 2014 through January 2017. The study window included two complete hydrologic years. Flow ranged from a minimum of 0.14 L $s^{-1}$ to a maximum of 1300 L $s^{-1}$. Concentrations of $CO_2$ within the stream and piezometer C7 were recorded over much of this time period, while DO was recorded in the stream for most of 2016 (Figure 3.3).

Both $CO_2$ and DO in the stream were near saturation during the winter when flow conditions were high and temperature was low (Figure 3.3). $CO_2$ concentrations of the stream were generally above saturation with a mean $pCO_2$ concentration of 954 ppmv, maximum in summer and early fall at 2750 ppmv, and minimum through the winter and early spring at 450 ppmv. During the summer, when discharge was low and temperatures were high, both DO and $CO_2$ deviated from saturation in opposite directions. DO concentrations were below saturation, while $CO_2$ concentrations were above saturation, consistent with net heterotrophic conditions that are expected of well shaded headwater streams (Vannote et al. 1980). $CO_2$ concentrations of piezometer C7 were consistently above saturation with a mean $pCO_2$ concentration of 6823 ppmv, maximum in late summer at 9000 ppmv, and minimum through the winter and early spring at 4400 ppmv. Additional timeseries plots of DIC and DO, and regression relationships used to define water chemistry of lateral inflow dominated piezometers, are provided in Appendix C.

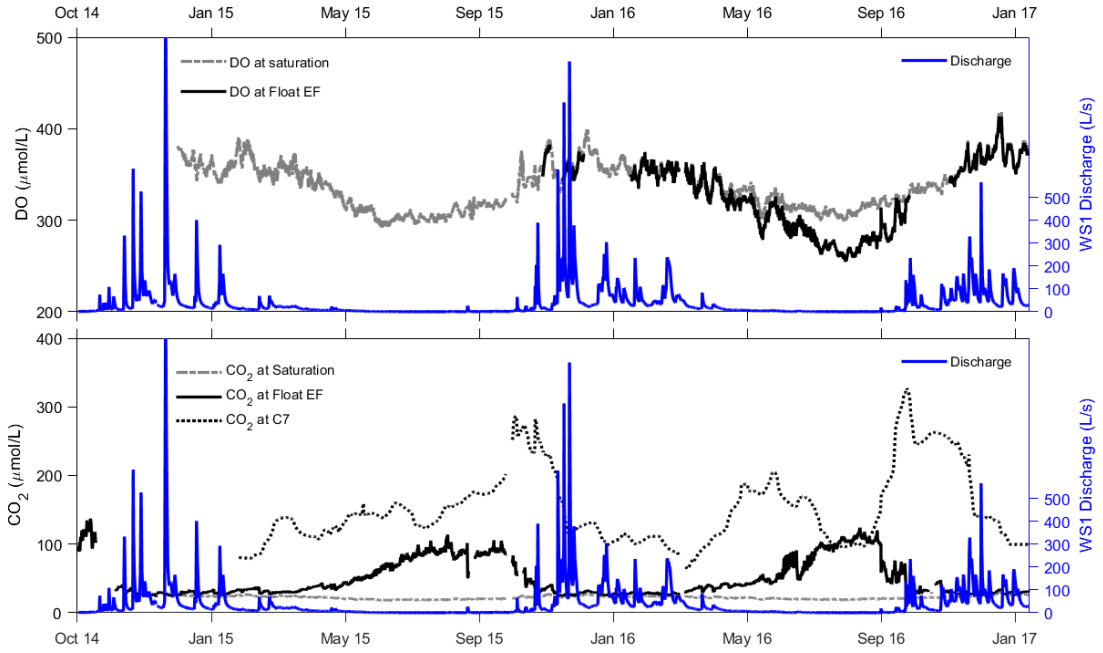


Figure 3.3 – DO and $CO_2$ time series measured within the stream (Float EF) and within a lateral inflow dominated piezometer (C7) over the October 2014 through January 2017 study period.

### *3.6.2 Aeration Rate*

Instantaneous measurements of the aeration rate were estimated using the oxygen carbon method (Figure 3.4). Aeration rate was positively correlated with stream discharge. A power law equation was used to regress $K_{600}$ to discharge performed moderately well with r-square value 52% ($p < 0.05$). Regression relationships from propane gas injections are also shown but had a poor fit (r-square = 20%) and small sample size (n = 10). Relationships with hydraulics were also investigated but found to overestimate the aeration rate compared with that found through propane gas injections or the oxygen carbon method.

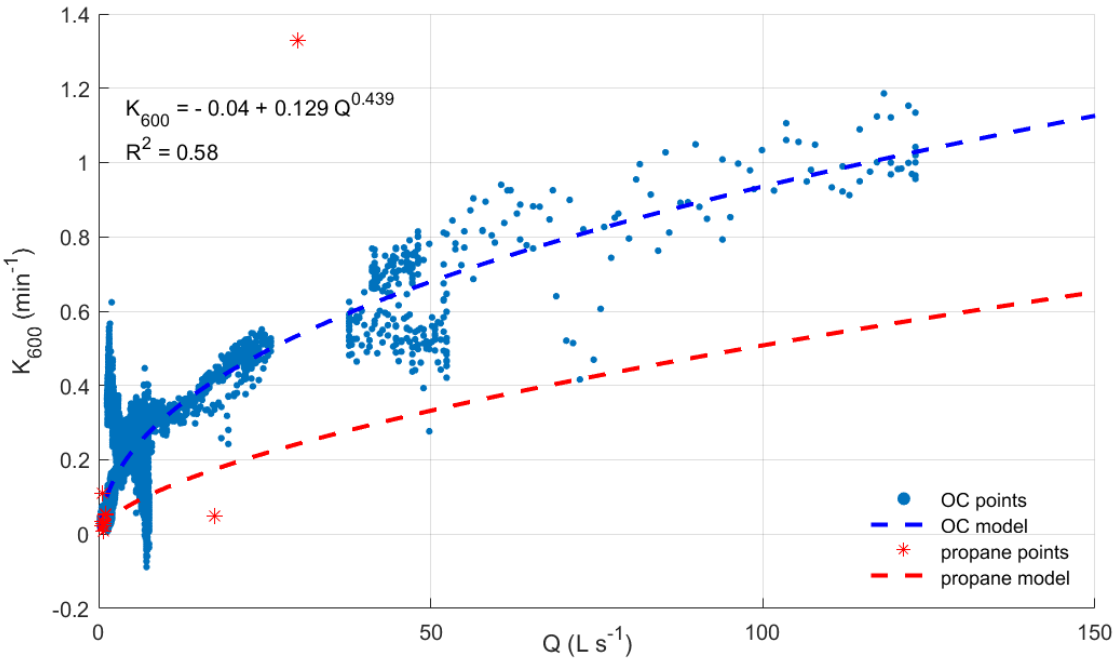


Figure 3.4 – Measurement of the aeration rate (K600) from oxygen carbon method and from propane injections, versus discharge (Q).

### *3.6.3 Stream Metabolism*

NEP was estimated from continuous time series data of DO and $CO_2$ using the single station methods. Results were found to be generally consistent with negative NEP values indicating heterotrophic conditions (Table 3.2). Mean NEP from DO timeseries was -2.67±0.02 g $O_2$ $m^{-2}$ $day^{-1}$ or 0.85 ±0.01 g C $m^{-2}$ $day^{-1}$.

Table 3.2 – Mean stream metabolism parameters estimated from time series data from October 2014 through January 2017. Positive values indicate production of $O_2$, and consumption of C. Estimates from $CO_2$ time series assume RQ = 1/PQ = 0.85. Net Ecosystem Production (NEP), Community Respiration (CR), and Gross Primary Production (GPP) are reported in units of $O_2$ produced per unit stream area per day.

| Time series used as input | *NEP* (g $O_2$ $m^{-2}$ $d^{-1}$) | *CR* (g $O_2$ $m^{-2}$ $d^{-1}$) | *GPP* (g $O_2$ $m^{-2}$ $d^{-1}$) |
|---|---|---|---|
| DO | -2.67 | -2.85 | 0.18 |
| $CO_2$ | -4.80 | -4.90 | 0.10 |
| Mean | -3.74 | -3.88 | 0.14 |

Differences between estimates from DO vs $CO_2$ were evident (Figure 3.5). The magnitude of Net Ecosystem Production (NEP) and Community Respiration (CR) rates estimated from $CO_2$ were higher (more negative) than estimates from DO. The offset tended to be systematic with consistent offsets in estimated NEP through extended periods of time. We speculate that this difference arises from the import of DIC along hyporheic flow paths that travel beneath and adjacent to the wetted channel beneath riparian terrace areas.

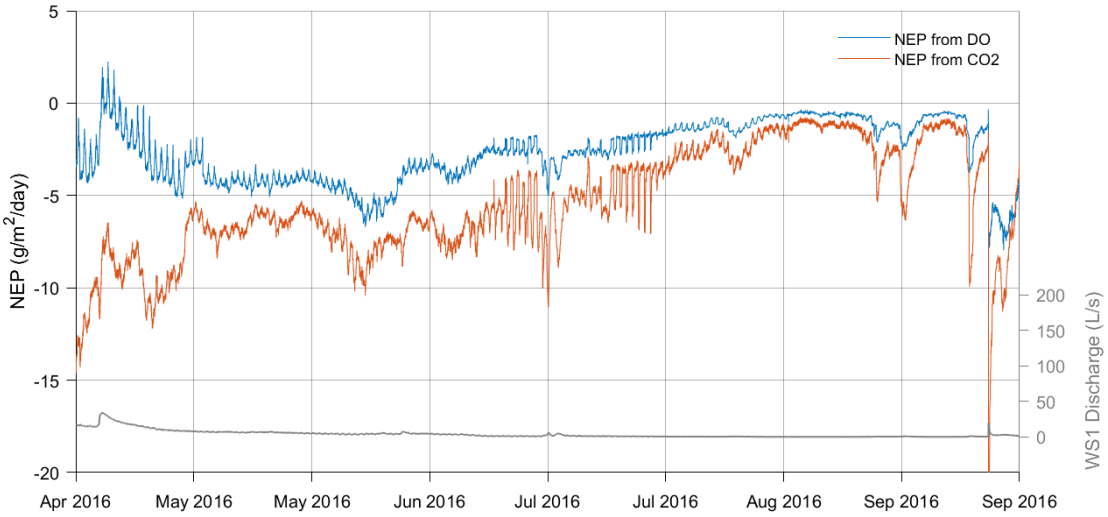


Figure 3.5 – Time series of Net Ecosystem Production (NEP) in units of $O_2$ per unit stream area from independent DO and $CO_2$ time series measured in the stream at Float EF through the spring and summer of 2016.

An offset between NEP from DO and NEP from $CO_2$ is also evident in temperature to NEP relationships (Figure 3.6), particularly at higher temperatures. The Arrhenius equation was used as a regression model for NEP. NEP rates at 15 °C were -7.2 g $O_2$ $m^{-2}day^{-1}$ from DO timeseries regressions, and -12.8 g $O_2$ $m^{-2}day^{-1}$ from $CO_2$ timeseries regressions. At lower temperatures, near 6 °C and below, the difference in modeled NEP is minimal.

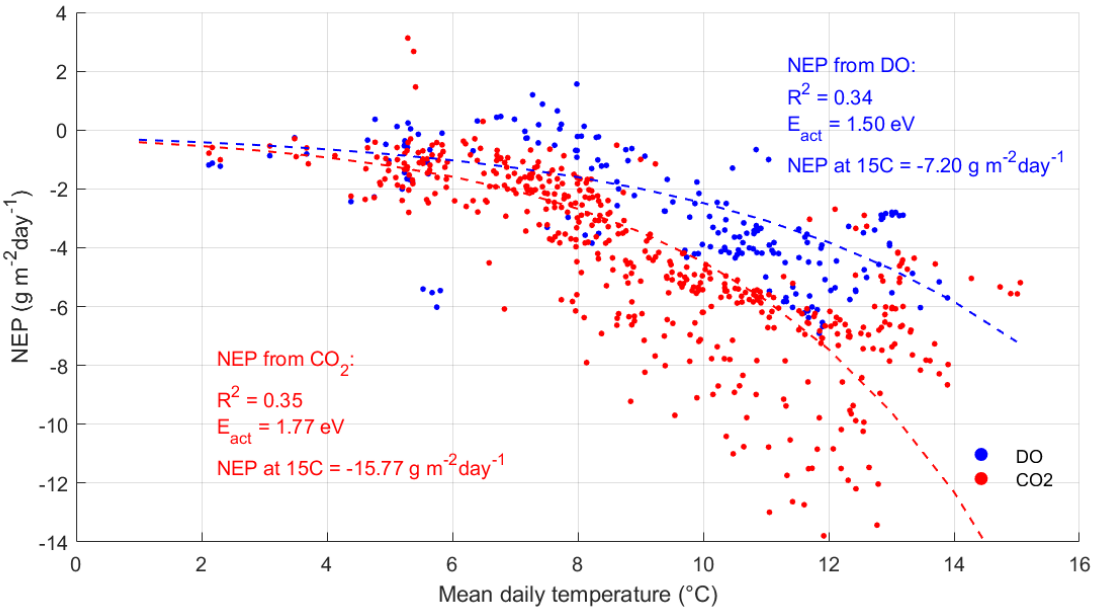


Figure 3.6 – Temperature versus Net Ecosystem Production (NEP) with Arrhenius equation regression lines. Characteristic parameters of the Arrhenius equation, activation energy (Eact and NEP at 15 °C) are shown. NEP is in units of $O_2$ produced per unit stream area per day.

### *3.6.4 DIC Imports and Exports*

Over the study period average imports of DIC to the WS1 stream were found to be $130 \pm \frac{\mathbf{40.5}}{\mathbf{36}}$ kg C $ha^{-1}yr^{-1}$ (Table 3.3). $DIC_{lateral}$ constituted 50% of total imports ($65.6 \pm \frac{17}{16.6}$ kg C $ha^{-1}yr^{-1}$), $DIC_{riparian}$ made up 23% ($29.9 \pm \frac{18.8}{16.3}$ kg C $ha^{-1}yr^{-1}$) and $DIC_{metabolism}$ made up 26% ($33.8 \pm \frac{17.7}{12.0}$ kg C $ha^{-1}yr^{-1}$). $CO_{2evasion}$ made up 59% ($76.9 \pm \frac{34.4}{30.1}$ kg C $ha^{-1}yr^{-1}$) of exports, and $DIC_{discharge}$ made up the remainder, 41% ($53.1 \pm \frac{6.1}{5.9}$ kg C $ha^{-1}yr^{-1}$).

Table 3.3 – Mean DIC import and exports for each month, and the year in kg C $ha^{-1}yr^{-1}$ with respect to catchment area. Input data was from October 2014 through January 2017. Positive values indicate imports of carbon to the stream or internal production of DIC within the stream.

| month | Jan | Feb | Mar | Apr | May | Jun | Jul | Aug | Sep | Oct | Nov | Dec | Year |
|---|---|---|---|---|---|---|---|---|---|---|---|---|---|
| $DIC_{lateral}$ | 117.6 | 93.9 | 96.2 | 44.0 | 18.7 | 9.4 | 3.0 | 1.1 | 4.1 | 41.3 | 105.1 | 253.0 | 65.6 |
| $DIC_{metabolism}$ | 20.0 | 24.7 | 23.8 | 27.0 | 34.0 | 48.3 | 50.2 | 43.1 | 38.0 | 40.5 | 30.2 | 28.7 | 34.0 |
| $DIC_{riparian}$ | 11.7 | 16.2 | 15.7 | 19.6 | 29.0 | 49.9 | 56.9 | 49.4 | 39.2 | 37.1 | 22.3 | 18.8 | 30.5 |
| $DIC_{discharge}$ | -94.5 | -79.2 | -78.2 | -35.9 | -15.2 | -7.6 | -2.5 | -1.0 | -3.3 | -32.5 | -83.5 | -204.4 | -53.2 |
| $CO2_{evasion}$ | -54.8 | -55.7 | -55.8 | -54.7 | -66.5 | -99.9 | -107.5 | -92.7 | -78.0 | -88.5 | -74.8 | -96.1 | -77.1 |
| | | | | | | | | | | | | Total | **130.1** |

There was strong seasonality to $DIC_{lateral}$ and $DIC_{discharge}$ (Figure 3.7 and 3.8). This was expected as these components are driven largely by discharge. Other parameters were comparatively uniform through the year, but also demonstrated some seasonality. $DIC_{riparian}$ and $DIC_{metabolism}$ were modeled as functions of temperature and increased in the summer and decreased in the winter. $CO_{2evasion}$ was determined by differencing all other terms and found to have a bimodal form with a peak in summer (driven by elevated NEP) and peak in winter (driven by lateral inflows). However, the seasonality of $CO_{2evasion}$ may be an artifact of having a short study window of only 27 months. The dataset used here included a number of large storm events that occurred in December of successive years. If more years of data were included, storm driven fluxes would be spread out more uniformly through the wet season and the bimodal form of $CO_{2evasion}$ would perhaps be less apparent.

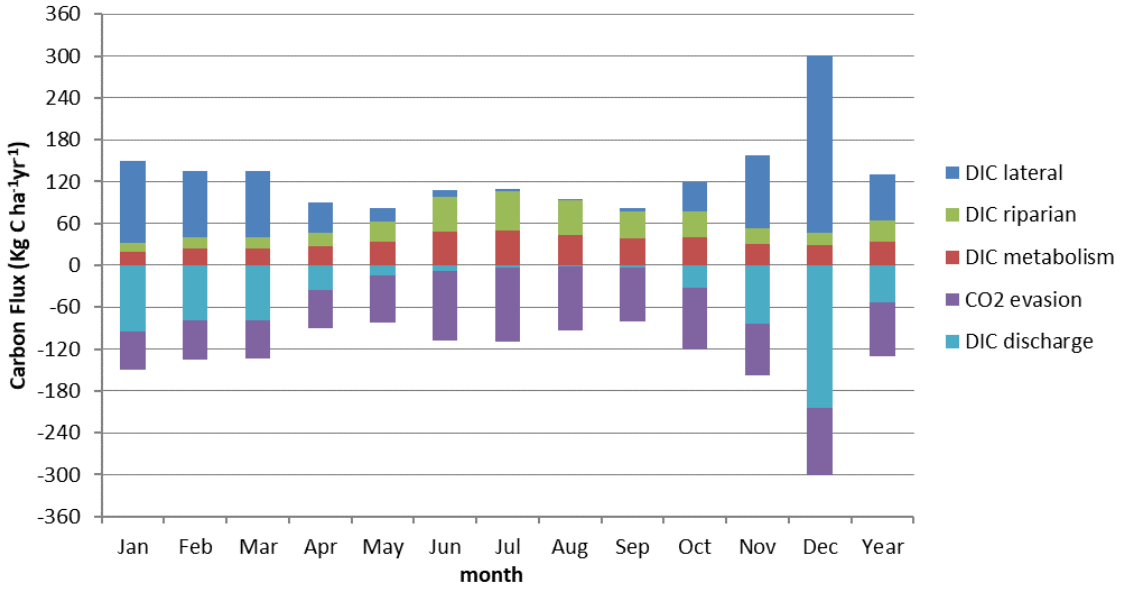


Figure 3.7 – Mean monthly and annual DIC imports and exports. Input data was from October 2014 through January 2017.

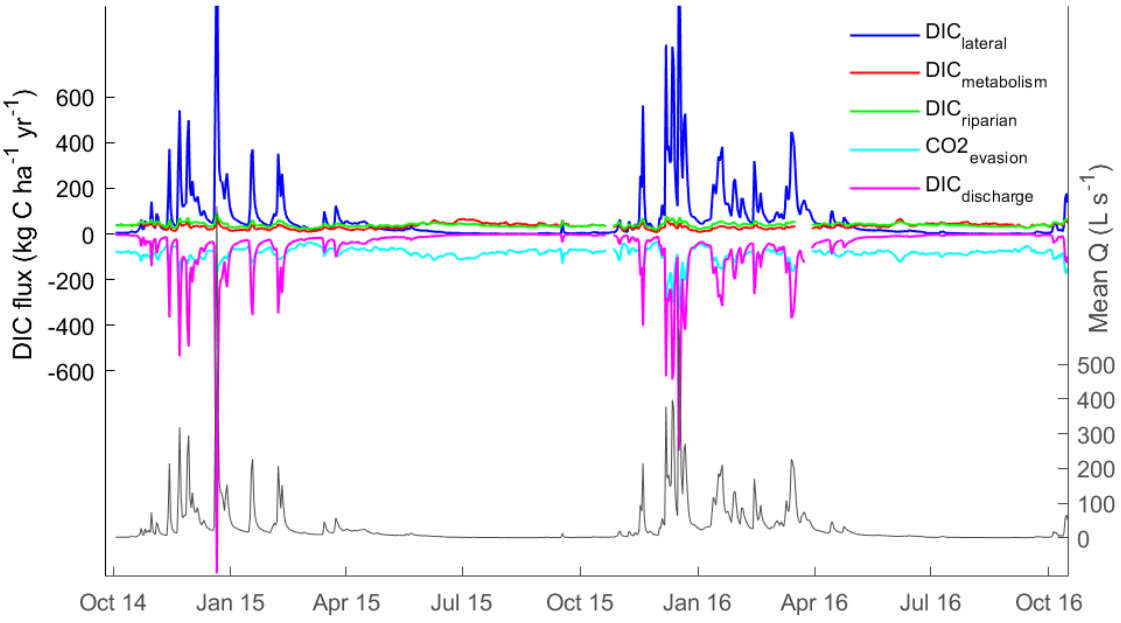


Figure 3.8 – Time series of DIC imports and exports October 2014 through October 2016.

## *3.7 Discussion*

### *3.7.1 DIC Exports*

Discharge of inorganic carbon from rivers to oceans is well understood as a function of rock weathering, and well constrained through measurements of discharge and carbonate chemistry of rivers (Cole et al. 2007). Thus, recent carbon budgets for streams and rivers have focused on constraining estimates of evasion of $CO_2$ from aquatic ecosystems to the atmosphere and instream processing of organic carbon (Butman and Raymond 2011, Raymond et al. 2013, Hotchkiss et al. 2015b). Butman and Raymond (2011) estimated average $CO_2$ outgassing of streams and rivers of the coterminous USA to be 124 ± 43 kg C $ha^{-1}yr^{-1}$, and 70 ± 26 kg C $ha^{-1}yr^{-1}$ for streams in the West. Our estimate of 76.8 ± $\frac{34.4}{30.1}$ kg C $ha^{-1}yr^{-1}$ is in alignment with these values, and also within confidence intervals of recent $CO_2$ evasion estimates of WS1 of 42.2 ± $\frac{209}{7.7}$ kg C $ha^{-1}yr^{-1}$ (Argerich et al. 2016). Per unit stream area, estimated $CO_2$ outgassing of 2421 ± $\frac{1084}{949}$ g C $m^{-2}yr^{-1}$ is consistent with mean estimates from Butman and Raymond (2011) of 2370 ± 800 g C $m^{-2}yr^{-1}$, and 3000 ± 1113 g C $m^{-2}yr^{-1}$ for streams in the West, and within confidence intervals for headwater streams in Sweden of 2869 ± $\frac{1435}{1004}$ g C $m^{-2}yr^{-1}$ (Wallin et al. 2018).

Most other studies estimated evasion rates through direct measurement of $pCO_2$ or estimated $pCO_2$ from carbonate chemistry of water samples, and either measurement of aeration rates or estimated of aeration rates from hydraulics (Marx et al. 2017). This study took an unusual approach of estimating all other imports and exports and deriving $CO_2$ evasion as the remainder. To verify the validity of this approach, we calculated $CO_2$ outgassing using $K_{CO2}$, $CO_{2def}$, and $A_s$ and found an average annual export of 39.2 ± $\frac{30.4}{26.2}$ kg C $ha^{-1}yr^{-1}$. This value is lower than expected, but within 95% confidence intervals. That there is consistency between estimates of $CO_2$ outgassing from alternative methods, other studies of WS1, and macro scale studies indicates that our methods to estimate imports of DIC were reasonable. DIC imports: $DIC_{lateral}$, $DIC_{metabolism}$ and $DIC_{riparian}$, were each

derived entirely from field measurements and/or site specific data. Values from literature were not used to estimate any component of the carbon budget.

### *3.7.2 DIC Imports - Lateral Inflows*

DIC imported to the stream from groundwater or hillslope runoff was estimated to be 65.6 ± $\frac{17}{16.6}$ kg C $ha^{-1}yr^{-1}$, generally consistent with estimates from Argerich et. Al (2016) and global scale studies. Strong seasonality in net flux of $DIC_{lateral}$ to the stream is apparent. This seasonality is driven by the rate of lateral inflows (assumed to be equivalent to stream flow). DIC concentrations of lateral inflows exhibited the opposite seasonal variation with maximum concentrations in the dry season and minimum concentrations in the wet season. Studies of hillslope runoff processes in nearby catchments have estimated mean residence time for precipitation to infiltrate the soil, travel through the weathered rock and/or groundwater systems, and emerge as streamflow of 23 to 55 days during the wet season, and 260 days (or longer) for summer baseflow (McGuire et al. 2005, 2007). Variation in residence times between seasons provides a basis for seasonal fluctuation in chemistry of lateral inflow (Chorover et al. 2017). Solute concentrations and DIC are expected to increase with residence time, consistent with observed increases in EC and DIC of lateral inflow dominated piezometers in the dry season and decreases in the wet season. However, regarding carbon fluxes, seasonal variation in DIC concentrations are orders of magnitude less than variation in lateral inflow rates, thus lateral imports of DIC are much greater during the wet season despite the lower DIC concentration in this period of the year. That aside, accurate estimates of DIC concentrations of lateral inflows, particularly during the wet season, are important for constraining the carbon budget of freshwater systems (Marx et al. 2017).

Errors associated with estimated $DIC_{lateral}$ are difficult to quantify due to spatial variation. Lateral inflow dominated piezometers (C7, D7, E7, and F7) were clustered together at the hillslope transition along the base of a north facing slope of the well field. It is unknown if concentrations at these sites are representative of lateral inflows of the greater catchment. The mean $pCO_2$ of lateral inflow water was estimated to be 6445

ppmv, in the range typical of $pCO_2$ in unsaturated riparian soils near piezometer F2 on the other side of the well field (Brandes 2017). Measurements of $pCO_2$ and DIC from a hillslope piezometer a few hundred meters upstream of the well field had values similar to that of lateral inflow dominated piezometers when sampled during the summer, but much lower concentrations, closer to that of stream water, during the winter (Corson-Rikert et al. 2016). These data suggest that DIC concentrations of lateral inflows used in this study may not be representative of the whole catchment. Further investigation of groundwater and hillslope $pCO_2$ and DIC concentrations over a range of residence times would be useful.

### *3.7.3 DIC Imports - Stream Metabolism*

Mean NEP (per unit stream area) of -2.67±0.02 g $O_2$ $m^{-2}$ $day^{-1}$ or 0.85 ±0.01 g C $m^{-2}$ $day^{-1}$ (coincidental agreement with value of *RQ*) was in the typical range of NEP rates measured at sites within the LTER (Argerich, personal communication), and near the mean (0.87 ±0.06 g C $m^{-2}$ $day^{-1}$) of all sites in the coterminous USA reported and used by (Hotchkiss et al. 2015b). Our initial intention had been to apply timeseries measurements of NEP directly in the final carbon budget; however, DO time series spanned less than half of the study period. To estimate NEP for the complete study period, an alternative method was needed; thus, the Arrhenius equation was used. The Arrhenius equation was also useful for smoothing out periods when measured NEP did not appear reasonable and would have skewed results. However, some patterns of interest were evident in measured NEP.

Storm events at the beginning of the wet season were generally correlated with increases in NEP (more negative), while storm events in mid-winter had less affect. Post-storm increases in NEP could support the hypothesis that respiration rates increase at the beginning of the wet season in response to an influx of organic carbon. Significant increases in DOC concentrations during October and November have been observed within the stream and well field of WS1 (Corson-Rikert et al. 2016). In a multiyear investigation of stream metabolism in Tennessee, USA, increases in NEP were observed in response to

storm events; however, the study did not account for the effect of lateral inflows of potentially low DO groundwater (Roberts et al. 2007). In winter, when temperatures are lower, DOC concentrations have been observed to be lower, respiration rates were also lower. These patterns suggest that NEP is driven in part by temperature and organic carbon supply. Another pattern of interest was that measured NEP decreased substantially when flow was below 1.0 L/s; however, there is concern that equations for hydraulics are not representative for very low flows. Further investigation of NEP at low flows, when a large proportion of total flow is transported through the subsurface, is warranted. For this study, we felt use of the Arrhenius equation to model NEP was appropriate.

Mean annual $DIC_{metabolism}$ was 44% of $CO_{2evasion}$. This fraction is high compared with results from Hotchkiss et al. (2015b), which found estimated internal $CO_2$ production for similar sized streams, with mean discharge between 10 and 100 L $s^{-1}$, to be 25% of $CO_2$ emissions. This study would thus indicate that stream metabolism is of greater influence to carbon budgets for small streams than previous studies have found; however, fluxes are generally consistent and largely within margins of error. Our direct estimate of $CO_{2evasion}$ from $CO_2$ concentrations and aeration rate was 39.2 kg C $ha^{-1}$ $yr^{-1}$ (30% of the total exports), in line with (Hotchkiss et al. 2015b).

### *3.7.4 DIC Imports – Near Stream Riparian Sources*

This is the first carbon budget for a temperate headwater stream, to our knowledge, to explicitly quantify imports of carbon from near-stream riparian sources. We found this flux to be substantial with a mean annual value $29.9 \pm \frac{18.8}{16.3}$ (23% of total imports) and on par with $DIC_{metabolism}$ of $33.8 \pm \frac{17.7}{12.0}$ kg C $ha^{-1}yr^{-1}$.

This "new" category of imported carbon is poorly understood but supported by field measurements. The systematic offset in NEP measured from $CO_2$ versus DO timeseries is the first line of evidence and was used to estimate $DIC_{riparian}$. Calculations of NEP accounted for lateral inflows, thus bias associated with lateral inflows is not expected to explain the offset. Measurements of DIC and DO in stream water dominated piezometers is a second line of evidence. Increases in DIC relative to stream water were

generally more than double decreases in DO on a molar basis (Figure C.7). Metabolic quotients of C released to $O_2$ consumed are expected to be close to 1.0, Bott (2006) recommended a value of 0.85 for RQ. Thus, respiration of dissolved or particulate organic carbon along hyporheic flow paths should result in a similar magnitude increase in DIC relative to decrease in DO. That the ratio of $O_2$ consumed to DIC produced was generally above 2.0 indicates there is an alternative source of DIC along hyporheic flow paths within the riparian zone.

Dosch (2014) estimated hyporheic exchange flows exported $37.5 \pm \frac{84.6}{33.5}$ kg C ha-1yr-1 from the riparian zone to the stream in WS1. Exports were not intended to be analogous with $DIC_{riparian}$ of this study; the analysis did not remove lateral inflow dominated piezometers from the dataset and did not subtract DIC that could be accounted for by measured reductions in DO. We speculate that much of the DIC exported through hyporheic exchange flows is sourced from root respiration within the riparian zone, similar to as occurs in wetland environments in the tropics (Abril et al. 2014). However, further study is necessary to corroborate this assertion.

Based on conceptual models of hyporheic exchange flows, $DIC_{riparian}$ may be significant to the carbon budget of low-order headwater streams in general that have proportionally high rates of hyporheic exchange flow relative to streamflow (Wondzell 2011). This hypothesis is premised on the assumption that $DIC_{riparian}$ is sourced from relatively long hyporheic flow paths that extend beneath and through riparian areas that host productive riparian vegetation. Similarly, riparian vegetation, or aerial macrophytes, with roots that extend directly into the wetted channel could also impart $CO_2$ into streams or rivers, without the reduction in DO associated with C processing through stream metabolism.

### *3.8 Chapter Summary*

Results of this study are consistent with literature and found that a temperate headwater stream imported and exported large volumes of carbon. A complete budget of inorganic imports and exports found DIC exports to be dominated by $CO_2$ evasion at 59%

(76.9 kg C $ha^{-1}yr^{-1}$), while export with streamflow was 41% (53.1 kg C $ha^{-1}yr^{-1}$) of mean annual basin wide flux. DIC imports were attributed to hillslope runoff and groundwater inflow was the dominant carbon source at 50% (65.6 kg C $ha^{-1}yr^{-1}$) of imports. The remaining 50% was partitioned between stream metabolism at 26% (33.8 kg C $ha^{-1}yr^{-1}$) and near stream riparian sources at 23% (29.9 kg C $ha^{-1}yr^{-1}$). This study is the first to quantify near stream riparian sources separate from lateral inflows. It is unclear if riparian sources are significant and ubiquitous to all streams and rivers. Riparian carbon fluxes are certainly deserving of further research.

## *3.9 Acknowledgements*

This research was made possible through support from the National Science Foundation (1417603). Meteorological data and site access were provided by the H. J. Andrews Experimental Forest research program, funded by the National Science Foundation (NSF) LTER (DEB 1440409), US Forest Service Pacific Northwest (USFS PNW), and Oregon State University (OSU). Additional funding was provided from USFS PNW and OSU through the joint venture agreement 10-JV-11261991-055. Water-chemistry samples were run by OSU and the USFS Cooperative Chemical Analytical Laboratory (CCAL).

*3.10 Literature Cited*

Abril, G., J.-M. Martinez, Lf. Artigas, P. Moreira-Turcq, M. F. Benedetti, L. Vidal, T. Meziane, J.-H. Kim, M. C. Bernardes, N. Savoye, J. Deborde, E. L. Souza, P. Alberic, M. F. Landim de Souza, and F. Roland. 2014. Amazon River carbon dioxide outgassing fuelled by wetlands. Nature 505:395–398.

Argerich, A., R. Haggerty, S. L. Johnson, S. M. Wondzell, N. Dosch, H. Corson-Rikert, L. R. Ashkenas, R. Pennington, and C. K. Thomas. 2016. Comprehensive multiyear carbon budget of a temperate headwater stream. Journal of Geophysical Research: Biogeosciences 121:1306–1315.

Arrhenius, S. 1915. Quantitative laws in biological chemistry. Bell, London.

Bott, T. L. 2006. Primary Productivity and Community Respiration. Pages 663–690 *in* F. R. Hauer and G. A. Lamberti, editors. Methods in Stream Ecology (Second Edition). Academic Press, San Diego.

Brandes, J. 2017. The Vadose Zone as a Hyporheic Carbon Source: A Look at Temporal Trends in Hyporheic Zone $pCO_2$.

Butman, D., and P. A. Raymond. 2011. Significant efflux of carbon dioxide from streams and rivers in the United States. Nature Geoscience 4:839–842.

Chorover, J., L. A. Derry, and W. H. McDowell. 2017. Concentration-Discharge Relations in the Critical Zone: Implications for Resolving Critical Zone Structure, Function, and Evolution. Water Resources Research 53:8654–8659.

Cole, and Caracao. 2001. Carbon in catchments: connecting terrestrial carbon losses with aquatic metabolism. Marine and Freshwater Research 52:101–110.

Cole, J. J., Y. T. Prairie, N. F. Caraco, W. H. McDowell, L. J. Tranvik, R. G. Striegl, C. M. Duarte, P. Kortelainen, J. A. Downing, J. J. Middelburg, and J. Melack. 2007. Plumbing the Global Carbon Cycle: Integrating Inland Waters into the Terrestrial Carbon Budget. Ecosystems 10:172–185.

Corson-Rikert, H. A., S. M. Wondzell, R. Haggerty, and M. V. Santelmann. 2016. Carbon dynamics in the hyporheic zone of a headwater mountain stream in the Cascade Mountains, Oregon. Water Resources Research 52:7556–7576.

Crawford, J. T., N. R. Lottig, E. H. Stanley, J. F. Walker, P. C. Hanson, J. C. Finlay, and R. G. Striegl. 2014. $CO_2$ and CH4 emissions from streams in a lake-rich landscape: Patterns, controls, and regional significance. Global Biogeochemical Cycles 28:197–210.

Dosch, N. T. 2014, September 12. Spatiotemporal dynamics and drivers of stream $pCO_2$ in a headwater mountain catchment in the Cascade Mountains, Oregon. Oregon State University, Masters Thesis.

Downing, J. 2012. Global abundance and size distribution of streams and rivers. Inland Waters 2:229–236.

del Giorgio, P. A., and P. J. L. Williams. 2005. Respiration in aquatic ecosystems. Oxford University Press, New York.

Hall, R. O., and J. L. Tank. 2005. Correcting whole-stream estimates of metabolism for groundwater input. Limnology and Oceanography: Methods 3:222–229.

Hope, D., S. M. Palmer, M. F. Billett, and J. J. C. Dawson. 2001. Carbon dioxide and methane evasion from a temperate peatland stream. Limnology and Oceanography 46:847–857.

Hotchkiss, E. R., R. O. Hall Jr, R. A. Sponseller, D. Butman, J. Klaminder, H. Laudon, M. Rosvall, and J. Karlsson. 2015a. Sources of and processes controlling $CO_2$ emissions change with the size of streams and rivers. Nature Geoscience 8:696–699.

Hotchkiss, E. R., R. O. Hall Jr, R. A. Sponseller, D. Butman, J. Klaminder, H. Laudon, M. Rosvall, and J. Karlsson. 2015b. Sources of and processes controlling $CO_2$ emissions change with the size of streams and rivers. Nature Geoscience 8:696–699.

Hotchkiss, E. R., R. O. H. Jr, R. A. Sponseller, D. Butman, J. Klaminder, H. Laudon, M. Rosvall, and J. Karlsson. 2015c. Sources of and processes controlling $CO_2$ emissions change with the size of streams and rivers. Nature Geoscience 8:696–699.

Johnson, M. S., M. F. Billett, K. J. Dinsmore, M. Wallin, K. E. Dyson, and R. S. Jassal. 2010. Direct and continuous measurement of dissolved carbon dioxide in freshwater aquatic systems—method and applications. Ecohydrology 3:68–78.

Johnson, S., and R. Fredriksen. 2016. Stream chemistry concentrations and fluxes using proportional sampling in the Andrews Experimental Forest, 1968 to present. Long-Term Ecological Research. Forest Science Data Bank, Corvallis, OR. [Database]. Available: http://andrewsforest.oregonstate.edu/data/abstract.cfm?dbcode=CF002 (17 February 2017).

Jones, J. B., and P. J. Mulholland. 1998. Influence of drainage basin topography and elevation on carbon dioxide and methane supersaturation of stream water. Biogeochemistry 40:57–72.

Kasahara, and Wondzell. 2003. Geomorphic controls on hyporheic exchange flow in mountain streams. Water Resources Research 39:1005.

Lewis, E., and W. R. Wallace. 1998. Program Developed for $CO_2$ System Calculations. ORNL/CDIAC-105. Carbon Dioxide Information Analysis Center, Oak Ridge National Laboratory, U.S. Department of Energy, Oak Ridge, Tennessee.

Marx, A., J. Dusek, J. Jankovec, M. Sanda, T. Vogel, R. van Geldern, J. Hartmann, and J. a. C. Barth. 2017. A review of $CO_2$ and associated carbon dynamics in headwater streams: A global perspective. Reviews of Geophysics 55:560–585.

Marzolf, E. R., P. J. Mulholland, and A. D. Steinman. 1994. Improvements to the Diurnal Upstream–Downstream Dissolved Oxygen Change Technique for Determining Whole-Stream Metabolism in Small Streams. Canadian Journal of Fisheries and Aquatic Sciences 51:1591–1599.

Marzolf, E. R., P. J. Mulholland, and A. D. Steinman. 1998. Reply: Improvements to the diurnal upstream-downstream dissolved oxygen change technique for determining whole-stream metabolism in small streams. Canadian Journal of Fisheries and Aquatic Sciences 55:1786–1787.

McCutchan, J. Jr. H., J. III. F. Saunders, W. Jr. M. Lewis, and M. G. Hayden. 2002. Effects of groundwater flux on open-channel estimates of stream metabolism. Limnology and Oceanography 47:321–324.

McGuire, K. J., J. J. McDonnell, M. Weiler, C. Kendall, B. L. McGlynn, J. M. Welker, and J. Seibert. 2005. The role of topography on catchment-scale water residence time. Water Resources Research 41.

McGuire, K. J., M. Weiler, and J. J. McDonnell. 2007. Integrating tracer experiments with modeling to assess runoff processes and water transit times. Advances in Water Resources 30:824–837.

Millero, F. J. 1979. The thermodynamics of the carbonate system in seawater. Geochimica et Cosmochimica Acta 43:1651–1661.

Minshall, G. W., R. C. Petersen, K. W. Cummins, T. L. Bott, J. R. Sedell, C. E. Cushing, and R. L. Vannote. 1983. Interbiome Comparison of Stream Ecosystem Dynamics. Ecological Monographs 53:2–25.

Montgomery, D. R., and J. M. Buffington. 1997. Channel-reach morphology in mountain drainage basins. Geological Society of America Bulletin 109:596–611.

Odum, H. T. 1956. Primary Production in Flowing Waters1. Limnology and Oceanography 1:102–117.

Öquist, M. G., M. Wallin, J. Seibert, K. Bishop, and H. Laudon. 2009. Dissolved Inorganic Carbon Export Across the Soil/Stream Interface and Its Fate in a Boreal Headwater Stream. Environmental Science & Technology 43:7364–7369.

Pennington, R., A. Argerich, and R. Haggerty. 2018. Measurement of gas-exchange rate in streams by the oxygen–carbon method. Freshwater Science 37:222–237.

Priest, Black, Woller, and Taylor. 1988. Geologic map of the McKenzie Bridge quadrangle, Lane Co., Oregon. Oregon Dept of Geology and Mineral Industries Geologic Map Series GSM-48, scale 1:62500.

Raymond, P. A., J. Hartmann, R. Lauerwald, S. Sobek, C. McDonald, M. Hoover, D. Butman, R. Striegl, E. Mayorga, C. Humborg, P. Kortelainen, H. Dürr, M. Meybeck, P. Ciais, and P. Guth. 2013. Global carbon dioxide emissions from inland waters. Nature 503:355–359.

Raymond, P. A., C. J. Zappa, D. Butman, T. L. Bott, J. Potter, P. Mulholland, A. E. Laursen, W. H. McDowell, and D. Newbold. 2012. Scaling the gas transfer velocity and hydraulic geometry in streams and small rivers. Limnology and Oceanography: Fluids and Environments 2:41–53.

Roberts, B. J., P. J. Mulholland, and W. R. Hill. 2007. Multiple Scales of Temporal Variability in Ecosystem Metabolism Rates: Results from 2 Years of Continuous Monitoring in a Forested Headwater Stream. Ecosystems 10:588–606.

Schmadel, N. M., A. S. Ward, and S. M. Wondzell. 2017. Hydrologic controls on hyporheic exchange in a headwater mountain stream. Water Resources Research 53:6260–6278.

Swanson, and Dooge. 1975. Geology and geomorphology of the H.J. Andrews Experimental Forest, western Cascades, Oregon Res. Pap. PNW-188. Portland, OR: U.S. Department of Agriculture, Forest Service, Pacific Northwest Forest and Range Experiment Station. 14 p.

Turner, D. P., A. R. Jacobson, W. D. Ritts, W. L. Wang, and R. Nemani. 2013. A large proportion of North American net ecosystem production is offset by emissions from harvested products, river/stream evasion, and biomass burning. Global Change Biology 19:3516–3528.

Vannote, R. L., G. W. Minshall, K. W. Cummins, J. R. Sedell, and C. E. Cushing. 1980. The River Continuum Concept. Canadian Journal of Fisheries and Aquatic Sciences 37:130–137.

Wallin, M. B., A. Campeau, J. Audet, D. Bastviken, K. Bishop, J. Kokic, H. Laudon, E. Lundin, S. Löfgren, S. Natchimuthu, S. Sobek, C. Teutschbein, G. A.

Weyhenmeyer, and T. Grabs. 2018. Carbon dioxide and methane emissions of Swedish low-order streams—a national estimate and lessons learnt from more than a decade of observations. Limnology and Oceanography Letters 3:156–167.

Ward, A. S., M. Fitzgerald, M. N. Gooseff, T. J. Voltz, A. M. Binley, and K. Singha. 2012. Hydrologic and geomorphic controls on hyporheic exchange during base flow recession in a headwater mountain stream. Water Resources Research 48:W04513.

Ward, A. S., M. N. Gooseff, M. Fitzgerald, T. J. Voltz, and K. Singha. 2014. Spatially distributed characterization of hyporheic solute transport during baseflow recession in a headwater mountain stream using electrical geophysical imaging. Journal of Hydrology 517:362–377.

Ward, A. S., M. N. Gooseff, and K. Singha. 2010. Characterizing hyporheic transport processes — Interpretation of electrical geophysical data in coupled stream–hyporheic zone systems during solute tracer studies. Advances in Water Resources 33:1320–1330.

Ward, N. D., T. S. Bianchi, P. M. Medeiros, M. Seidel, J. E. Richey, R. G. Keil, and H. O. Sawakuchi. 2017. Where Carbon Goes When Water Flows: Carbon Cycling across the Aquatic Continuum. Frontiers in Marine Science 4.

Wondzell, S. M. 2006. Effect of morphology and discharge on hyporheic exchange flows in two small streams in the Cascade Mountains of Oregon, USA. Hydrological Processes 20:267–287.

Wondzell, S. M. 2011. The role of the hyporheic zone across stream networks. Hydrological Processes 25:3525–3532.

# 4 Conclusion

Development of methods and field measurement of the aeration rates through use of the newly formulated oxygen carbon method was a success. Predicted gas exchange rates over a three-day period during baseflow conditions on a fourth order mountain stream were consistent with the measured aeration rate found through propane gas injection. Long term monitoring over multiple months in Watershed 1, a second order headwater stream, allowed for measurement of the aeration rate over a range of discharge conditions. The aeration rate was a critical parameter in the measurement of stream metabolism and development of a stream carbon budget.

Results of the carbon budget for Watershed 1 were consistent with literature and found that the temperate headwater stream imported and exported large volumes of carbon. DIC exports were dominated by $CO_2$ evasion at 59% (77.1 kg C $ha^{-1}yr^{-1}$), while DIC export with streamflow constituted 41% (53.2 kg C $ha^{-1}yr^{-1}$). Hillslope runoff and groundwater inflow were the dominant carbon source at 50% (65.6 kg C $ha^{-1}yr^{-1}$) of imports. The remaining 50% was partitioned between stream metabolism at 26% (34 kg C $ha^{-1}yr^{-1}$) and near stream riparian sources at 23% (30.5 kg C $ha^{-1}yr^{-1}$). These C fluxes are significant and on par with published rates of terrestrial NEP. This is the first study of a low-order stream to quantify near stream riparian sources separate from lateral inflows or stream metabolism. It is unclear if riparian sources are significant and ubiquitous across riverscapes.

The carbon budget was developed through use of high resolution timeseries data allowing for event driven fluxes to be incorporated. Analysis was multidisciplinary in nature and contributes to our understanding of hydrologic and biogeochemical processes that regulate C processing in headwater streams.

# BIBLIOGRAPHY

Abril, G., J.-M. Martinez, Lf. Artigas, P. Moreira-Turcq, M. F. Benedetti, L. Vidal, T. Meziane, J.-H. Kim, M. C. Bernardes, N. Savoye, J. Deborde, E. L. Souza, P. Alberic, M. F. Landim de Souza, and F. Roland. 2014. Amazon River carbon dioxide outgassing fuelled by wetlands. Nature 505:395–398.

Argerich, A., R. Haggerty, S. L. Johnson, S. M. Wondzell, N. Dosch, H. Corson-Rikert, L. R. Ashkenas, R. Pennington, and C. K. Thomas. 2016. Comprehensive multiyear carbon budget of a temperate headwater stream. Journal of Geophysical Research: Biogeosciences 121:1306–1315.

Aristegi, L., O. Izagirre, and A. Elosegi. 2009. Comparison of several methods to calculate reaeration in streams, and their effects on estimation of metabolism. Hydrobiologia 635:113–124.

Arrhenius, S. 1915. Quantitative laws in biological chemistry. Bell, London.

Aufdenkampe, A. K., E. Mayorga, P. A. Raymond, J. M. Melack, S. C. Doney, S. R. Alin, R. E. Aalto, and K. Yoo. 2011. Riverine coupling of biogeochemical cycles between land, oceans, and atmosphere. Frontiers in Ecology and the Environment 9:53–60.

Barnes, I. 1965. Geochemistry of Birch Creek, Inyo County, California a travertine depositing creek in an arid climate. Geochimica et Cosmochimica Acta 29:28.

Battin, T. J., L. A. Kaplan, S. Findlay, C. S. Hopkinson, E. Marti, A. I. Packman, J. D. Newbold, and F. Sabater. 2008. Biophysical controls on organic carbon fluxes in fluvial networks. Nature Geoscience 1:95–100.

Bencala, K. E., and R. A. Walters. 1983. Simulation of solute transport in a mountain pool-and-riffle stream: A transient storage model. Water Resources Research 19:718–724.

Bennett, J. P. 1972. Reaeration in open-channel flow. Geological Survey Professional Paper 737. U.S. Geological Survey, Washington, DC.

Birkel, C., C. Soulsby, I. Malcolm, and D. Tetzlaff. 2013. Modeling the dynamics of metabolism in montane streams using continuous dissolved oxygen measurements. Water Resources Research 49:5260–5275.

Birnbaum, Z. W., E. Lukacs, P. Révész, and P. Révész. 1967. The Laws of Large Numbers. Academic Press/Elsevier Science, Burlington.

Bott, T. L. 2006. Primary Productivity and Community Respiration. Pages 663–690 *in* F. R. Hauer and G. A. Lamberti, editors. Methods in Stream Ecology (Second Edition). Academic Press, San Diego.

Brandes, J. 2017. The Vadose Zone as a Hyporheic Carbon Source : A Look at Temporal Trends in Hyporheic Zone $pCO_2$.

Butman, D., and P. A. Raymond. 2011. Significant efflux of carbon dioxide from streams and rivers in the United States. Nature Geoscience 4:839–842.

Chapra, S., and D. Di Toro. 1991. Delta Method For Estimating Primary Production, Respiration, And Reaeration In Streams. Journal of Environmental Engineering 117:640–655.

Chorover, J., L. A. Derry, and W. H. McDowell. 2017. Concentration-Discharge Relations in the Critical Zone: Implications for Resolving Critical Zone Structure, Function, and Evolution. Water Resources Research 53:8654–8659.

Cole, and Caracao. 2001. Carbon in catchments: connecting terrestrial carbon losses with aquatic metabolism. Marine and Freshwater Research 52:101–110.

Cole, J. J., Y. T. Prairie, N. F. Caraco, W. H. McDowell, L. J. Tranvik, R. G. Striegl, C. M. Duarte, P. Kortelainen, J. A. Downing, J. J. Middelburg, and J. Melack. 2007. Plumbing the Global Carbon Cycle: Integrating Inland Waters into the Terrestrial Carbon Budget. Ecosystems 10:172–185.

Cole, J., G. Lovett, S. Findlay, and Cary Conference. 1991. Comparative analyses of ecosystems : patterns, mechanisms, and theories. Springer-Verlag, New York.

Corson-Rikert, H. A., S. M. Wondzell, R. Haggerty, and M. V. Santelmann. 2016. Carbon dynamics in the hyporheic zone of a headwater mountain stream in the Cascade Mountains, Oregon. Water Resources Research 52:7556–7576.

Covar, A. 1976. Selecting the Proper Reaeration Coefficient for Use in Water Quality Models. Presented at the US EPA Conference on Environmental Simulation and Modeling, April 19–22, Cincinnati, Ohio.

Crawford, J. T., N. R. Lottig, E. H. Stanley, J. F. Walker, P. C. Hanson, J. C. Finlay, and R. G. Striegl. 2014. $CO_2$ and CH4 emissions from streams in a lake-rich landscape: Patterns, controls, and regional significance. Global Biogeochemical Cycles 28:197–210.

Crawford, J. T., R. G. Striegl, K. P. Wickland, M. M. Dornblaser, and E. H. Stanley. 2013. Emissions of carbon dioxide and methane from a headwater stream network of interior Alaska. Journal of Geophysical Research: Biogeosciences 118:482–494.

Davies, J. T., A. A. Kilner, and G. A. Ratcliff. 1964. The effect of diffusivities and surface films on rates of gas absorption. Chemical Engineering Science 19:583–590.

Day, T. J. 1976. On the precision of salt dilution gauging. Journal of Hydrology 31:293–306.

Demars, B. O. l., J. Russell Manson, J. S. Ólafsson, G. M. Gíslason, R. Gudmundsdóttir, G. Woodward, J. Reiss, D. E. Pichler, J. J. Rasmussen, and N. Friberg. 2011. Temperature and the metabolic balance of streams. Freshwater Biology 56:1106–1121.

Demars, B. O. L., J. Thompson, and J. R. Manson. 2015. Stream metabolism and the open diel oxygen method: Principles, practice, and perspectives. Limnology and Oceanography: Methods 13:356–374.

Dosch, N. T. 2014, September 12. Spatiotemporal dynamics and drivers of stream $pCO_2$ in a headwater mountain catchment in the Cascade Mountains, Oregon. Oregon State University, Masters Thesis.

Downing, J. 2012. Global abundance and size distribution of streams and rivers. Inland Waters 2:229–236.

Fischer, H. B. 1972. A Lagrangian method of predicting pollutant dispersion in Bolinas Lagoon, Marin County, California. Geological Survey Professional Paper 582-B. U.S. Geological Survey.

Fredriksen, R. L., F. M. McCorison, and F. J. Swanson. 1983. Material transfer in a western Oregon forested watershed. U.S. Dept. of Agriculture, Forest Service.

del Giorgio, P. A., and P. J. L. Williams. 2005. Respiration in aquatic ecosystems. Oxford University Press, New York.

Hall, R. O., and J. L. Tank. 2005. Correcting whole-stream estimates of metabolism for groundwater input. Limnology and Oceanography: Methods 3:222–229.

Hensley, R. T., and M. J. Cohen. 2016. On the emergence of diel solute signals in flowing waters. Water Resources Research 52:759–772.

Holtgrieve, G. W., D. E. Schindler, T. A. Branch, and Z. T. A'mar. 2010. Simultaneous quantification of aquatic ecosystem metabolism and reaeration using a Bayesian statistical model of oxygen dynamics. Limnology and Oceanography 55:1047–1063.

Holtgrieve, G. W., D. E. Schindler, and K. Jankowski. 2016. Comment on Demars et al. 2015, "Stream metabolism and the open diel oxygen method: Principles, practice, and perspectives." Limnology and Oceanography: Methods 14:110–113.

Hope, D., S. M. Palmer, M. F. Billett, and J. J. C. Dawson. 2001. Carbon dioxide and methane evasion from a temperate peatland stream. Limnology and Oceanography 46:847–857.

Hornberger, G., and M. Kelly. 1975. Atmospheric Reaeration in a River Using Productivity Analysis. Journal of the Environmental Engineering Division-Asce 101:729–739.

Hotchkiss, E. R., R. O. Hall Jr, R. A. Sponseller, D. Butman, J. Klaminder, H. Laudon, M. Rosvall, and J. Karlsson. 2015a. Sources of and processes controlling $CO_2$ emissions change with the size of streams and rivers. Nature Geoscience 8:696–699.

Hotchkiss, E. R., R. O. Hall Jr, R. A. Sponseller, D. Butman, J. Klaminder, H. Laudon, M. Rosvall, and J. Karlsson. 2015b. Sources of and processes controlling $CO_2$

emissions change with the size of streams and rivers. Nature Geoscience 8:696–699.

Hotchkiss, E. R., and R. O. Hall Jr. 2014. High rates of daytime respiration in three streams: Use of δ18O and $O_2$ to model diel ecosystem metabolism. Limnology and Oceanography 59:798–810.

Hotchkiss, E. R., R. O. H. Jr, R. A. Sponseller, D. Butman, J. Klaminder, H. Laudon, M. Rosvall, and J. Karlsson. 2015c. Sources of and processes controlling $CO_2$ emissions change with the size of streams and rivers. Nature Geoscience 8:696–699.

Jähne, B., K. O. Münnich, R. Bösinger, A. Dutzi, W. Huber, and P. Libner. 1987. On the parameters influencing air-water gas exchange. Journal of Geophysical Research: Oceans 92:1937–1949.

Johnson, M. S., M. F. Billett, K. J. Dinsmore, M. Wallin, K. E. Dyson, and R. S. Jassal. 2010. Direct and continuous measurement of dissolved carbon dioxide in freshwater aquatic systems—method and applications. Ecohydrology 3:68–78.

Johnson, S., and R. Fredriksen. 2016. Stream chemistry concentrations and fluxes using proportional sampling in the Andrews Experimental Forest, 1968 to present. Long-Term Ecological Research. Forest Science Data Bank, Corvallis, OR. [Database]. Available: http://andrewsforest.oregonstate.edu/data/abstract.cfm?dbcode=CF002 (17 February 2017).

Johnston, and Williams. 2006. Field comparison of Optical and Clark cell dissolved oxygen sensors in the Tualatin River, Oregon, 2005. U.S. Geological Survey, Reston, Va.

Jones, J. B., and P. J. Mulholland. 1998. Influence of drainage basin topography and elevation on carbon dioxide and methane supersaturation of stream water. Biogeochemistry 40:57–72.

Kadmon, R., O. Farber, and A. Danin. 2003. A Systematic Analysis of Factors Affecting the Performance of Climatic Envelope Models. Ecological Applications 13:853–867.

Kaplan, L. A., and T. L. Bott. 1982. Diel fluctuations of DOC generated by algae in a piedmont stream. Limnology and Oceanography 27:1091–1100.

Kasahara, and Wondzell. 2003. Geomorphic controls on hyporheic exchange flow in mountain streams. Water Resources Research 39:1005.

Kelly, M. G., M. R. Church, and G. M. Hornberger. 1974. A solution of the inorganic carbon mass balance equation and its relation to algal growth rates. Water Resources Research 10:493–497.

Kelly, M. G., N. Thyssen, and B. Moeslund. 1983. Light and the annual variation of oxygen- and carbon-based measurements of productivity in a macrophyte-dominated river1. Limnology and Oceanography 28:503–515.

Khadka, M. B., J. B. Martin, and J. Jin. 2014. Transport of dissolved carbon and $CO_2$ degassing from a river system in a mixed silicate and carbonate catchment. Journal of Hydrology 513:391–402.

Kilpatrick, F. A., and E. D. Cobb. 1985. Measurement of Discharge Using Tracers: U.S. Geological Survey Techniques of Water-Resources Investigations, book 3, chap. A16. Page 52.

Kilpatrick, Rathbun, Yotsukura, and Parker. 1989. Determination of stream reaeration coefficients by use of tracers. Dept of the Interior, US Geological Survey; Denver, CO.

Knapp, J. L. A., K. Osenbrück, and O. A. Cirpka. 2015. Impact of non-idealities in gas-tracer tests on the estimation of reaeration, respiration, and photosynthesis rates in streams. Water Research 83:205–216.

Koffi, E. N., P. J. Rayner, M. Scholze, and C. Beer. 2012. Atmospheric constraints on gross primary productivity and net ecosystem productivity: Results from a carbon-cycle data assimilation system. Global Biogeochemical Cycles 26:GB1024.

Leith, F. I., K. J. Dinsmore, M. B. Wallin, M. F. Billett, K. V. Heal, H. Laudon, M. G. Öquist, and K. Bishop. 2015. Carbon dioxide transport across the hillslope–riparian–stream continuum in a boreal headwater catchment. Biogeosciences 12:1881–1892.

Lewis, E., and W. R. Wallace. 1998. Program Developed for $CO_2$ System Calculations. ORNL/CDIAC-105. Carbon Dioxide Information Analysis Center, Oak Ridge National Laboratory, U.S. Department of Energy, Oak Ridge, Tennessee.

Lorah, M. M., and J. S. Herman. 1988. The chemical evolution of a travertine-depositing stream: geochemical processes and mass transfer reactions. Water Resources Research 24:1541–1552.

Luo, Y. 2006. Soil respiration and the environment. Elsevier Academic Press, Amsterdam ; Boston.

Marx, A., J. Dusek, J. Jankovec, M. Sanda, T. Vogel, R. van Geldern, J. Hartmann, and J. a. C. Barth. 2017. A review of $CO_2$ and associated carbon dynamics in headwater streams: A global perspective. Reviews of Geophysics 55:560–585.

Marzolf, E. R., P. J. Mulholland, and A. D. Steinman. 1994. Improvements to the Diurnal Upstream–Downstream Dissolved Oxygen Change Technique for Determining Whole-Stream Metabolism in Small Streams. Canadian Journal of Fisheries and Aquatic Sciences 51:1591–1599.

Marzolf, E. R., P. J. Mulholland, and A. D. Steinman. 1998. Reply: Improvements to the diurnal upstream-downstream dissolved oxygen change technique for determining whole-stream metabolism in small streams. Canadian Journal of Fisheries and Aquatic Sciences 55:1786–1787.

McCutchan, J. H., W. M. Lewis, and J. F. Saunders. 1998. Uncertainty in the Estimation of Stream Metabolism from Open-Channel Oxygen Concentrations. Journal of the North American Benthological Society 17:155–164.

McCutchan, J. Jr. H., J. III. F. Saunders, W. Jr. M. Lewis, and M. G. Hayden. 2002. Effects of groundwater flux on open-channel estimates of stream metabolism. Limnology and Oceanography 47:321–324.

McGuire, K. J., J. J. McDonnell, M. Weiler, C. Kendall, B. L. McGlynn, J. M. Welker, and J. Seibert. 2005. The role of topography on catchment-scale water residence time. Water Resources Research 41.

McGuire, K. J., M. Weiler, and J. J. McDonnell. 2007. Integrating tracer experiments with modeling to assess runoff processes and water transit times. Advances in Water Resources 30:824–837.

Millero, F. J. 1979. The thermodynamics of the carbonate system in seawater. Geochimica et Cosmochimica Acta 43:1651–1661.

Minshall, G. W., R. C. Petersen, K. W. Cummins, T. L. Bott, J. R. Sedell, C. E. Cushing, and R. L. Vannote. 1983. Interbiome Comparison of Stream Ecosystem Dynamics. Ecological Monographs 53:2–25.

de Montety, V., J. B. Martin, M. J. Cohen, C. Foster, and M. J. Kurz. 2011. Influence of diel biogeochemical cycles on carbonate equilibrium in a karst river. Chemical Geology 283:31–43.

Montgomery, D. R., and J. M. Buffington. 1997. Channel-reach morphology in mountain drainage basins. Geological Society of America Bulletin 109:596–611.

Moran, M. A., and R. G. Zepp. 1997. Role of photoreactions in the formation of biologically labile compounds from dissolved organic matter. Limnology and Oceanography 42:1307–1316.

Mulholland, P. J., C. S. Fellows, J. L. Tank, N. B. Grimm, J. R. Webster, S. K. Hamilton, E. Martí, L. Ashkenas, W. B. Bowden, W. K. Dodds, W. H. Mcdowell, M. J. Paul, and B. J. Peterson. 2001. Inter-biome comparison of factors controlling stream metabolism. Freshwater Biology 46:1503–1517.

National Oceanic and Atmospheric Administration. 2016. Annual Mean Carbon Dioxide Data.

Odum, H. T. 1956. Primary Production in Flowing Waters1. Limnology and Oceanography 1:102–117.

Oh, N. H., and D. D. Richter. 2004. Soil acidification induced by elevated atmospheric $CO_2$. Global Change Biology 10:1936–1946.

Öquist, M. G., M. Wallin, J. Seibert, K. Bishop, and H. Laudon. 2009. Dissolved Inorganic Carbon Export Across the Soil/Stream Interface and Its Fate in a Boreal Headwater Stream. Environmental Science & Technology 43:7364–7369.

Palumbo, J., and L. Brown. 2013. Assessing the Performance of Reaeration Prediction Equations. Journal of Environmental Engineering 140.

Pennington, R., A. Argerich, and R. Haggerty. 2018. Measurement of gas-exchange rate in streams by the oxygen–carbon method. Freshwater Science 37:222–237.

Perkins, D. M., G. Yvon-Durocher, B. O. L. Demars, J. Reiss, D. E. Pichler, N. Friberg, M. Trimmer, and G. Woodward. 2012. Consistent temperature dependence of respiration across ecosystems contrasting in thermal history. Global Change Biology 18:1300–1311.

Plummer, L. N., and E. Busenberg. 1982. The solubilities of calcite, aragonite and vaterite in $CO_2$-$H_2O$ solutions between 0 and 90°C, and an evaluation of the aqueous model for the system $CaCO_3$-$CO_2$-$H_2O$. Geochimica et Cosmochimica Acta 46:1011–1040.

Priest, Black, Woller, and Taylor. 1988. Geologic map of the McKenzie Bridge quadrangle, Lane Co., Oregon. Oregon Dept of Geology and Mineral Industries Geologic Map Series GSM-48, scale 1:62500.

Rathbun, R. E., D. Y. Tai, D. J. Shultz, and D. W. Stephens. 1978. Laboratory Studies of Gas Tracers for Reaeration. Journal of the Environmental Engineering Division 104:215–229.

Raven, J. A., and J. Beardall. 2005. Respiration in aquatic photolithotrophs. Page Respiration in aquatic ecosystems. Oxford University Press, New York.

Raymond, P. A., and J. J. Cole. 2001. Gas exchange in rivers and estuaries: Choosing a gas transfer velocity. Estuaries 24:312–317.

Raymond, P. A., J. Hartmann, R. Lauerwald, S. Sobek, C. McDonald, M. Hoover, D. Butman, R. Striegl, E. Mayorga, C. Humborg, P. Kortelainen, H. Dürr, M. Meybeck, P. Ciais, and P. Guth. 2013. Global carbon dioxide emissions from inland waters. Nature 503:355–359.

Raymond, P. A., C. J. Zappa, D. Butman, T. L. Bott, J. Potter, P. Mulholland, A. E. Laursen, W. H. McDowell, and D. Newbold. 2012. Scaling the gas transfer velocity and hydraulic geometry in streams and small rivers. Limnology and Oceanography: Fluids and Environments 2:41–53.

Reichert, P., U. Uehlinger, and V. Acuña. 2009. Estimating stream metabolism from oxygen concentrations: Effect of spatial heterogeneity. Journal of Geophysical Research: Biogeosciences 114:G03016.

Riley, A. J., and W. K. Dodds. 2013. Whole-stream metabolism: strategies for measuring and modeling diel trends of dissolved oxygen. Freshwater Science 32:56–69.

R.K. Pachauri, and L.A. Meyer. (n.d.). IPCC, 2014: Climate Change 2014: Synthesis Report. Contribution of Working Groups I, II and III to the Fifth Assessment Report of the Intergovernmental Panel on Climate Change. Page 151. IPCC, Geneva, Switzerland.

Roberts, B. J., P. J. Mulholland, and W. R. Hill. 2007. Multiple Scales of Temporal Variability in Ecosystem Metabolism Rates: Results from 2 Years of Continuous Monitoring in a Forested Headwater Stream. Ecosystems 10:588–606.

Ryther, J. H. 1956. The Measurement of Primary Production1. Limnology and Oceanography 1:72–84.

Schmadel, N. M., A. S. Ward, and S. M. Wondzell. 2017. Hydrologic controls on hyporheic exchange in a headwater mountain stream. Water Resources Research 53:6260–6278.

Sherman, L. A., and P. Barak. 2000. Solubility and Dissolution Kinetics of Dolomite in Ca–Mg–HCO /CO Solutions at 25°C and 0.1 MPa Carbon Dioxide. Soil Science Society of America Journal 64:1959–1968.

Spiro, B., and A. Pentecost. 1991. One day in the life of a stream—a diurnal inorganic carbon mass balance for a travertine-depositing stream (waterfall beck, Yorkshire). Geomicrobiology Journal 9:1–11.

Stumm, J., and J. Morgan. 1996. Aquatic Chemistry: Chemical Equilibria and Rates in Natural Waters (3rd ed., Environmental science and technology). Wiley, New York.

Swanson, and Dooge. 1975. Geology and geomorphology of the H.J. Andrews Experimental Forest, western Cascades, Oregon Res. Pap. PNW-188. Portland, OR: U.S. Department of Agriculture, Forest Service, Pacific Northwest Forest and Range Experiment Station. 14 p.

Thyssen, N., and M. G. Kelly. 1985. Water-air exchange of carbon dioxide and oxygen in a river: measurement and comparison of rates. Archiv für Hydrobiologie 105:219–228.

Tobias, C., and J. K. Böhlke. 2011. Biological and geochemical controls on diel dissolved inorganic carbon cycling in a low-order agricultural stream: Implications for reach scales and beyond. Chemical Geology 283:18–30.

Tobias, C. R., J. K. Böhlke, and J. W. Harvey. 2007. The oxygen-18 isotope approach for measuring aquatic metabolism in high productivity waters. Limnology and Oceanography 52:1439–1453.

Tsivoglou, E. C., and L. A. Neal. 1976. Tracer Measurement of Reaeration: III. Predicting the Reaeration Capacity of Inland Streams. Journal (Water Pollution Control Federation) 48:2669–2689.

Tsivoglou, E., and L. Neal. (n.d.). Tracer Measurement of Reaeration .3. Predicting Reaeration Capacity of Inland Streams. Journal Water Pollution Control Federation 48:2669–2689.

Turner, D. P., A. R. Jacobson, W. D. Ritts, W. L. Wang, and R. Nemani. 2013. A large proportion of North American net ecosystem production is offset by emissions from harvested products, river/stream evasion, and biomass burning. Global Change Biology 19:3516–3528.

Turner, D. P., W. D. Ritts, Z. Yang, R. E. Kennedy, W. B. Cohen, M. V. Duane, P. E. Thornton, and B. E. Law. 2011. Decadal Trends in Net Ecosystem Production and Net Ecosystem Carbon Balance for a Regional Socioecological System.

U.S. Geological Survey. 1981. Water Quality Branch Technical Memorandum No. 81.11.

Vannote, R. L., G. W. Minshall, K. W. Cummins, J. R. Sedell, and C. E. Cushing. 1980. The River Continuum Concept. Canadian Journal of Fisheries and Aquatic Sciences 37:130–137.

Wallin, M. B., A. Campeau, J. Audet, D. Bastviken, K. Bishop, J. Kokic, H. Laudon, E. Lundin, S. Löfgren, S. Natchimuthu, S. Sobek, C. Teutschbein, G. A. Weyhenmeyer, and T. Grabs. 2018. Carbon dioxide and methane emissions of Swedish low-order streams—a national estimate and lessons learnt from more than a decade of observations. Limnology and Oceanography Letters 3:156–167.

Wanninkhof, R., P. J. Mulholland, and J. W. Elwood. 1990. Gas exchange rates for a first-order stream determined with deliberate and natural tracers. Water Resources Research 26:1621–1630.

Ward, A. S., M. Fitzgerald, M. N. Gooseff, T. J. Voltz, A. M. Binley, and K. Singha. 2012. Hydrologic and geomorphic controls on hyporheic exchange during base flow recession in a headwater mountain stream. Water Resources Research 48:W04513.

Ward, A. S., M. N. Gooseff, M. Fitzgerald, T. J. Voltz, and K. Singha. 2014. Spatially distributed characterization of hyporheic solute transport during baseflow recession in a headwater mountain stream using electrical geophysical imaging. Journal of Hydrology 517:362–377.

Ward, A. S., M. N. Gooseff, and K. Singha. 2010. Characterizing hyporheic transport processes — Interpretation of electrical geophysical data in coupled stream–hyporheic zone systems during solute tracer studies. Advances in Water Resources 33:1320–1330.

Ward, N. D., T. S. Bianchi, P. M. Medeiros, M. Seidel, J. E. Richey, R. G. Keil, and H. O. Sawakuchi. 2017. Where Carbon Goes When Water Flows: Carbon Cycling across the Aquatic Continuum. Frontiers in Marine Science 4.

Wondzell, S. M. 2006. Effect of morphology and discharge on hyporheic exchange flows in two small streams in the Cascade Mountains of Oregon, USA. Hydrological Processes 20:267–287.

Wondzell, S. M. 2011. The role of the hyporheic zone across stream networks. Hydrological Processes 25:3525–3532.

Wright, J. C., and I. K. Mills. 1967. Productivity Studies on the Madison River, Yellowstone National Park1. Limnology and Oceanography 12:568–577.

Yoon, T. K., H. Jin, N.-H. Oh, and J.-H. Park. 2016. Technical note: Applying equilibration systems to continuous measurements of $pCO_2$ in inland waters. Biogeosciences Discuss. 2016:1–34.

Young, R. G., and A. D. Huryn. 1998. Comment: Improvements to the diurnal upstream-downstream dissolved oxygen change technique for determining whole-stream metabolism in small streams. Canadian Journal of Fisheries and Aquatic Sciences 55:1784–1785.

# APPENDICES

# Appendix A – Oxygen Carbon Method Supplemental Information

## *Measurements*

A constant rate injection of NaCl salt tracer was conducted August 11, 2015 to measure discharge and mean travel time. Discharge, mean travel time, and mean velocity were calculated from the conservative tracer breakthrough curves (Kilpatrick and Cobb 1985) using electrical conductivity (EC) as a surrogate for concentration. EC was measured and logged at the upstream and downstream end of the study reach with WTW (Weilheim, Germany) Cond 3310 meters. Mean travel time was calculated by measuring the offset in time to achieve half plateau EC values at the upstream and downstream station. Discharge was calculated by dilution gaging. Mean depth was calculated from discharge, velocity, and mean width. Alkalinity samples were run by Oregon State University and United States Forest Service Cooperative Chemical Analytical Laboratory by titrating samples to a pH of 4.5 on a Hach (Loveland Colorado) Radiometer TIM840 AutoTitrator.

DO and temperature were measured with YSI (Yellow Springs, Ohio) 600 OMS - V2 sondes, model 6150 ROX DO. Prior to deployment, DO sondes were calibrated and left to run in water saturated air for three hours in the lab. This operation was repeated at the end of the deployment, when the sondes were back in the lab to check for drift. To cross-calibrate sensors, once in the field and right before and after deployment, all sondes were placed adjacent to one another for two hours in the stream collecting data prior and post.

Molar concentration $CO_2$ was measured at the upstream and downstream end of the study reach using Vaisala (Vantaa, Finland) Carbocap GMM220 $CO_2$ sensors, modified following Johnson et al. (2010), wired to Campbell Scientific dataloggers. Sensors were attached to the bottom of floats to maintain a consistent water depth. Sensors were calibrated prior to deployment in 1010 ppm $CO_2$ standard air. Similar to DO sondes, $CO_2$ sensors were placed adjacent to one another for two hours in the stream collecting data prior and post deployment. $CO_2$ data was post processed and converted to partial pressure

$CO_2$ according to barometric pressure, water temperature, and water depth per Johnson et al. 2010).

*Carbonate Chemistry Simplification*

As formulated in this study the OC method relies on measurement of DO, $CO_2$ and DIC. Continuous measurement of DIC is technically challenging, however for low alkalinity waters, DIC measurement is unnecessary for the OC method. In this study we calculated DIC from continuously measured $CO_2$ and mean alkalinity of point samples. DIC can be calculated from two out of the following concentrations: pH, $CO_2$, alkalinity, $HCO_3^-$, and $CO_3^{2-}$ (Stumm and Morgan 1996). If alkalinity were not expected to be a constant, continuous measurement of pH could be used as an alternative to alkalinity as a means to calculate DIC. pH bulbs have a tendency to drift, require frequent calibration, and have limited precision (Ben-Yaakov, 1981). However, significant simplification can be made for low alkalinity water (below about 500 μeq/L when $CO_2$ is above saturation) where $\Delta CO_2$ can be substituted for $\Delta DIC$. A plot of $CO_2$ vs DIC at 20 ˚C, 1 atm, and fixed alkalinity of 500 μmol/L is provided in Figure A.1, and demonstrates the near 1:1 relationship between $CO_2$ to DIC over a large range of $CO_2$ concentrations. An additional figure (Figure A.2) is also included that plots $\Delta DIC/\Delta CO_2$ vs $pCO_2$ for waters over a range of alkalinities. Carbonate speciation was calculated using CO2SYS version 1.1 coded in Matlab (Lewis and Wallace 1998). Our study site had low alkalinity water (382 μeq/L), and the influence on mean $K_{DO}$ by OC from the above simplification was less than 1%. For waters with high alkalinity (above about 500 μmol/L), we do not recommend substituting $\Delta CO_2$ for $\Delta DIC$. Under these circumstances DIC ought to be measured or calculated; however, as noted above, practical challenges exist to collection of continuous and accurate carbonate chemistry data.

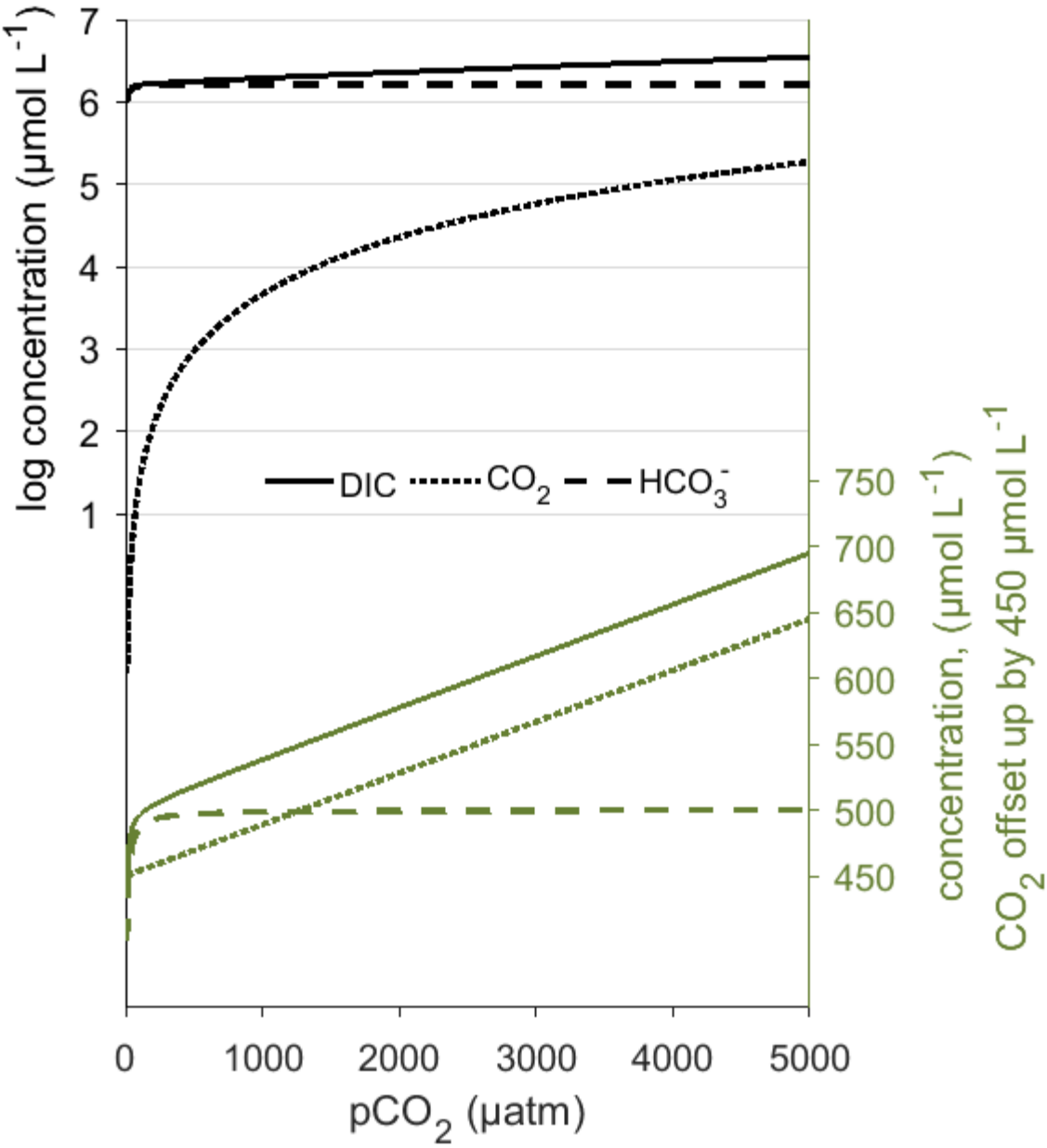


Figure A.1 – DIC, dissolved $CO_2$, and $HCO_3^{2-}$ calculated from partial pressure $CO_2$ and alkalinity using CO2SYS version 1.1 coded in Matlab (Lewis and Wallace 1998), at 1 atm, and fixed alkalinity of 500 µeq/L. $CO_2$ and DIC are parallel when $CO_2$ concentrations are above 500 µatm. This relationship allows for ΔDIC to be substituted by $\Delta CO_2$ in freshwater systems with alkalinities below about 500 µeq/L if $CO_2$ concentrations are above about 500 µatm. Temperature dependent equilibrium constants from (Millero 1979) were selected for calculations.

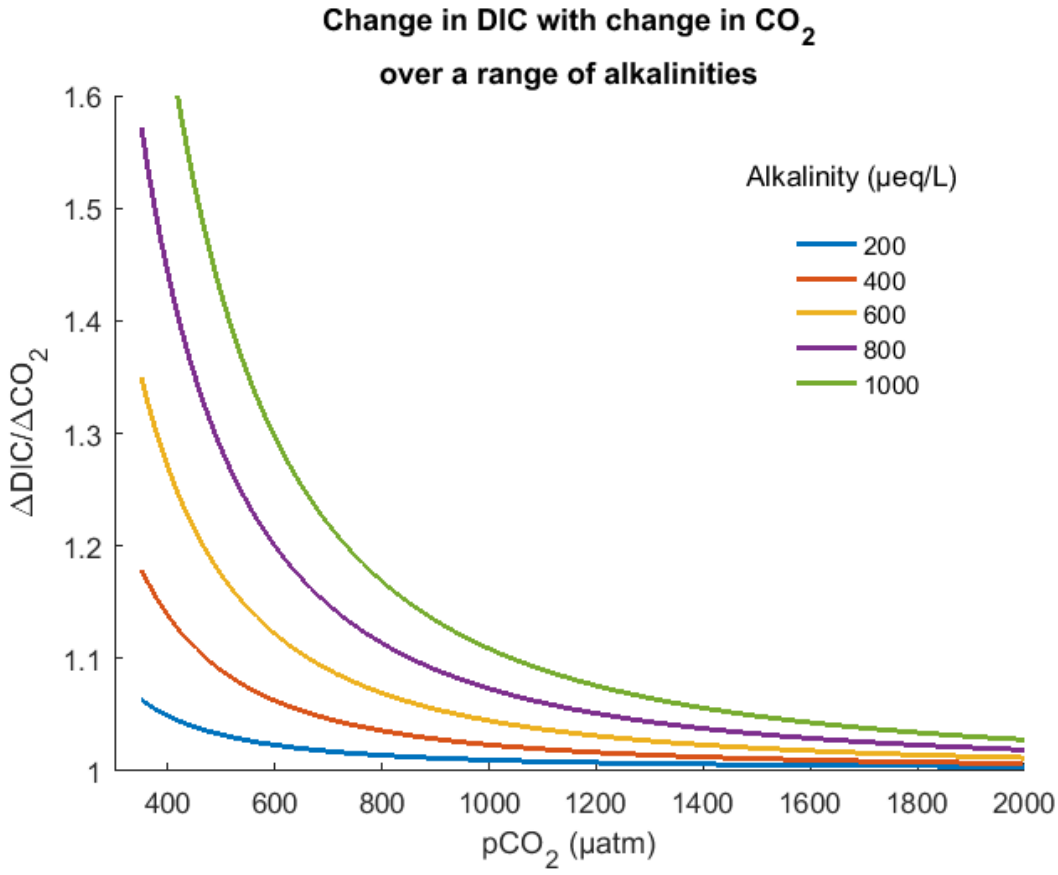


Figure A.2 – Change in *DIC* over change in $CO_2$ is plotted versus $pCO_2$ over a range in alkalinities. As alkalinity increases the change in *DIC* over change in $CO_2$ increases, making substitution of $\Delta CO_2$ for ΔDIC inaccurate.

*Literature Cited*

Ben-Yaakov, S. 1981. Electrochemical measurements. Pages 100-122 in Whitfield, M., and D. Jagner (editors). Marine electrochemistry: a practical introduction. Wiley, Chichester, New York.

Johnson, M. S., M. F. Billett, K. J. Dinsmore, M. Wallin, K. E. Dyson, and R. S. Jassal. 2010. Direct and continuous measurement of dissolved carbon dioxide in freshwater aquatic systems—method and applications. Ecohydrology 3:68–78.

Kilpatrick, F. A., and E. D. Cobb. 1985. Measurement of Discharge Using Tracers: U.S. Geological Survey Techniques of Water-Resources Investigations, book 3, chap. A16. Page 52.

Lewis, E., and W. R. Wallace. 1998. Program Developed for $CO_2$ System Calculations. ORNL/CDIAC-105. Carbon Dioxide Information Analysis Center, Oak Ridge National Laboratory, U.S. Department of Energy, Oak Ridge, Tennessee.

Millero, F. J. 1979. The thermodynamics of the carbonate system in seawater. Geochimica et Cosmochimica Acta 43:1651–1661.

Stumm, J., and J. Morgan. 1996. Aquatic Chemistry: Chemical Equilibria and Rates in Natural Waters (3rd ed., Environmental science and technology). Wiley, New York.

Appendix B: Determining Travel Time and Groundwater Dominated Piezometers Using Tracer Injections and Temperature Time Series

An array of 31 EC/temperature sensors (Campbell 547A) were deployed at the WS1 Well Field (Figure B.1). The sensor array measured EC within the stream and 30 piezometers continuously at a 10 minute interval. EC and temperature were also measured using a handheld WTW (Weilheim, Germany) Cond 3310 meter on a roughly monthly interval. Handheld measurements were used for QA/QC and drift correction. The EC/Temperature data was used to estimate travel times from the stream along hyporheic flow paths to each piezometer and identify piezometers that are dominated by lateral inflows of hillslope or groundwater.

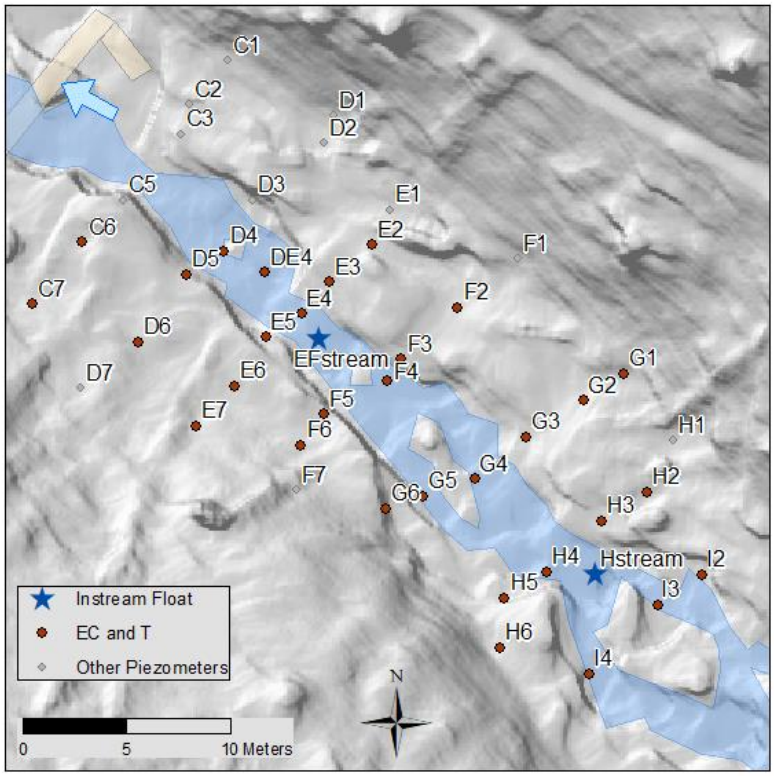


Figure B.1– WS1 Well Field and location of stainless-steel piezometers and instream monitoring locations (Instream Float). Sites with continuous deployment of Electrical Conductivity (EC) and Temperature (T) are shown as red dots.

Conservative salt tracer injections were conducted on five separate occasions between 2014 and 2016, over a range of flow conditions ranging from 0.9 L/s to 20 L/s.

Salt was added as a constant rate injection or pulse injections. The injection point was a site roughly 30 meters upstream of transect I (the upstream most transect of the WS1 Well Field).

*Travel Time*

Travel time from the stream to each piezometer was estimated by both fitting a transfer function model to observed EC signals (recorded in the stream and piezometer), and performing a windowed cross correlation. Transfer function analysis was performed on tracer break through curves when tracer (NaCl) was injected. Equation **Error! Reference source not found.** describes the transfer function model, which is a convolution.

$$EC_{out}(t) = \int_0^t EC_{in}(t) \cdot g(t-\tau)\mathrm{d}\tau \qquad \text{(Eq. B.1)}$$

Where $EC_{out}$ is the electrical conductivity observed at the site of interest, $EC_{in}$ is the input electrical conductivity (typically of the stream), $t$ is time, $\tau$ is a time lag, and $g$ is the transfer function. The shape of the transfer function is interpreted as the probability distribution of travel times from the stream to the well (Jury 1982). The transfer function was given a predefined form as a gamma distribution, after (Luo et al. 2006), and fit to observed data using Matlab's model fitting function 'fmincon' to minimize the root mean squared error of the modeled output from the observed. Prior to model fitting the input and output data were normalized by dividing the data by their respective zeroth moment ($M_0$)

$$M_0 = \int EC(t) \cdot \mathrm{d}t \qquad \text{(Eq. B.2)}$$

The transfer function method was found to perform sufficiently well to model the output signal recorded at most wells from the input signal (Figure B.2).

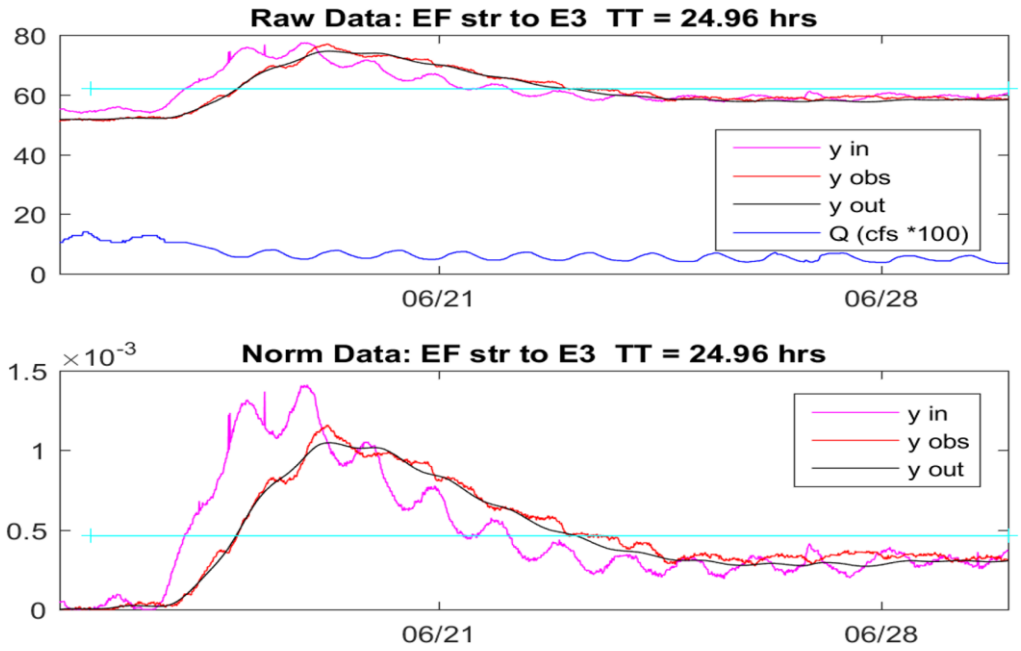


Figure B.2 – Example input data series (y in), observed data series (y obs), and transfer function model output (y out) for piezometer E3. Upper plot is the raw data. Lower plot is the normalized data. The light blue horizontal line is the window of time used for model fitting.

Windowed cross correlation was also used to estimate travel times from the stream to piezometer sites. Cross correlation is a common statistical technique that measures the similarity between two time series as a function of displacement. In this case, when the EC signal of the well is displaced back in time equivalent to the travel time, the correlation between the two datasets is at a maximum. Cross correlation was performed on 28 day long subsets (windows) of the EC time series. Only correlations which were found to be significant (alpha value > 0.05) using the artificial skill method were retained (Jenkins and Watts 1968) (Figure B.3)

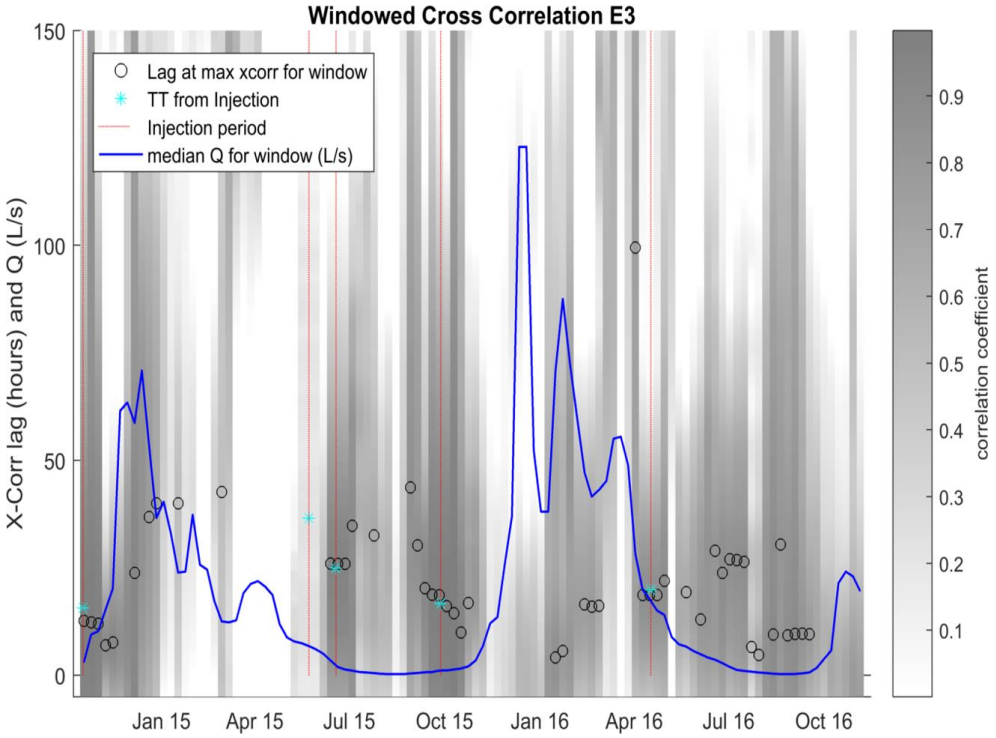


Figure B.3 – Example output from the windowed cross correlation (X-Corr). The open circles represent the lag (travel time) with the highest correlation for a given date (mid-point of a 28 day window). Teal asterisks represent the measured travel time (TT) from solute injection using the transfer function model, showing good agreement with estimates from the cross correlation.

*Groundwater Dilution*

The zeroth moment was also used to determine piezometers that were dominated or diluted by lateral inflows. The ratio of $M_0$ observed at a piezometer to $M_0$ observed in the stream ($M_0$ Ratio) is expected to indicate the degree of dilution by lateral inflows of groundwater. Once a tracer is fully mixed in the stream, all sites farther downstream or down a hyporheic flow path will have the same value of $M_0$ as is recorded in the stream (Jerald L. Schnoor 1996). Thus, if the $M_0$ Ratio at a site is near zero, then no tracer reached the site and it is assumed that the site is lateral inflow dominated. If the $M_0$ Ratio is close to 1.0, then the site is assumed to be stream water dominated. In practice there are many confounding factors including the potential that the stream is not well mixed at the

downwelling site, or the downwelling site of a hyporheic flow path is upstream of the tracer injection location. In the vicinity of the WS1 Well Field, we expect the stream to mix rapidly in a short distance; however, we suspect that some piezometer sites in the upper most transects I and H have downwelling locations that are within the mixing zone or above the injection point.

*Temperature Anomaly*

Temperature was also used a natural tracer for groundwater inflows. The temperature of groundwater is expected to exhibit less seasonality compared to that of stream water. During the summer when air temperature is high, groundwater will be cooler on average than stream water. Conversely, during the winter when air temperature is cold, groundwater will be warmer on average than stream water.

The temperature anomaly was defined as the difference of the average temperature at a site from the average temperature of the stream. Average temperature was found by Applying a low pass filter (21 day moving average) to temperature timeseries datasets. The low pass filter smoothed out all diurnal or short period storm driven temperature fluctuations. Groundwater dilution was estimated by defining groundwater to have the temperature as was recorded in C7 and applying an end member mixing model to estimate the ratio of stream water to groundwater required to produce the observed temperature of the site.

*Results*

Estimated travel times from the stream to piezometers and ratios of $M_0$ Ratios were analyzed and are summarized in Table B.1 and Figure B.5. Estimates of travel times for individual piezometer sites were generally consistent between injections, indicating that travel time does not change appreciably with discharge. Travel times for individual piezometers were also generally consistent with those measured in 1997 ((Wondzell 2006). This was surprising given that nearly 20 years had passed and the original PVC piezometers had been replaced by stainless steel units. However, major channel reconfiguration had not occurred during this period.

Table B.1 – Estimated travel time (TT) and $M_0$ Ratios for piezometers within the WS1 Well Field.

| | Apr-2016 | | Apr-2015 | | Oct-2014 | | Jun-2015 | | Sep-2015 | | Median TT | Cross Correlation 2014 through 2016 |
|---|---|---|---|---|---|---|---|---|---|---|---|---|
| | 20 L/s | | 10 L/S | | 2.0 L/s | | 1.8 L/S | | 1.0 L/s | | | varied |
| | TT (hours) | M0 Ratio | TT (hours) | M0 Ratio | TT (hours) | M0 Ratio | TT (hours) | M0 Ratio | TT (hours) | M0 Ratio | TT (hours) | TT (hours) |
| **C6** | NAN | NAN | 45.2 | 0.71 | 114.7 | 0.47 | 68.0 | 0.39 | 69.2 | 0.31 | 68.6 | 87.2 |
| **C7** | NAN | NAN | NAN | NAN | NAN | NAN | 67.8 | 0.33 | 62.6 | 0.35 | 65.2 | 65.2 |
| **D4** | NAN | NAN | 1.1 | 0.58 | 2.5 | 1.00 | 2.3 | 0.99 | NAN | NAN | 2.3 | 1.8 |
| **D5** | 21.5 | 0.32 | 74.1 | 0.67 | 83.3 | 0.69 | NAN | 0.09 | 54.0 | 0.69 | 64.0 | 32.4 |
| **D6** | NAN | 0.18 | 7.1 | 1.02 | 130.6 | 0.62 | 47.8 | 0.68 | 115.7 | 0.51 | 81.8 | 124.0 |
| **D7** | NAN | 0.09 | NAN | NAN | NAN | NAN | NAN | 0.00 | NAN | 0.00 | NAN | NAN |
| **DE4** | 17.6 | 0.77 | 1.1 | 0.99 | 11.3 | 0.94 | 1.9 | 1.01 | NAN | NAN | 6.6 | 3.0 |
| **E2** | 33.2 | 0.08 | NAN | NAN | 112.1 | 0.53 | NAN | 0.44 | 50.5 | 1.01 | 50.5 | 49.2 |
| **E3** | 19.9 | 0.34 | 36.55 | 0.73 | 15.6 | 1.08 | 24.9 | 1.34 | 16.7 | 1.17 | 19.9 | 18.6 |
| **E4** | NAN | NAN | NAN | NAN | 4.7 | 1.03 | NAN | NAN | NAN | NAN | 4.7 | 8.7 |
| **E5** | 49.6 | 0.36 | 70.7 | 0.68 | 47.9 | 0.80 | 66.9 | 0.76 | 5.2 | 0.97 | 49.6 | 15.3 |
| **E6** | NAN | 0.04 | 5.7 | 0.78 | 104.8 | 0.91 | 10.9 | 0.94 | 65.1 | 0.40 | 38.0 | 47.0 |
| **E7** | NAN | 0.14 | NAN | 0.00 | NAN | NAN | NAN | 0.00 | NAN | 0.08 | NAN | NAN |
| **F2** | NAN | NAN | 65.6 | 0.32 | 62.9 | 0.75 | 59.9 | 1.86 | 70.5 | 0.61 | 64.3 | 32.1 |
| **F3** | 15.3 | 0.56 | 2.2 | 0.81 | 3.7 | 1.05 | NAN | NAN | 9.4 | 1.30 | 6.6 | 5.6 |
| **F4** | 6.8 | 0.89 | 3.5 | 0.85 | 3.4 | 1.05 | 6.0 | 1.40 | 8.6 | 1.30 | 6.0 | 5.5 |
| **F5** | 83.8 | 0.21 | 23.5 | 1.11 | 46.3 | 0.87 | 24.8 | 0.85 | 60.1 | 0.71 | 46.3 | 26.3 |
| **F6** | NAN | NAN | 42.7 | 0.44 | NAN | NAN | 50.6 | 0.37 | 27.8 | 0.56 | 42.7 | 49.3 |
| **G1** | NAN | 0.02 | 44.8 | 1.27 | 88.0 | 0.44 | 59.8 | 1.39 | 178.7 | 1.11 | 73.9 | 19.0 |
| **G2** | NAN | 0.29 | 72.2 | 0.77 | 77.4 | 0.79 | NAN | 0.62 | 163.9 | 0.82 | 77.4 | 103.8 |
| **G3** | 34.0 | NAN | NAN | NAN | 89.7 | 0.62 | 65.7 | 2.12 | 156.6 | 1.34 | 77.7 | 105.1 |
| **G4** | 2.0 | 0.65 | NAN | NAN | 8.3 | 1.06 | 64.3 | 1.39 | 153.5 | 0.70 | 36.3 | 6.0 |
| **G5** | NAN | NAN | NAN | NAN | 2.4 | 1.10 | 2.5 | 1.05 | NAN | NAN | 2.4 | 2.7 |
| **G6** | 96.9 | 0.16 | 37.9 | 3.81 | 141.5 | 1.32 | 66.9 | 0.77 | 29.5 | 0.57 | 66.9 | 28.1 |
| **H2** | NAN | NAN | 21.9 | 5.18 | 52.9 | 0.84 | NAN | NAN | NAN | NAN | 37.4 | 10.0 |
| **H3** | 6.0 | 1.03 | 15.3 | 1.75 | 36.5 | 0.87 | 19.9 | 4.59 | 38.4 | 1.78 | 19.9 | 19.4 |
| **H4** | 3.1 | 0.96 | 25.9 | 2.81 | 22.4 | 0.65 | 14.8 | 1.99 | NAN | NAN | 18.6 | 6.2 |
| **H5** | NAN | 0.04 | 44.1 | 1.78 | 136.0 | 0.76 | NAN | 0.11 | NAN | NAN | 90.0 | 14.2 |
| **H6** | NAN | 0.03 | 36.1 | 0.75 | 66.2 | 0.34 | | 0.22 | 61.8 | 0.24 | 61.8 | 67.0 |
| **I2** | 28.1 | 0.72 | NAN | NAN | NAN | NAN | 11.6 | 4.94 | 41.7 | 1.73 | 28.1 | 34.4 |
| **I3** | 4.7 | 0.91 | 23.5 | 3.07 | 11.1 | 1.18 | 0.7 | 3.00 | 155.0 | 0.51 | 11.1 | 4.1 |
| **I4** | NAN | 0.2 | 4.4 | 2.24 | 6.2 | 0.70 | NAN | 0.37 | 1.0 | 0.10 | 4.4 | 4.0 |
| Mean | 28.2 | 0.4 | 30.6 | 1.4 | 54.9 | 0.8 | 35.2 | 1.2 | 69.4 | 0.8 | 40.8 | 33.2 |
| Count | 15 | 23 | 23 | 24 | 27 | 27 | 22 | 29 | 23 | 25 | 30 | 30 |

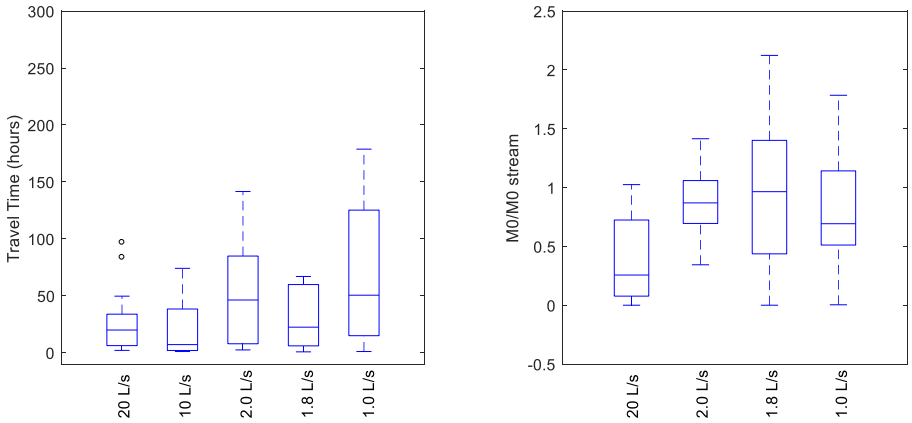


Figure B.4 – Mean travel time and $M_0$ Ratios for piezometers within the WS1 well field. Box plots show medians (center horizontal line), quartiles (boxes), 90 percent confidence intervals (whiskers) and outliers (circles).

The mean of travel times for all sites increased with decreasing discharge (Figure B.5). This trend is consistent with that found by (Ward et al. 2017). However, this trend is confounded by the spatial contraction of the hyporheic zone during high flow. At high flows, the tracer break through curves were extremely weak for many long travel time sites, generally located farther from the stream. If no tracer was observed an estimate of travel time was not given. Thus, at high flow the number of piezometers with a travel time estimate is small and these sites tend to cluster near the stream and have shorter travel times. Conversely, at low flow, a greater number of sites have measurable travel times, including many sites with long travel times farther from the stream.

Estimates of travel time from cross correlation agreed well with those estimated from tracer break through curves. When analyzing data that included a tracer injection break through curve within the model window, the agreement between methods was good (Figure B.4). The cross correlation method was also found to perform well for sites with relatively short travel times less than roughly 24 hours and did not require any tracer injection. Thus, for sites with relatively short travel time natural fluctuations in EC were sufficient for the cross correlation method to be effective. For sites with longer travel

times, the cross correlation method identified few correlations that were statistically significant unless a salt tracer had been introduced.

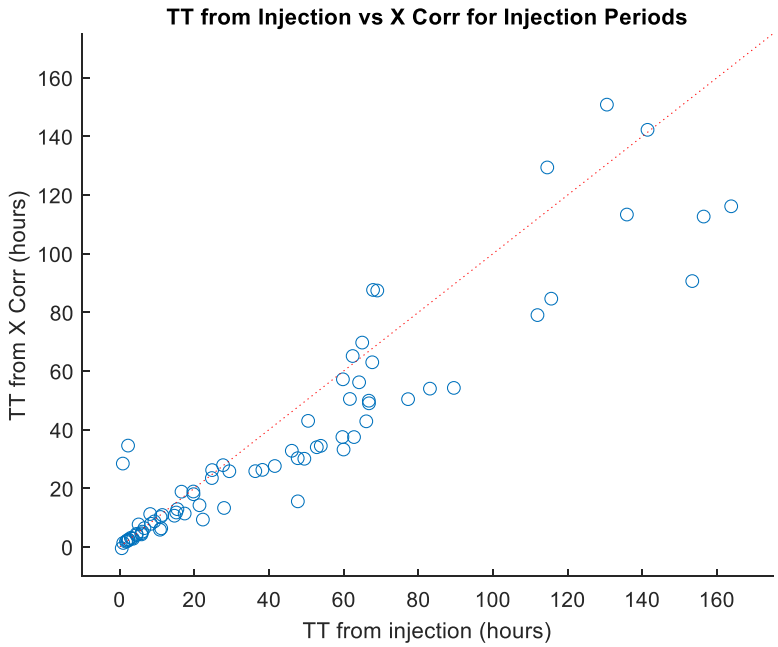


Figure B.5 – Comparison of travel time (TT) estimates from analysis of tracer injection by the transfer function method to TT from cross correlation (X-Corr). The two methods agreed well during times when tracer injections had been conducted.

$M_0$ Ratios decreased significantly from tracer injections completed at low flows (2 L/s or less) to tracer injections completed at intermediate flows (20 L/s). $M_0$ Ratios were observed to decrease markedly for sites outside the active channel near the toe of the hillslope (Figure B.7). The change in $M_0$ Ratio was interpreted to indicate that the hyporheic zone contracts with increasing discharge, and that much of the riparian terrace is dominated by groundwater or hillslope water during periods of elevated flow. The contraction of the hyporheic zone with increasing discharge is expected, and was predicted through finite element modeling of the study reach and greater WS1 by (Schmadel et al. 2017). Results from this study support those results.

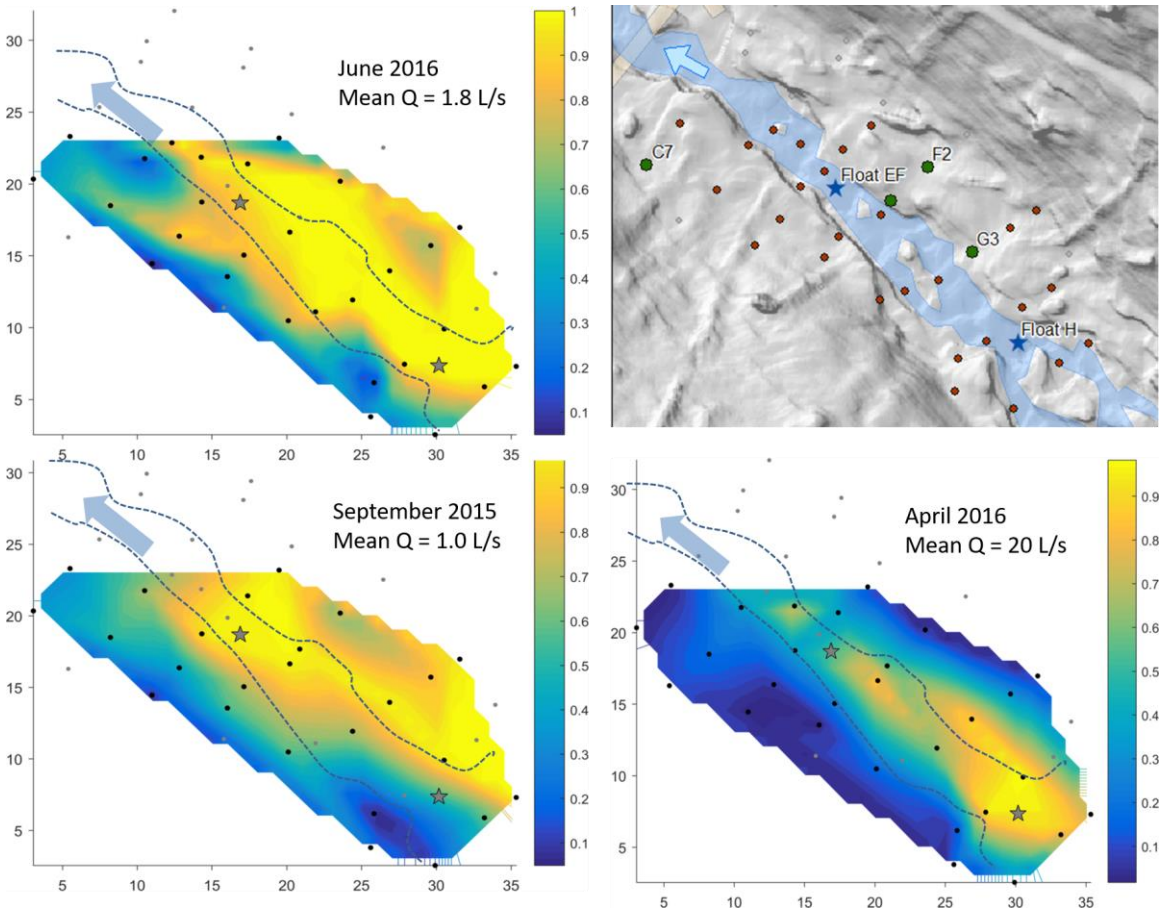


Figure B.6 – $M_0$ Ratio for various tracer injections over a range in flow conditions. Many sites outside the active channel transition from having high $M_0$ Ratio (hyporheic water dominated) to having low $M_0$ Ratio (lateral inflow dominated) between flows of 2.0 and 20 L/S.

$M_0$ Ratios were found to have small values at all flow conditions for sites at the hillslope transition, particularly on left bank of the Well Network. These sites include piezometer C7, D7, E7, and F7. It was observed that tracer injections did not propagate to these sites, even over plateau injections of multiple days, when flows were above 2.0 L/s. At very low flows of October 2014 and 2015, EC was observed to increase in or after the time period of the injection, but the form of the EC break through curves in these piezometers was perplexing with shapes inconsistent with a tracer break through curve. These sites were interpreted to be groundwater or hillslope water dominated for most, if not all, of the year.

Analysis of temperature time series was in agreement with results from tracer injections, and indicates sites along the hillslope transition on the south side of well network are groundwater dominated. During the summer, groundwater is expected to be cooler than stream water. The sites farthest southwest (nearest the break in slope at the hillslope to riparian terrace transition) were observed to have a temperature anomalies of -1.5 to -2 ℃ relative the stream in July of 2015 and 2016 (Figure B.8). These same sites were observed to have a temperature anomalies of +1.0 to +1.5 ℃ relative the stream in January of 2016. These spatial trends are interpreted to indicate persistent groundwater influx from the hillslope, and that piezometers C7, D7, E7, and F7 are groundwater dominated through much of the year.

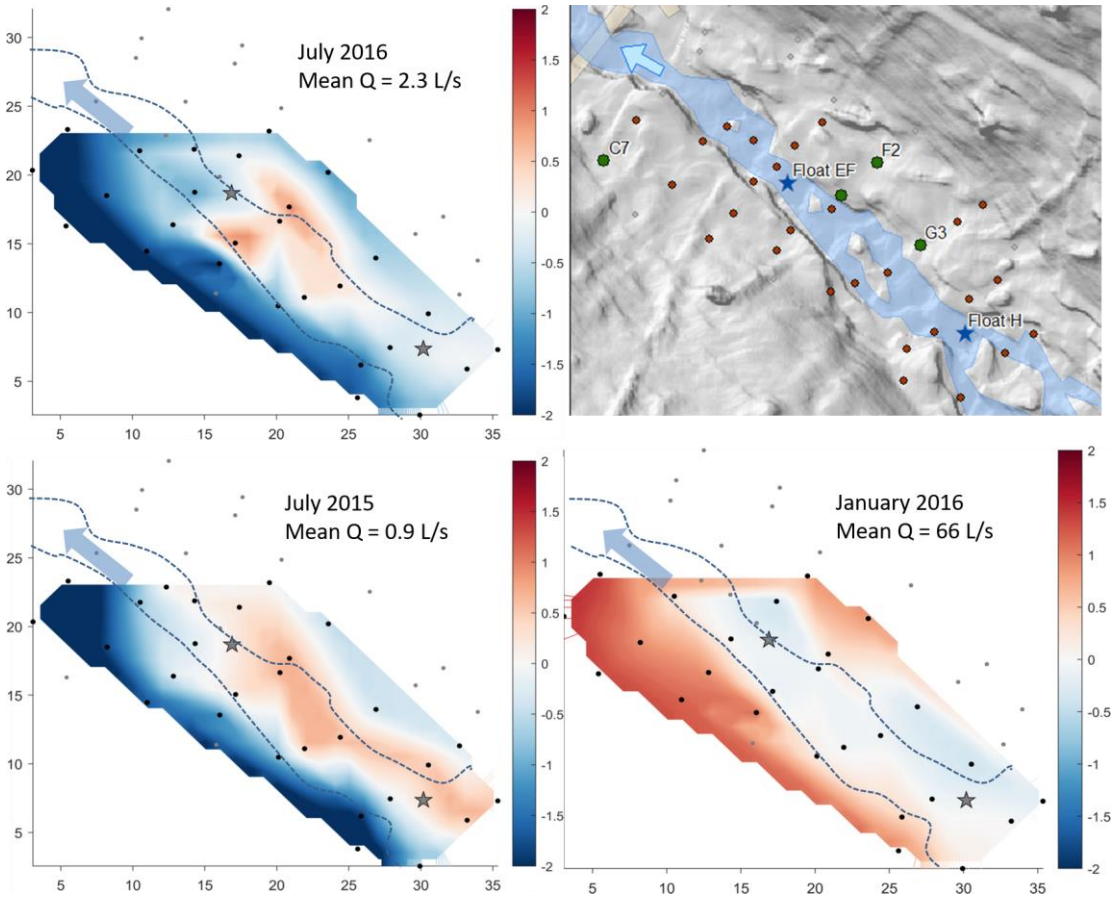


Figure B.7 – Temperature anomaly at various time of the year. Temperature anomaly is strongest along the southwest side of the riparian terrace. Temperature anomaly is less pronounced on the northeast side of the riparian terrace.

*Literature Cited*

Jenkins, G. M., and D. G. Watts. 1968. Spectral analysis and its applications.

Jerald L. Schnoor. 1996. Environmental modeling: fate and transport of pollutants in water, air, and soil. Wiley.

Jury, W. A. 1982. Simulation of solute transport using a transfer function model. Water Resources Research 18:363–368.

Luo, J., O. A. Cirpka, M. N. Fienen, W. Wu, T. L. Mehlhorn, J. Carley, P. M. Jardine, C. S. Criddle, and P. K. Kitanidis. 2006. A parametric transfer function methodology for analyzing reactive transport in nonuniform flow. Journal of Contaminant Hydrology 83:27–41.

Schmadel, N. M., A. S. Ward, and S. M. Wondzell. 2017. Hydrologic controls on hyporheic exchange in a headwater mountain stream. Water Resources Research 53:6260–6278.

Ward, A. S., N. M. Schmadel, S. M. Wondzell, M. N. Gooseff, and K. Singha. 2017. Dynamic hyporheic and riparian flow path geometry through base flow recession in two headwater mountain stream corridors. Water Resources Research 53:3988–4003.

Wondzell, S. M. 2006. Effect of morphology and discharge on hyporheic exchange flows in two small streams in the Cascade Mountains of Oregon, USA. Hydrological Processes 20:267–287.

Appendix C – Additional Figures for Carbon Fluxes of a Headwater Stream

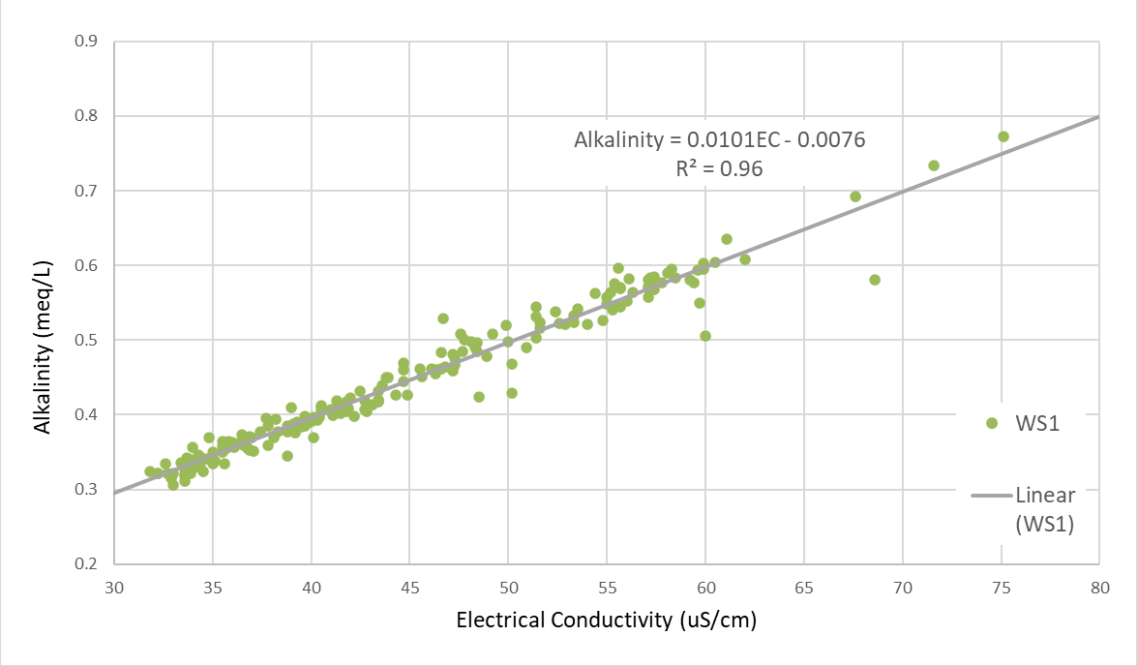


Figure C.1 – Electrical Conductivity versus Alkalinity from flow proportional sampling of the Watershed 1 gage.

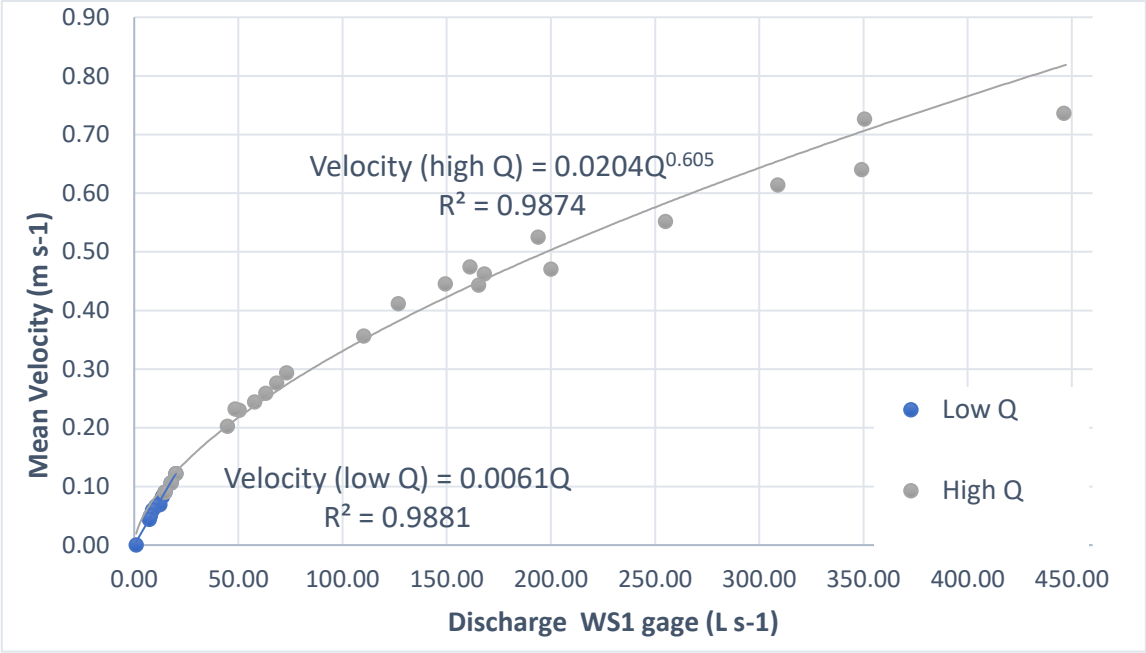


Figure C.2 – Discharge at Wastershed 1 gage vs mean stream velocity over a wide range of flow conditions.

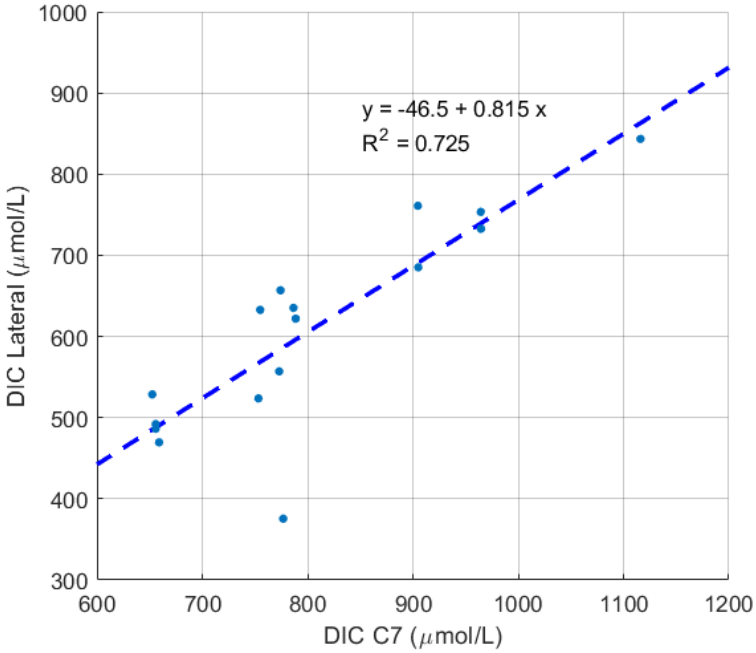


Figure C.3 – DIC from timeseries data at piezometer C7 versus measurements of DIC from water samples at piezometers C7, D7, E7, and F7, referred to in this plot as DIC Lateral.

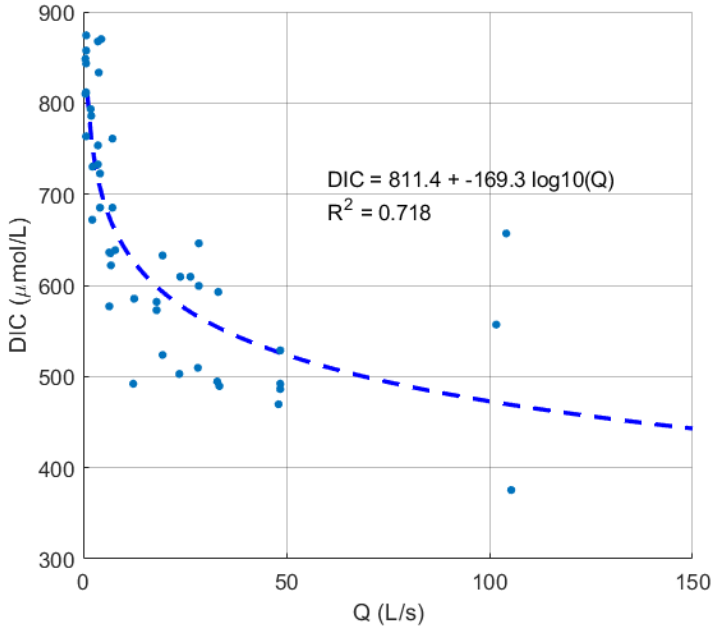


Figure C.4 – Discharge at the Watershed 1 gage versus DIC from water samples at piezometers C7, D7, E7, and F7.

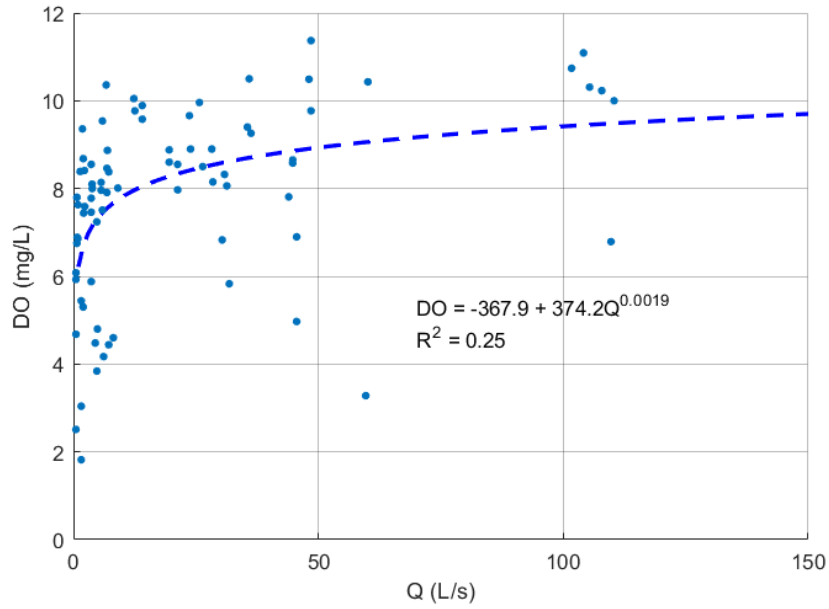


Figure C.5 – Discharge at the Watershed 1 gage versus DO from water samples at piezometers C7, D7, E7, and F7.

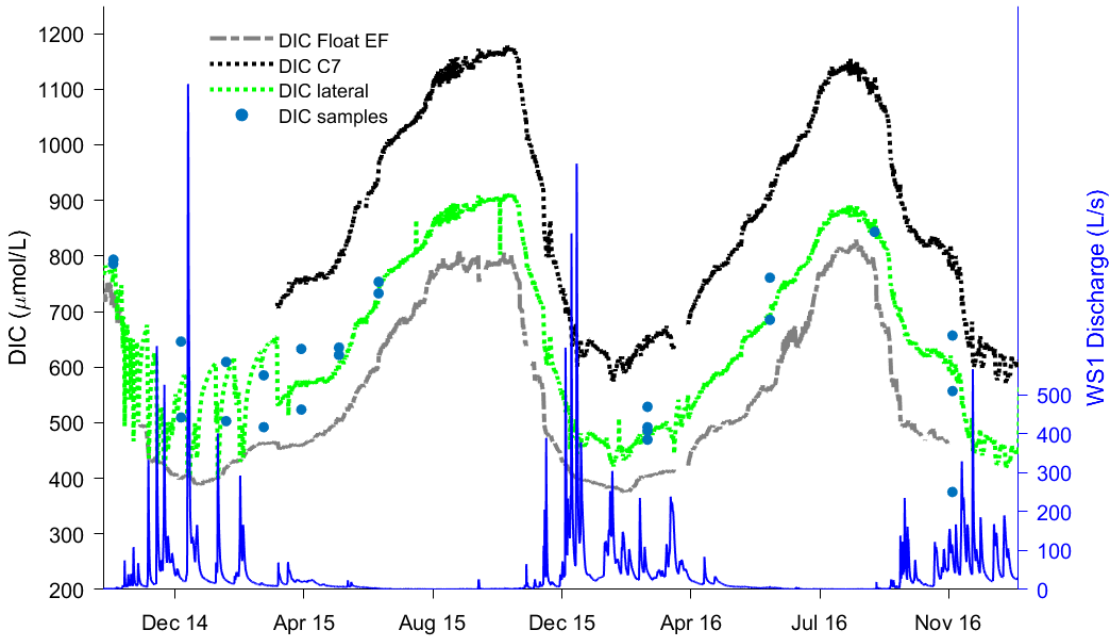


Figure C.6 – DIC time series for the stream at Float EF, piezometer C7 and modeled DIC for lateral inflows.

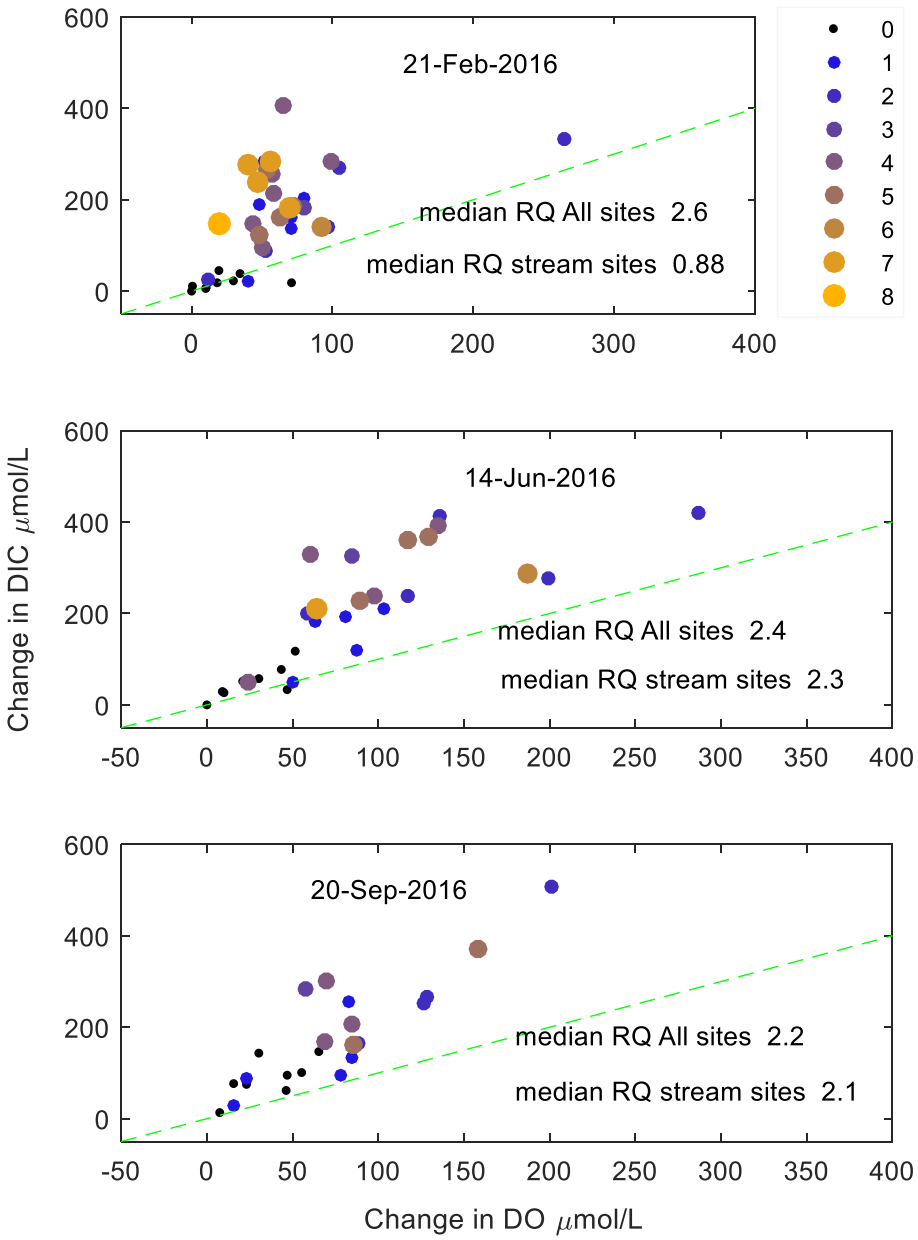


Figure C.7 – Change in DO from the stream to piezometer sites in µmol $O_2$ $L^{-1}$ versus change in DIC in µmol C $L^{-1}$, on various sample runs in 2016. The size and color of each point corresponds to the minimum distance the piezometer is from the wetted channel at winter baseflow. RQ is the ratio of -ΔDIC/ΔDIC. Stream sites are piezometers that are within the wetted channel at winter baseflow. Data is courtesy of Satish Serchan.